



## **Dose assessment in Computed Tomography based on Monte Carlo simulation for a 320 detector- row cone-beam scanner**

**Maria Cros Torrents**

**ADVERTIMENT.** L'accés als continguts d'aquesta tesi doctoral i la seva utilització ha de respectar els drets de la persona autora. Pot ser utilitzada per a consulta o estudi personal, així com en activitats o materials d'investigació i docència en els termes establerts a l'art. 32 del Text Refós de la Llei de Propietat Intel·lectual (RDL 1/1996). Per altres utilitzacions es requereix l'autorització prèvia i expressa de la persona autora. En qualsevol cas, en la utilització dels seus continguts caldrà indicar de forma clara el nom i cognoms de la persona autora i el títol de la tesi doctoral. No s'autoritza la seva reproducció o altres formes d'explotació efectuades amb finalitats de lucre ni la seva comunicació pública des d'un lloc aliè al servei TDX. Tampoc s'autoritza la presentació del seu contingut en una finestra o marc aliè a TDX (framing). Aquesta reserva de drets afecta tant als continguts de la tesi com als seus resums i índexs.

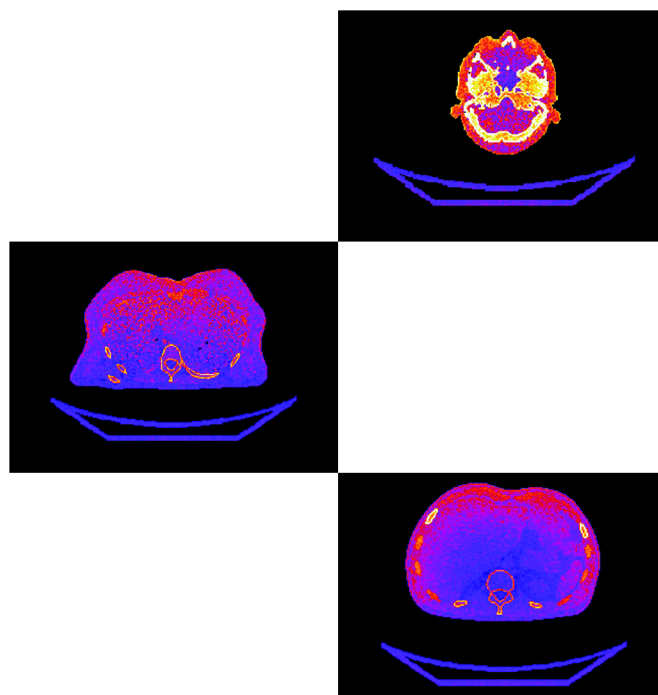
**ADVERTENCIA.** El acceso a los contenidos de esta tesis doctoral y su utilización debe respetar los derechos de la persona autora. Puede ser utilizada para consulta o estudio personal, así como en actividades o materiales de investigación y docencia en los términos establecidos en el art. 32 del Texto Refundido de la Ley de Propiedad Intelectual (RDL 1/1996). Para otros usos se requiere la autorización previa y expresa de la persona autora. En cualquier caso, en la utilización de sus contenidos se deberá indicar de forma clara el nombre y apellidos de la persona autora y el título de la tesis doctoral. No se autoriza su reproducción u otras formas de explotación efectuadas con fines lucrativos ni su comunicación pública desde un sitio ajeno al servicio TDR. Tampoco se autoriza la presentación de su contenido en una ventana o marco ajeno a TDR (framing). Esta reserva de derechos afecta tanto al contenido de la tesis como a sus resúmenes e índices.

**WARNING.** Access to the contents of this doctoral thesis and its use must respect the rights of the author. It can be used for reference or private study, as well as research and learning activities or materials in the terms established by the 32nd article of the Spanish Consolidated Copyright Act (RDL 1/1996). Express and previous authorization of the author is required for any other uses. In any case, when using its content, full name of the author and title of the thesis must be clearly indicated. Reproduction or other forms of for profit use or public communication from outside TDX service is not allowed. Presentation of its content in a window or frame external to TDX (framing) is not authorized either. These rights affect both the content of the thesis and its abstracts and indexes.

# Dose assessment in Computed Tomography based on Monte Carlo simulation for a 320 detector-row cone-beam scanner

---

MARIA CROS TORRENTS



UNIVERSITAT ROVIRA I VIRGILI

Dose assessment in Computed Tomography based on Monte Carlo simulation for a 320 detector- row cone-beam scanner

Maria Cros Torrents

Dose assessment in Computed Tomography based on  
Monte Carlo simulation for a 320 detector-row  
cone-beam scanner

PhD Thesis

**Maria Cros Torrents**

Supervised by: PhD Marçal Salvadó Artells

Unitat de Física Mèdica, Departament de Ciències Mèdiques Bàsiques



UNIVERSITAT ROVIRA I VIRGILI

2017

UNIVERSITAT ROVIRA I VIRGILI

Dose assessment in Computed Tomography based on Monte Carlo simulation for a 320 detector- row cone-beam scanner

Maria Cros Torrents



DEPARTAMENT DE CIÈNCIES MÈDIQUES BÀSIQUES

UNITAT DE FÍSICA MÈDICA

C/ Sant Llorenç, 21

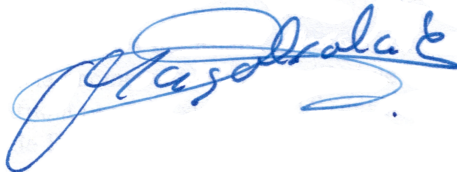
43201 Reus (Tarragona)

Tel.: (+34) 977759382

I STATE that the present study, entitled “**Dose assessment in Computed Tomography based on Monte Carlo simulation for a 320 detector-row cone-beam scanner**”, presented by Maria Cros Torrents for the award of the degree of Doctor, has been carried out under my supervision at the Medical Physics Unit of the Department of Basic Medical Science of this university, and that it fulfils all the requirements to be eligible for the European Doctorate Award.

Reus, 23<sup>th</sup> May 2017

Doctoral Thesis Supervisor



PhD. Marçal Salvadó Artells

UNIVERSITAT ROVIRA I VIRGILI

Dose assessment in Computed Tomography based on Monte Carlo simulation for a 320 detector- row cone-beam scanner

Maria Cros Torrents

*Potser sense saber-ho,  
m'has fet arribar fins aquí.  
A tu, papa.*





# Acknowledgments

This thesis work could not have been performed without the help and collaboration of multiple people.

First, I would like to express my sincere thanks to my supervisor Marçal Salvadó, head of the Medical Physics Unit of the Universitat Rovira i Virgili. Gràcies Marçal, pel teu suport, per les estones de discussió científica i per l'orientació durant la realització d'aquesta tesi. I sobretot, gràcies per la comprensió en cada moment i per fer el camí tan fàcil.

I would also like to thank the members of the Medical Physics Unit and the Radiation Protection Service of the Universitat Rovira i Virgili, for giving me the opportunity of being part of them. Al Miguel López, per haver-me obert les portes al món de la recerca i per haver-nos deixat aprendre de tota la seva experiència laboral i de vida. Al Juan José Morant, per haver aportat aquesta visió de la ciència tan real i tan pràctica al nostre treball del dia a dia, recordant-me que tot el que fem té un sentit més enllà de les portes del despatx. Al Diego Molina, per la seva dedicació al nostre projecte i l'extrema eficiència que, després d'uns anys, encara no he deixat d'admirar.

Al Ramon, per ser aquell company d'estudis i de feina que es va convertir en un gran amic a qui li he pogut explicar sempre allò que em preocupava i allò que m'alegrava. Gràcies Ramon, primer per ajudar-me amb els estudis de física quan calia, i després per ajudar-me a formar part del grup de Física Mèdica. En definitiva, gràcies per ser-hi sempre en l'espai-temps adequat. A la Irene, pel seu immens suport i ajuda en la meua feina i sobretot, per haver-me acollit tan bé a Leiden durant els tres mesos que guardo com a millor record d'aquests anys. Gràcies Irene, pels moments de ciència compartits i per les llargues converses d'amigues que sempre semblaven no tenir fi. A l'Elena, per les hores de treball i d'amistat que hem anat construint juntes al despatx, fent de tot plegat, un camí més lleuger. Gràcies Elena, per donar naturalitat a la realitat, arrancant-nos somriures fins i tot en els moments més complicats.

I would like to express my sincere appreciation to the people from LUMC. To Koos Geleijns, head of Medical Physics at LUMC, for opening the door of the hospital, for giving me the opportunity to do a research stay in Leiden and for becoming my second supervisor during the development of the thesis. To Raoul Joemai, for sharing your knowledge, for giving new ideas and for the help that you have always offered to my work. I would also like to thank all the LUMC staff who helped me during my stay, specially, to my colleagues at K4-44 for making me feel welcome at all times.

I would like to thank to Universitat Rovira i Virgili for the scholarship AEE2015-Biomedicina in the framework of *Ajuts per a estades curtes a l'estranger*, which financed my research in LUMC (The Netherlands).

I would like to acknowledge CSUC (Consorci de Serveis Universitaris de Catalunya) for

the technical support provided during the performing of all the Monte Carlo simulations in their supercomputers.

Finally, I would express my special gratitude to everyone who has shared this period of time close to me. Gràcies a les *Drugas*, per fer més fàcil el *subterfugi* durant els anys a la Facultat de Física. Gràcies als amics i amigues per la seva comprensió quan se m'acumulava la feina. En especial, als amics del "Jo també faig el doctorat". I sobretot, gràcies als de més a la vora. A l'Elisabet i a l'Enric per la infinita paciència. Al papa i a la mama, Joan i Maria del Carme, per haver-me fet pla el camí que m'ha permès arribar fins aquí. Gràcies per haver-me ensenyat a voler aprendre i per haver estat segurs, en el moment precís, d'allò que jo hi hauria estat massa tard.

# List of acronyms and abbreviations

AF	Adult female
AM	Adult male
CT	Computed Tomography
CTA	Computed Tomography angiography
CTDI	Computed Tomography dose index
CTDI <sub>vol</sub>	Volumetric Computed Tomography dose index
CTDI <sub>w</sub>	Weighted Computed Tomography dose index
CTP	Computed Tomography perfusion
DLP	Dose-length product
ESD	Entrance skin dose
FBP	Filtered back projection
FOV	Field of view
HU	Hounsfield units
ICRP	International Commission on Radiological Protection
kVp	Peak kilovoltage
mAs	Tube charge per rotation
MC	Monte Carlo
MDCT	Multi-slice detector Computed Tomography
MOSFET	Metal oxide semiconductor field-effect transistors
PMMA	Polymethylmethacrylate
RBM	Red bone marrow
SSDE	Size-specific dose estimates
TCM	Tube current modulation
TLD	Thermoluminescent dosimeter

*LIST OF ACRONYMS AND ABBREVIATIONS*

# List of contributions

## Thesis papers

This thesis is based on the following peer-reviewed publications, which will be referred to in the text using capital Roman numerals:

- [I] Salvadó M, Cros M, Joemai RMS, Calzado A, Geleijns J. Monte Carlo simulation of the dose distribution of ICRP adult reference computational phantoms for acquisitions with a 320 detector-row cone-beam CT scanner. *Phys Med* 2015;31:452-462 (DOI: 10.1016/j.ejmp.2015.04.007)
- [II] Geleijns J, Joemai RMS, Cros M, Hernandez-Giron I, Calzado A, Dewey M, Salvadó M. A Monte Carlo simulation for the estimation of patient dose in rest and stress cardiac computed tomography with a 320-detector row CT scanner. *Phys Med* 2015;31:1029-34 (DOI: 10.1016/j.ejmp.2015.08.008)
- [III] Cros M, Geleijns J, Joemai RMS, Salvadó M. Perfusion CT of the brain and liver and of lung tumors: Use of Monte Carlo simulation for patient dose estimation for examinations with a cone-beam 320-MDCT scanner. *Am Jour Roentgenol* 2016;206:129-35 (DOI: 10.2214/AJR.15.14913)
- [IV] Cros M, Joemai RMS, Geleijns J, Molina D, Salvadó M. SimDoseCT: dose reporting software based on Monte Carlo simulation for a 320 detector-row cone-beam CT scanner and ICRP computational adult phantoms. *Phys Med Biol* 2017 (DOI: doi.org/10.1088/1361-6560/aa77ea)

## Software registration

In the context of this thesis, a software has been registered in the Benelux Office for Intellectual Property. It corresponds to the software development described in Paper [IV].

M. Cros, R.M.S. Joemai, J. Geleijns, D. Molina and M. Salvadó *SimDoseCT: Computed Tomography dose reporting software*. Benelux Office for Intellectual Property, i-DEPOT evidence number 105319, 11th May 2017.

## Presentations in conferences

Oral presentations based on the contents of this thesis have been given at:

M. Cros, J. Geleijns, R.M.S. Joemai and M. Salvadó. SimDoseCT: programa para la evaluación de dosis en un escáner volumétrico de Tomografía Computarizada. Oral presentation (presenter). V Congreso conjunto de las Sociedades Españolas de Física Médica y Protección Radiológica. Girona, 2017.

M. Cros, J. Geleijns, R.M.S. Joemai and M. Salvadó. A Monte Carlo Simulation for Patient Dose Evaluation in Brain Perfusion CT with a 320 Detector-row Cone-beam CT Scanner using ICRP Computational Phantoms. Oral presentation (presenter). IV Congreso conjunto de las Sociedades Españolas de Física Médica y Protección Radiológica. Valencia, 2015.

M. Cros, J. Geleijns, R M S Joemai, I. Hernandez-Giron, A. Calzado, M. Dewey and M. Salvadó. Patient Dose Estimation in Cardiac Computed Tomography with a 320 Detector Row Scanner Based on Monte Carlo Simulation. Oral presentation (presenter). 8th European Conference on Medical Physics. Athens, 2014. Available: <https://doi.org/10.1016/j.ejmp.2014.07.091>

M. Cros, J. Geleijns and M. Salvadó. Cálculo de dosis en maniqués antropomórficos ICRP 110 mediante simulación de protocolos generales para un equipo de TC de 320 secciones. Oral presentation (presenter). III Congreso conjunto de las Sociedades Españolas de Física Médica y Protección Radiológica. Cáceres, 2013.

## Other publications

Other scientific contributions related to the contents of this thesis have been published:

Casanovas R, Cros M, Salvadó M. Simulació Montecarlo del transport de la radiació per a aplicacions en medicina i protecció radiològica. *Revista de física* 2014;5:21-29.

## Book chapters and editions

During this thesis, the following book chapters were written:

J.J. Morant, R. Casanovas, M. Alcaraz, M. Cros. *Física de las radiaciones*. J.J. Morant, M. Alcaraz, E. Velasco (eds.). *Formación básica en protección radiológica. Curso de protección radiológica dirigido al personal técnico de las empresas de venta y asistencia técnica de equipos de rayos X dentales*. Servicio de publicaciones de la Universidad de Murcia. 1a Edición, pp. 11-68. 2013, ISBN: 978-84-15463-89-4.

M. López, F. Borrull, M. Salvadó, C. Aguilar, R. Casanovas, M. Cros, I. Hernández, J.J. Morant, A. Nieto, S. Peñalver. Edition of the proceedings of the conference *VII Jornadas sobre calidad en el control de la radiactividad ambiental*, Tarragona (Spain), 2012. Available: [http://www.csn.es/images/stories/publicaciones/otras\\_publicaciones/coediciones/vii\\_jornades\\_de\\_calidad\\_web.pdf](http://www.csn.es/images/stories/publicaciones/otras_publicaciones/coediciones/vii_jornades_de_calidad_web.pdf).

## Other remarks

During the development of this thesis, other remarks can be highlighted:

Best Oral Presentation Award at the 8th European Conference on Medical Physics (Athens, 2014) for the paper *Patient Dose Estimation in Cardiac Computed Tomography with a 320 Detector Row Scanner Based on Monte Carlo Simulation*.

Research stay in LUMC (Leiden University Medical Center, Leiden, The Netherlands) in the Radiology Department (Head of Department: Koos Geleijns) during the period between September and December 2015.





# Contents

<b>Acknowledgments</b>	<b>ix</b>
<b>List of acronyms and abbreviations</b>	<b>xi</b>
<b>List of contributions</b>	<b>xiii</b>
<b>Contents</b>	<b>xvii</b>
<b>Summary</b>	<b>xix</b>
<b>1 Introduction</b>	<b>1</b>
1.1 Computed Tomography . . . . .	1
1.1.1 Basic principles of CT . . . . .	1
1.1.2 Evolution of CT scanners . . . . .	2
1.2 The 320 detector-row cone-beam scanner . . . . .	4
1.2.1 Technical specifications . . . . .	5
1.2.2 Scan modes and clinical applications . . . . .	6
1.3 CT Dosimetry . . . . .	7
1.4 Patient dose estimation . . . . .	8
<b>2 Motivation, hypothesis and objectives</b>	<b>11</b>
<b>3 PhD thesis outline</b>	<b>13</b>
<b>4 Materials, methods and results</b>	<b>15</b>
4.1 Scanner modelling and validation of the simulation program . . . . .	17
4.2 Dose assessment in specific studies . . . . .	31
4.2.1 Dose assessment in cardiac CT . . . . .	31
4.2.2 Dose assessment in perfusion CT . . . . .	39
4.3 Development of software for dose assessment . . . . .	49
<b>5 Discussion</b>	<b>71</b>
5.1 Results discussion . . . . .	71
5.2 Discussion on the state of the art . . . . .	73
<b>6 Conclusions</b>	<b>75</b>
6.1 Main conclusions . . . . .	75
6.2 Future work . . . . .	77
<b>7 Bibliography</b>	<b>79</b>
<b>A Software registration</b>	<b>83</b>



# Summary

## Introduction

Computed Tomography (CT) has become one of the imaging techniques most used in the field of diagnostic radiology. Since the introduction of the multi-slice CT scanners, a continuous process of technological evolution has made possible a new range of diagnostic applications. These scanners allowed to obtain more anatomical information using advanced dose reduction techniques and to acquire with high resolution in order to improve image quality and reduce artefacts.

But the continuous increase of the number of patients undergoing CT explorations and the impact of clinical applications have implied an exponential increase of the doses due to CT examinations in medicine. This is particularly relevant in some newest explorations that involve high doses, such as CT perfusion (CTP), CT angiography (CTA), dynamic scans (4D CT) and others.

Additionally, the introduction of new CT equipment has introduced several technical advances in recent years, such as a 320 detector-row CT scanner (Aquilion ONE) for cone-beam acquisitions with a volume coverage of 160 mm in a single 0.35 s full rotation. These features lead to a reduction of the scan time and a minimization of the movement artefacts.

With the appearance of the 320 detector-row CT scanners, the existing CT dose metrics had to be revised and new approaches for Computed Tomography dose index (CTDI) dosimetry for cone-beam scanners were suggested. In parallel, some specific CT explorations and acquisitions have been adapted to this scanner since its coverage allowed for imaging of whole organs in a single axial rotation.

According to ALARA principle, radiation doses to patients have to be As Low As Reasonably Achievable. Hence, considering the fast technical advances in x-ray imaging during last years and the increase in the amount of CT examinations, there is a need to be aware about radiation exposure in current acquisition protocols in order to optimize the clinical application of CT and to minimize possible radiation-induced health effects.

There are different methods to estimate doses such as dosimetric studies in anthropomorphic phantoms, Monte Carlo (MC) simulation studies or k-factors that convert the dose-length product (DLP) to effective dose. Besides, several dosimetric software tools have been developed to facilitate the determination of the effective dose and the organ doses from MC data sets.

MC code simulates the radiation transport through voxelized space taking into account the geometry and x-ray characteristics of the CT scanner and compute the energy deposition from interactions of the beam in each voxel of the irradiated phantom.

Hence, this method provides a versatile and accurate tool to estimate organ doses and effective dose in CT examinations. Regarding the literature, several studies about dose assessment in CT using MC simulation-based methods have been published. However, most are based on CT scanners with narrow collimation geometries and mathematical phantoms, becoming outdated with the publication of the latest recommendation from the International Commission on Radiological Protection (ICRP) such as the adult computational phantoms and the commercialization of the new CT contemporary scanners.

For this reason, there is a need to develop methods for patient doses assessment in CT examinations that are up to date with current scanner technology and design, current acquisition protocols and the latest reference in computational phantoms.

## Motivation and objectives

The motivation of this thesis was the development of a MC simulation tool taking into account all relevant technical characteristics of the 320 detector-row cone-beam CT scanner and the latest recommendations of the ICRP with the aim of assessing doses in patients undergoing CT examinations. In this framework, the starting hypothesis of this project is that the use of methods based on MC simulation using the ICRP adult computational phantoms can be a useful tool to estimate patient doses undergoing examinations with a 320 detector-row cone-beam CT scanner.

The main specific objectives of this thesis are:

1. To devise a MC simulation tool for dose assessment that accurately reproduces the 320 detector-row cone-beam CT scanner operation taking into account all parameters that influence dose.
2. To validate the MC program by comparing results from simulations with the actual dose measurements in the scanner.
3. To apply the MC simulation program to assess doses using the ICRP adult computational phantoms. In particular, to calculate organ doses and effective doses of four clinical acquisition CT protocols used in the scanner with and without automatic tube current modulation (TCM).
4. To apply the MC simulation program to assess doses for the cardiac CT protocol performed in a international multicenter study (CORE320) which includes CT calcium scoring, CT coronary angiography and CT myocardial perfusion using the 320 detector-row scanner and the ICRP adult computational phantoms. To study the influence of the positioning of the patient during the cardiac CT scan.
5. To apply the MC simulation program to estimate the patient dose from perfusion CT examinations of the brain, lung tumors and the liver on a 320 detector-row scanner with the ICRP adult computational phantoms.
6. To determine the conversion factors (k-factors) to estimate effective dose from DLP for each CT protocol.
7. To develop a software based on MC simulation to easily assess and report doses for standard patients undergoing CT examinations in a 320 detector-row cone-beam scanner.

## Results

This thesis is compounded from four papers. They described the procedure followed to tailor the scanner model in a MC simulation program, the validation of the MC code, the use of the program for dose estimation in different CT examinations and the development of the dosimetric software tool for dose assessment and reporting.

Paper [I] was focused on the modelling and validation of a MC simulation program for patient dose assessment for a 320 detector-row CT scanner. All the technical features of the scanner were successfully reproduced. The MC program was validated by comparing simulations results with actual dose measurements acquired under the same conditions. Once validated, patient dose assessment was performed for four clinical axial acquisitions using the ICRP adult reference phantoms. The results were nearly always lower than those obtained from other dose calculator tools or published in other studies, which were obtained using mathematical phantoms in different CT systems. The influence on dose of TCM in one of the acquisitions was also analysed, leading to dose decrease and greater uniformity of the dose distributions.

The MC simulation program was used in Paper [II] and Paper [III] in order to estimate organ absorbed dose and effective dose in standard patients for specific CT acquisition protocols. The former evaluated doses from a cardiac CT protocol, including CT calcium scoring, CT coronary angiography and CT myocardial perfusion with a 320 detector-row volumetric CT scanner according to the internationally recognized recommendations of the ICRP. The effect on patient dose of off-centering the patient and the positioning of the arms were evaluated. The latter was focused on perfusion CT examinations. The MC simulation tool was used to calculate the organ doses and the effective dose in the adult reference computational phantoms undergoing CTP Brain, CTP Lung Tumour and CTP Liver studies. Additionally dose assessment was performed for the skin and the eye lens. These CTP protocols performed in a 320 detector-row CT scanner operate safely below threshold doses for deterministic effects. Conversion factors (k-factors) were obtained to estimate effective doses from DLP in both cardiac and perfusion CT protocols. Results showed that in many studies the dose assessment for cardiac and body perfusion acquisitions is performed with a k-factor that underestimates effective doses. Contrarily, dose is overestimated in head examinations.

Finally, the development of a software dosimetric tool for accurate dose assessment in CT with the 320 detector-row cone-beam scanner was described in Paper [IV]. The software, called SimDoseCT, was based on look-up tables generated from MC simulation. By selecting the appropriate acquisition technique through a graphical user interface, the software reports organ absorbed doses and effective doses from all possible acquisitions within the CT scanner, like axial (volumetric), helical and scanogram acquisitions. The validation and testing of the software demonstrated the accurate methodology of SimDoseCT and its usefulness for dose assessment in CT.

## Conclusions

This dissertation presents a framework for dose estimates in standard patients undergoing CT examinations with a 320 detector-row cone-beam scanner. A set of k-factors and also a software dosimetric tool for an accurate estimation of organ absorbed doses and effective doses were created with the aim of improving the easy dose evaluation for

standard adult patients in CT contemporary scanners. The initial intended goals of the study were covered with the methodology and results described in the four papers that constituted this thesis. Future research could be focused on technical extensions in the dosimetric software such as the implementation of the TCM, size-specific dose estimates (SSDE) or paediatric patients. In addition, new studies combining dosimetry with image quality evaluation could be performed for the optimization in CT latest technologies.

# Chapter 1

## Introduction

### 1.1 Computed Tomography

Computed Tomography (CT) was introduced into clinical practice in 1971 by G.N. Hounsfield and J. Ambrose, who conducted the first clinical CT examination based on two contiguous axial images of a patient's head. A few years earlier, Cornack had described a technique for calculating the x-ray attenuation distribution inside the body and he had derived a mathematical theory for image reconstruction. Hounsfield and Cornack were awarded the Nobel Prize for Physiology and Medicine in 1979, which recognised their pioneer work in CT [1, 2].

The technological development of this imaging modality led to new practice examinations in any part of the body such as cardiac CT, CT angiography (CTA), CT perfusion (CTP) or paediatric CT and new techniques including helical acquisitions which were performed in 1989 for the first time. The introduction of multi-slice detector CT (MDCT) systems in 1998 allowed major advances in CT imaging, resulting in a reduction of the rotation time (from several minutes to 0.5 seconds) and in an increase of the volume coverage speed. Besides, the spatial and low-contrast resolution in the CT images has significantly improved over the years. Therefore, the MDCT with sub-second rotation times allows for the scanning of long ranges in shorter scan times and consequently, the capability to acquire images from organs like heart or lungs reducing the movement artifacts. [2, 3].

Nowadays, a wide range of CT scanners are available for different clinical applications. In addition to the scanners used to acquire diagnostic images from different organs or tissues of the body, there are specific scanners for radiation treatment planning in radiotherapy, for guided interventionism or devices that combines CT with other imaging techniques such as magnetic resonance (CT-MRI), positron emission tomography (PET-CT) or single photon emission computed tomography (SPECT-CT) [4].

Computed Tomography has become one of the imaging technique most used in the field of diagnostic radiology. The technological advances during the 1990s led to a strong increase in the number of CT examinations and also a growth in the contribution to collective radiation exposure due to medical examinations. For this reason, dose assessment is of capital importance to improve the optimization of the clinical CT protocols, reducing the radiation risks. [5].

#### 1.1.1 Basic principles of CT

Computed tomography refers to a computerized x-ray imaging procedure based on scanning thin sections of the body with a narrow x-ray beam that quickly rotates



around the body, producing signals that are processed by a computer to generate cross-sectional images. Compared to conventional radiography, which depicts a three-dimensional object as a two-dimensional image, CT stacks all the acquired images together to form a three-dimensional image of the patient that allows for easier identification of basic body structures, distinguishing between tissues with similar densities [3].

The fundamental operation of CT is based on reconstructing an object from its projections. The structures in a CT image are represented using different shades of grey depending on the absorption of photons in their path when running through the object. The photons emitted from the x-ray source interact with different tissues in the body and only a part of them traverse the patient. In order to know the attenuation of each x-ray through the body, the intensity of the beam has to be measured before entering into the object ( $I_0$ ) and also behind it ( $I$ ) by radiation detectors. Then, considering a homogeneous object and monochromatic radiation, the attenuation value ( $\mu$ ) through the distance  $d$  can be calculated using equation 1.1.

$$I = I_0 \cdot e^{-\mu \cdot d} \quad (1.1)$$

The attenuation value that is obtained in only one direction path is not enough for the determination of the spatial distribution of different structures inside a three-dimensional object. For inhomogeneous objects it is necessary to determine the distribution ( $\mu(x, y)$ ). Therefore, it is required to measure the attenuation profiles or projections for successive angular positions. Modern scanners measure between 800 and 1500 projections in each tube rotation [6].

This information, which constitutes the “Radon transform” or sinogram of the image, gives the detector readings as a function of the acquisition angle. An inverse transformation is processed by the computer to determine  $\mu(x, y)$ . But the simple back projection leads to an unsharp image which is not enough to correctly reconstruct the image. To avoid this unsharpening, a high pass filtering procedure like convolution kernel is needed to be applied. The so-called filtered-backprojection (FBP) procedure is used to generate the image, in which the areas with lower attenuation appear in black and when the x-ray beam is completely absorbed by the body, the area on the image is white. The degree of attenuation is measured using the Hounsfield units (HU), assigning the number 0 to distilled water and -1000 to air, being 1000 the number that corresponds to dense bone. Therefore, the HU value is directly related to the linear attenuation coefficient [1, 6].

### 1.1.2 Evolution of CT scanners

The first CT scanner developed by Godfrey Hounsfield and his team at EMI Central Research Laboratories (London) in 1971 corresponds to the design that is referred to as first-generation CT. They were based on a thin x-ray beam 3mm-wide traversing over the patient and collected by the detector. Once measured, the detector was linearly translated to cover the entire object. When the linear measurements finished, the detector rotated 1 degree together with the x-ray tube to acquire the next angular position measurements until a 180 deg arc was covered. Since this procedure took scan times up to 4.5 minutes, image quality was low due to patient motion.

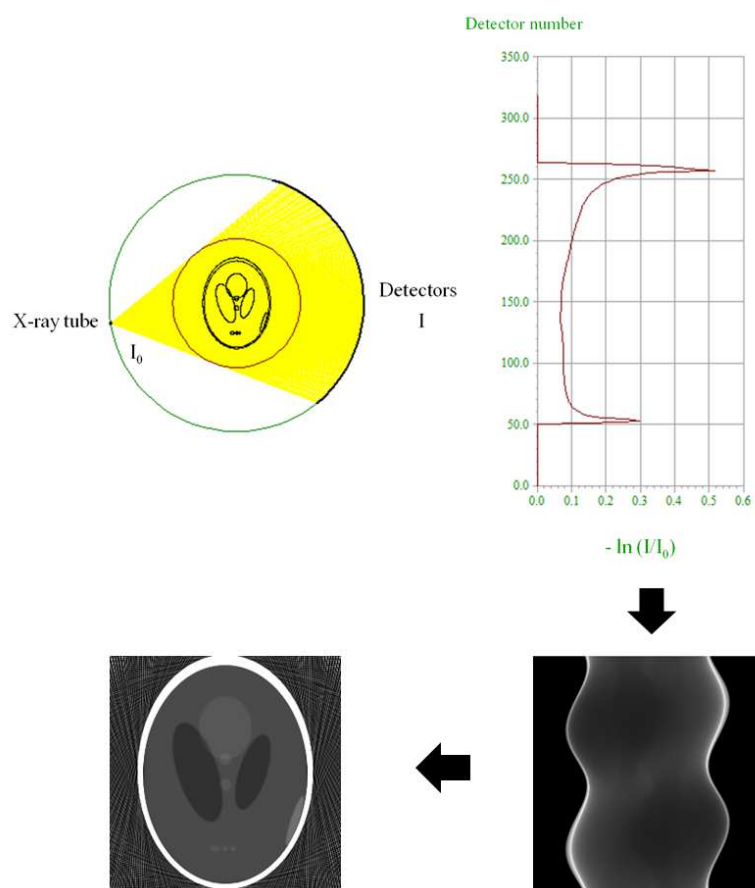


Figure 1.1: Schematic representation of the transmission measurements acquired in a single projection as the tube rotates around the patient. The initial x-ray beam ( $I_0$ ) is attenuated along the path within the Shepp-Logan head phantom. At the other side of the x-ray tube, photons fluence is measured by each detector. The plot of the attenuation, measured as  $-\ln(I/I_0)$ , is used to generate the sinogram and the reconstructed image using the FBP. Adapted from CTSim [7].

In order to reduce scan time, the technological development led to the second-generation CT scanner. In this case, the thin beam used in the old scanners was replaced by a fan-shaped x-ray beam, but it did not cover all the field of view (FOV) either. Then, this was still a translation-rotation scanner, even if it reduced scan times under 20 sec.

The next advances in CT had the same objective as in the previous years: to reduce the scan times. The third-generation CT scanner consisted of a detector array and a fan-shaped beam that covered the entire FOV. The detectors were located on an arc concentric to the x-ray tube and they both could rotate together around the patient. With this progress, the scatter radiation that reaches the detectors decreased and also the reduction of the scan time (2 s per rotation) improved the image quality.

A drawback of the third-generation scanners was the occurrence of artefacts because the same detectors were used repeatedly and a misalignment of a single detector could produce ring artefacts. Even if they are most widely today, the fourth-generation CT scanners were developed, where the detector array is located as an enclosed ring in a 360 deg circle, thereby remains stationary while the x-ray tube rotates with the gantry around the patient. However, the number of detectors in use at any time is controlled

by the beam width. In fact, due to the high number of detectors required and its corresponding electronics, this generation of scanners have become phased out.

In 1998, the introduction of multislice scanners, applied to the third-generation devices, was an important advance in CT technology and its clinical application. This kind of scanners contained 4 active rows and consequently, the speed and the volume coverage increased. A few years later, scanners with 16 and 64 detector rows appeared and in addition to reducing scan time, the spatial resolution improved. These new advances allowed the reconstruction of 3D images with high quality [2–4].

The multislice or multidetector scanners with up to 64 rows (maximum Z coverage of 32 mm) did not allow for acquisition of a entire organ. Therefore, the examination usually consists on helical scan with multiple rotations. In 2007, a 320-multislice scanner, called Aquilion ONE, was introduced by Toshiba. This scanner is a third-generation multidetector CT scanner equipped with 320 x 0.5 mm solid-state detector rows that produce a maximum Z axis coverage of 160 mm at isocenter. The coverage allows for imaging of whole organs in a single axial rotation (Figure 1.2).

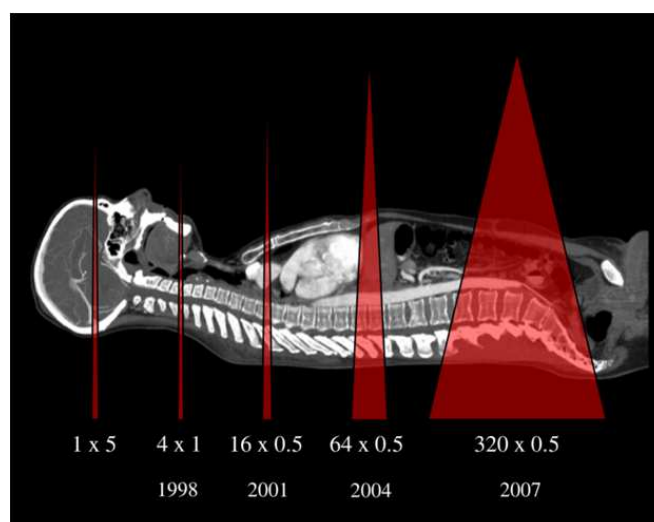


Figure 1.2: Evolution of the Z axis coverage since the beginning of multislice scanners to the introduction of the 320 detector-row cone-beam CT scanner.

## 1.2 The 320 detector-row cone-beam scanner

The 320 detector-row cone-beam CT scanner (Aquilion ONE, Toshiba) (Figure 1.3) in which this study is focused on, operates at sixteen different beam collimations allowing a Z axis coverage of the beam between 2 and 160 mm (i.e. 160, 140, 128, 120, 100, 80, 60, 50, 40, 32, 20, 16, 12, 8, 4 and 2 mm). This dynamic volume CT scanner presents special features such as the ability to capture entire organs in short times, for example the scan of the entire heart in one heartbeat. Moreover, since the overlap required in helical scanning is eliminated, patient exposure dose can be reduced.



Figure 1.3: The 320 detector-row cone-beam CT scanner, Aquilion ONE (Toshiba).

### 1.2.1 Technical specifications

The x-ray tube, with tungsten as anode material, produces the x-rays from a focal spot that allows different sizes (small:  $0.9 \times 0.8 \text{ mm}^2$  or large:  $1.6 \times 1.4 \text{ mm}^2$ ) depending on the acquisition parameters. The x-ray generator voltage range is between 80 and 135 kVp allowing different tube potential options (i.e. 80, 100, 120 and 135 kVp).

The beam generated by the x-ray tube has to be collimated in order to adjust the cone beam to the desired slice width. The use of a focal spot (that is not an ideal point focus) together with the collimator leads to the occurrence of penumbral regions, which makes the XY profile a trapezoid instead of a perfect rectangle. Besides, as a consequence of the broad beam width, an asymmetry appears evident in the Z profile resulting from the anode heel effect. In addition to the filtration provided by the tube itself, the scanner contains flat filters to reduce beam-hardening artefacts and beam shaping filters (or so-called bow tie filters) to modify the x-ray beam intensity inside the FOV thus to reduce the dynamic range of detector signal by compensating for patient's cross-sectional shape. Three different bow tie filters are available in the Aquilion ONE scanner, which corresponds to each FOV: small (240 mm), medium (320 mm) and large (500 mm) [1, 8].

This scanner contains 320 rows with solid-state detectors that transform the incident x-ray intensity into a corresponding electrical signal with the aim of generating the digital image. In the solid-state detectors (scintillators), all the photons reached are absorbed, thereby the efficiency is almost 100%. In front of the detectors, collimators are incorporated to minimize signal contributions from scattered radiation. The set of detectors is curved in the axial plane (XY) and has a rectangular shape along the longitudinal axis (Z) [4].

The gantry, a 72 cm-diameter ring, contains all the technological elements (including the x-ray tube, collimators, filters and detectors) in a rotatory system. The distance from focal spot to isocenter is 60 cm and the distance from focal spot to detectors is 107.2 cm.

The table supports a weight up to 300 kg and allows a movement range of 33–98.8 cm in vertical direction and 20–195 cm longitudinally.

The tube current can be set from 10 to 50 mA in 5 mA steps and from 50 to 580

mA in 10 mA steps. The minimum rotation time is 0.35 s, allowing other time values (i.e. 0.375, 0.4, 0.45, 0.5, 0.65, 0.75, 1.0, 1.5, 2.0 or 3.0 s). The scanner incorporates the adaptive exposure control (SURE Exposure 3D) that allows the modulation of the tube current (TCM) in the XY plane and Z direction. Thus, the system optimizes the radiation exposure required for the acquisition with regard to the natural variations in size, shape and density across different regions of the body between patients.

With the same objective, Aquilion ONE includes the Adaptive Iterative Dose Reduction 3D (AIDR 3D). AIDR is an iterative algorithm that consists on removing background noise while preserving diagnostic information and it results in robust noise reduction, which is essential for achieving ultra-low-dose examinations in routine clinical imaging.

### 1.2.2 Scan modes and clinical applications

The Aquilion ONE CT scanner has two scan modes for cross-sectional imaging with a rotating x-ray tube: an axial (volumetric) or a helical acquisition. In addition, the scanner is able to perform dynamic volume scans. With the acquisition options offered by Aquilion ONE, several advanced clinical applications are allowed.

The CT scan is always preceded by a projection imaging with a static x-ray tube for planning purposes, which is referred to as a scanogram. The scanner performs two orthogonal low-dose scanograms (frontal and lateral views) using a beam width of 2 mm and with the patient table in continuous movement in order to fix the start and end position of the acquisition and estimate the tube current depending on the size of the patient.

The volume scan (axial) is based on one single complete rotation of the x-ray tube without movement of the table. Since Aquilion ONE allows a coverage up to 160 mm, entire organs like the brain and the heart can be scanned in a single axial scan.

When the scan range exceeds 160 mm, scanning is performed as a set of axial acquisitions until covering all the volume of interest while patient table is moved before each shot. The multiple data sets are automatically combined to a wide volume.

For the helical mode, the x-ray tube is continuously rotating around the patient with constant output while the table is moving at constant speed through the gantry. The acquisition parameters (i.e. table speed ( $s$ ), rotation time ( $t$ ), collimation ( $b$ ) and number of simultaneous acquired sections ( $N$ )) determine the CT pitch factor ( $p$ ) defined in equation 1.2.

$$p = \frac{s \cdot t}{b \cdot N} \quad (1.2)$$

For an overlapping acquisition, the CT pitch factor is smaller than 1 and for an acquisition with interspaces it is larger than 1. A pitch factor of 1 yields a contiguous acquisition [1, 4].

Dual energy helical scanning is also allowed in the Aquilion ONE scanner. This acquisition alternates between high and low kV in each gantry rotation. The fact of producing photons with different energies provides additional information about the materials with different attenuation [3].

Dynamic volume scan is used to record temporal changes in the attenuation characteristics of the object examined. In clinical applications the assessment of contrast medium dynamics into regions of the body is of the greatest interest. For example blood flow dynamics can be assessed and quantified with perfusion software in head examinations, lung function can be observed during free breathing in chest examinations and blood flow can be observed during the injection of contrast in angiography examinations.

Aquilion ONE introduced some low-dose advanced clinical applications compared to other scanners. One of them is myocardial perfusion combined with coronary CTA, in which the whole-head acquisition in a single rotation allows the identification of coronary arteries responsible for ischemia. Another application is brain or body perfusion in which the blood perfusion of an organ can be analysed from dynamic scan images providing additional information for the diagnosis.

### 1.3 CT Dosimetry

According to ALARA principle of keeping radiation doses to patients As Low As Reasonably Achievable, there is an interest in the development of methods to evaluate patient doses in CT examinations with the goal of optimising radiation exposure without compromising the required image quality for a correct diagnostic.

Currently, metrics in CT dosimetry are based on CTDI concepts. The CTDI is a measure of the average dose in the scanned region normalized to a tube current time product. The first definition was advanced by the Food and Drug Administration in the USA (FDA) in the late 1970s [9]. The CTDI is derived from measurements in two cylindrical polymethylmethacrylate CT dosimetry phantoms representing the attenuation of respectively the adult head (16 cm diameter PMMA) or the body (32 cm diameter PMMA). The phantoms contain one central and four peripheral holes in which a 100 mm long ionization chamber is inserted. The five CTDI measurements were used to yield one CTDI value, called the weighted CTDI ( $CTDI_w$ ), with the weighting factors for deriving  $CTDI_w$  being respectively 1/3 for the centre CTDI and 2/3 for the averaged peripheral CTDI. With the introduction of helical CT scanners, the volume CTDI ( $CTDI_{vol}$ ), defined as  $CTDI_w$  divided by the helical pitch, was developed to take into account the effect of the helical pitch used in the irradiation.

But when new CT scanners with maximum nominal beam width exceeding the 100 mm length of the standard ionization chamber appeared, the definition of CTDI had to be updated [8] (Figure 1.4). Therefore, in 2009 the International Electrotechnical Commission (IEC) adapted the definition of CTDI for use in wide cone beam scanners, by limiting the denominator to 100 mm, even when the product  $N \cdot T$  exceeds 100 mm [10]:

$$CTDI_{100} = \frac{1}{\min\{N \cdot T, 100mm\}} \int_{-50mm}^{50mm} D(z) dz \quad (1.3)$$

where  $\min\{\}$  is the ‘min operation’ which gives the smallest of the two numbers  $N \cdot T$  (mm) or 100 (mm). In the case of the 320 detector row Aquilion ONE scanner, the

denominator must be 100 mm instead of 160 mm (320 detectors  $\times$  0.5 mm). In fact, for a beam width of 160 mm, this dose quantity should not be referred to as CTDI but as average dose ( $D_{100,w,avg}$ ) [8].

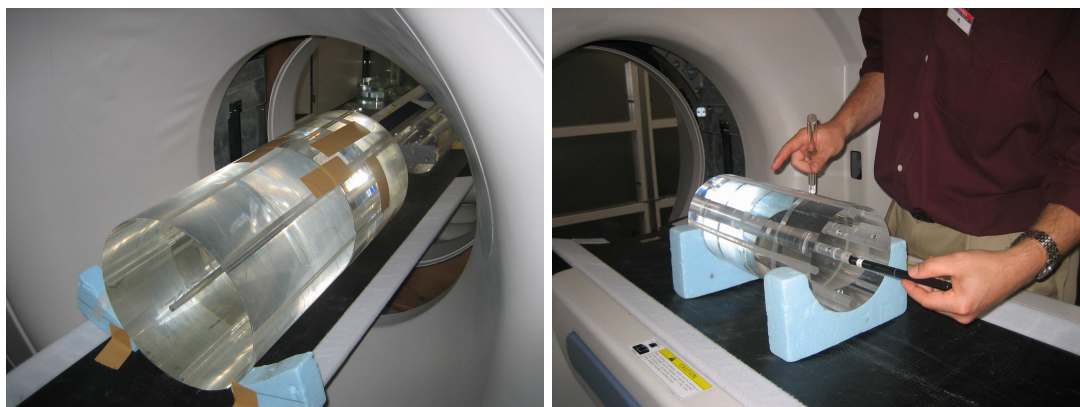


Figure 1.4: Measurement of CTDI within a body (left) and a head (right) PMMA phantoms in a 320 detector-row cone-beam CT scanner.

Statements of  $CTDI_{vol}$  values are obligatory for each CT exam and are required to be provided by the manufacturers on the CT scanner console. Since  $CTDI_{vol}$  does not take into account the scanned range, the dose-length product (DLP) (in  $mGy \cdot cm$ ) is used to obtain a first estimate of the dose characterising a complete examination. The DLP is calculated by multiplying the  $CTDI_{vol}$  (in  $mGy$ ) by the length of the exposed range (in  $cm$ ) [5].

However, these quantities are determined using cylindrical phantoms and only provide rough estimates of patient dose levels involved in the examination. According to the International Commission on Radiological Protection (ICRP) [11], the effective dose (E) is the best available dose descriptor since it takes into account the radiation-induced health effects and consequently, it allows a comparison between different techniques in diagnostic radiology.

## 1.4 Patient dose estimation

There are different methods to estimate the effective dose and numerous studies of patient dose can be found in the literature. The dosimetric studies using detectors such as thermoluminescent dosimeters (TLD) or metal oxide semiconductor field-effect transistors (MOSFET) on anthropomorphic phantoms improved the CTDI dosimetry in homogeneous cylindrical phantoms. However, they required reference calibration and energy corrections and since they are considered “point” measurements, they can not probably be extrapolable to the entire organs or the whole body [12].

In order to be able to make more precise dose estimates, calculations performed with Monte Carlo (MC) simulation method are widely used in several studies. Computations that use MC methods follow the paths of a large number of x-rays as they interact with a computational phantom and perform the interaction processes depending on the probability. In fact, the MC program simulates the radiation transport through voxelized objects (i.e. organs and tissues). The simulation of photons transport in

the energy range typical for CT scanners is based on processes of Rayleigh scattering, Compton scattering and photoelectric effect and the associated creation of fluorescent photons or Auger electrons. There are different commonly used and well-established MC packages such as EGS, PENELOPE, MCNP or GEANT. From the simulations, the total energy absorbed in the voxels was divided by the corresponding mass to calculate the (average) absorbed dose in the regions of interest such as tissues and organs.

MC simulations need to be validated before their results can be trusted. Ideally, MC-based computer programs are validated by generating a simulation that replicates an empirical test and then by comparing simulation and empirical results. For this reason, a detailed knowledge of the scanner features and characteristics of the x-ray beam (tube voltage and primary filtration, bow tie filter, heel effect, beam width, penumbra, rotation, tube charge) is required. Since data about the scanner are not easy to be provided by the manufacturer, necessary information for the MC simulation is usually obtained from indirect measurements [13, 14].

When MC simulations are performed, computational phantoms are used as a mathematical representation of the human body to track the radiation interactions and energy deposition in the body. The very simple phantoms (i.e. cylindrical phantoms) preceded the Medical Internal Radiation Dose (MIRD) phantom, that was developed by Oak Ridge National Laboratory (ORNL) in 1960s. It was the first anthropomorphic phantom representing a hermaphrodite adult for internal dosimetry and it describes human anatomy by using simple mathematical equations of analytical geometry. Several improved mathematical phantoms such as male and female adults, paediatric series, and enhanced organ models have been developed following the first hermaphrodite adult phantom. However, since mathematical phantoms provide only approximations of the true anatomical features of the human body, alternative voxel phantoms based on three-dimensional imaging techniques such as magnetic resonance (MR) and CT appeared [15]. Due to the wide range of voxel phantoms derived from the first MIRD phantoms, ICRP worked for developing the voxel reference phantoms with the aim of unifying dosimetric studies. Two voxel phantoms representing the standard adult female (AF) and adult male (AM) were developed to provide a more realistic and accurate representation of human anatomy [16]. The voxel phantoms represent an average female (height 163 cm, weight 60 kg, body mass index (BMI) 22.6 kg/m<sup>2</sup>) and an average male (height 176 cm, weight 73 kg, BMI 23.6 kg/m<sup>2</sup>) [17].

MC simulations have provided alternative methods to estimate the patient doses. The DLP-to-E conversion factors (the so-called k-factors) allows the estimation of the effective dose from the DLP value. Since effective dose can be obtained from MC simulations and DLP is derived from CTDI<sub>vol</sub>, the ratio of DLP-to-E can be given for respective anthropomorphic voxel phantoms [18]. It has to be noted that these conversion factors are only useful to estimate effective dose since they do not take the patient size into account and do not provide organ absorbed dose values. [5].

In order to give more complete information, several dosimetric software tools have been developed to facilitate the determination of the effective dose and the organ doses from pre-calculated tables derived from MC simulations. They all rely on the calculation of the total dose in each organ by adding the dose contribution of single slabs belonging in a specified scan range [5]. However, the existing software today, i.e. ImpactDose [19], CT-Expo [20], Waza-Ari [21, 22], ImPACT [23] and Virtual Dose [24], are based on pre-calculated tables with doses from outdated mathematical phantoms and scanners from the late 1980s.





## Chapter 2

# Motivation, hypothesis and objectives

The arrival of new CT equipment has introduced many technical peculiarities in recent years, such as a 320 detector-row CT scanner (Aquilion ONE) for cone-beam acquisitions. From the appearance of Aquilion ONE, some reference dose quantities have had to be reconsidered. Moreover, some specific CT explorations and studies have been emerged considering the special features of this scanner. Hence, there is a need for dose assessment in CT examinations with the 320 detector-row cone-beam CT scanner.

For this reason, the motivation of this thesis was the development of a MC simulation-based tool taking into account all relevant technical characteristics of the 320 detector-row cone-beam CT scanner and the latest recommendations of the ICRP with the aim of assessing doses in patients undergoing CT examinations. Since most current software for reporting doses are based on outdated scanners or inaccurate mathematical phantoms, this study planned on develop a tool for an accurately organ and effective doses estimation in latest CT technology such as the 320 detector-row cone-beam scanner using the adult reference computational phantoms from the ICRP.

In this framework, the starting hypothesis of this project is that the use of methods based on MC simulation using the ICRP adult computational phantoms can be a useful tool to estimate patient doses undergoing examinations with a 320 detector-row cone-beam CT scanner.

The main specific objectives of this thesis are:

1. To devise a MC simulation tool for dose assessment that accurately reproduces the 320 detector-row cone-beam CT scanner operation taking into account all parameters that influence dose.
2. To validate the MC program by comparing results from simulations with the actual dose measurements in the scanner.
3. To apply the MC simulation program to assess doses using the ICRP adult computational phantoms. In particular, to calculate organ doses and effective doses of four clinical acquisition CT protocols used in the scanner with and without automatic tube current modulation.
4. To apply the MC simulation program to assess doses for the cardiac CT protocol performed in a international multicenter study (CORE320) which includes CT calcium scoring, CT coronary angiography and CT myocardial perfusion using

the 320 detector-row scanner and the ICRP adult computational phantoms. To study the influence of the positioning of the patient during the cardiac CT scan.

5. To apply the MC simulation program to estimate the patient dose from perfusion CT examinations of the brain, lung tumors and the liver on a 320 detector-row scanner with the ICRP adult computational phantoms.
6. To determine the conversion factors (k-factors) to estimate effective dose from DLP for each CT protocol.
7. To develop a software based on MC simulation to easily assess and report doses for standard patients undergoing CT examinations in a 320 detector-row cone-beam scanner.

## Chapter 3

# PhD thesis outline

This thesis presents a collection of four papers, which have been published in peer-reviewed scientific journals, in the field of medical physics and radiology.

- [I] Salvadó M, Cros M, Joemai RMS, Calzado A, Geleijns J. Monte Carlo simulation of the dose distribution of ICRP adult reference computational phantoms for acquisitions with a 320 detector-row cone-beam CT scanner. *Phys Med* 2015;31:452-462 (DOI: 10.1016/j.ejmp.2015.04.007)
- [II] Geleijns J, Joemai RMS, Cros M, Hernandez-Giron I, Calzado A, Dewey M, Salvadó M. A Monte Carlo simulation for the estimation of patient dose in rest and stress cardiac computed tomography with a 320-detector row CT scanner. *Phys Med* 2015;31:1029-34 (DOI: 10.1016/j.ejmp.2015.08.008)
- [III] Cros M, Geleijns J, Joemai RMS, Salvadó M. Perfusion CT of the brain and liver and of lung tumors: Use of Monte Carlo simulation for patient dose estimation for examinations with a cone-beam 320-MDCT scanner. *Am Jour Roentgenol* 2016;206:129-35 (DOI: 10.2214/AJR.15.14913)
- [IV] Cros M, Joemai RMS, Geleijns J, Molina D, Salvadó M. SimDoseCT: dose reporting software based on Monte Carlo simulation for a 320 detector-row cone-beam CT scanner and ICRP computational adult phantoms. *Phys Med Biol* 2017 (DOI: doi.org/10.1088/1361-6560/aa77ea)

After a general introduction in Chapter 1, the motivation of this thesis and the objectives are described in Chapter 2. The four papers are gathered in Chapter 4 and are presented in chronological order of development and publication. They are organised in three different sections.

The first section is formed by Paper [I], which describes the modelling of a 320 detector-row cone-beam scanner to develop and validate a MC simulation program for patient dose assessment based on the ICRP anthropomorphic adult reference computational phantoms. Dose assessment for four clinical acquisition general protocols is also included.

Paper [II] and Paper [III] constitute a section that deal with dose assessment in specific studies with the 320 detector-row cone-beam scanner following the recommendations of the ICRP. They provide organ doses and effective dose from a cardiac CT acquisition protocol and from perfusion CT examinations of the brain, lung tumors and liver, respectively.

The last section of Chapter 4 includes Paper [IV], which describes the development and test of software for dose assessment in standard patients undergoing CT examinations in a 320 detector-row cone-beam scanner. The software is based on pre-calculated tables that provides organ and effective doses from MC simulations for the ICRP adult reference phantoms.

Finally, a general discussion on the results from the different papers together with a discussion on the state of the art is presented in Chapter 5. Main conclusions of the thesis and future work related to the present study are stated in Chapter 6.

## Chapter 4

# Materials, methods and results

This chapter presents the main part of the thesis, which is composed of the following four papers. They are organized in sections of the present chapter and they follow the chronological order of publication that also corresponds to the methodological order in the development of the thesis. The papers are referred to using capital Roman numerals in the text.

- [I] Salvadó M, Cros M, Joemai RMS, Calzado A, Geleijns J. Monte Carlo simulation of the dose distribution of ICRP adult reference computational phantoms for acquisitions with a 320 detector-row cone-beam CT scanner. *Phys Med* 2015;31:452-462 (DOI: 10.1016/j.ejmp.2015.04.007)
- [II] Geleijns J, Joemai RMS, Cros M, Hernandez-Giron I, Calzado A, Dewey M, Salvadó M. A Monte Carlo simulation for the estimation of patient dose in rest and stress cardiac computed tomography with a 320-detector row CT scanner. *Phys Med* 2015;31:1029-34 (DOI: 10.1016/j.ejmp.2015.08.008)
- [III] Cros M, Geleijns J, Joemai RMS, Salvadó M. Perfusion CT of the brain and liver and of lung tumors: Use of Monte Carlo simulation for patient dose estimation for examinations with a cone-beam 320-MDCT scanner. *Am Jour Roentgenol* 2016;206:129-35 (DOI: 10.2214/AJR.15.14913)
- [IV] Cros M, Joemai RMS, Geleijns J, Molina D, Salvadó M. SimDoseCT: dose reporting software based on Monte Carlo simulation for a 320 detector-row cone-beam CT scanner and ICRP computational adult phantoms. *Phys Med Biol* 2017 (DOI: doi.org/10.1088/1361-6560/aa77ea)



## 4.1 Scanner modelling and validation of the simulation program

- [I] Salvadó M, Cros M, Joemai RMS, Calzado A, Geleijns J. Monte Carlo simulation of the dose distribution of ICRP adult reference computational phantoms for acquisitions with a 320 detector-row cone-beam CT scanner. *Phys Med* 2015;31:452-462 (DOI: 10.1016/j.ejmp.2015.04.007)

### Abstract

*Purpose:* The purpose of this study was to develop and validate a Monte Carlo (MC) simulation tool for patient dose assessment for a 320 detector-row CT scanner, based on the recommendations of International Commission on Radiological Protection (ICRP). Additionally, the simulation was applied on four clinical acquisition protocols, with and without automatic tube current modulation (TCM).

*Methods:* The MC simulation was based on EGS4 code and was developed specifically for a 320 detectorrow cone-beam CT scanner. The ICRP adult reference phantoms were used as patient models. Dose measurements were performed free-in-air and also in four CTDI phantoms: 150 mm and 350 mm long CT head and CT body phantoms. The MC program was validated by comparing simulations results with these actual measurements acquired under the same conditions. The measurements agreed with the simulations across all conditions within 5 %. Patient dose assessment was performed for four clinical axial acquisitions using the ICRP adult reference phantoms, one of them using TCM.

*Results:* The results were nearly always lower than those obtained from other dose calculator tools or published in other studies, which were obtained using mathematical phantoms in different CT systems. For the protocol with TCM organ doses were reduced by between 28 and 36%, compared to the results obtained using a fixed mA value.

*Conclusions:* The developed simulation program provides a useful tool for assessing doses in a 320 detector-row cone-beam CT scanner using ICRP adult reference computational phantoms and is ready to be applied to more complex protocols.







## Original paper

## Monte Carlo simulation of the dose distribution of ICRP adult reference computational phantoms for acquisitions with a 320 detector-row cone-beam CT scanner

M. Salvadó <sup>a,\*</sup>, M. Cros <sup>a</sup>, R.M.S. Joemai <sup>b</sup>, A. Calzado <sup>c</sup>, J. Geleijns <sup>b</sup>

<sup>a</sup> Faculty of Medicine and Health Sciences, Universitat Rovira i Virgili, C/Sant Llorenç, 21, 43201 Reus, Spain

<sup>b</sup> Radiology Department, Leiden University Medical Center, Albinusdreef 2, 2333 ZA Leiden, The Netherlands

<sup>c</sup> Radiology Department, Universidad Complutense de Madrid, Avenida Complutense, 28040 Madrid, Spain



## ARTICLE INFO

## Article history:

Received 1 December 2014

Received in revised form

5 March 2015

Accepted 12 April 2015

Available online 8 May 2015

## Keywords:

Monte Carlo simulation  
Computed Tomography dose assessment  
ICRP adult reference computational  
phantoms  
320 Detector-row cone beam CT scanner

## ABSTRACT

**Purpose:** The purpose of this study was to develop and validate a Monte Carlo (MC) simulation tool for patient dose assessment for a 320 detector-row CT scanner, based on the recommendations of International Commission on Radiological Protection (ICRP). Additionally, the simulation was applied on four clinical acquisition protocols, with and without automatic tube current modulation (TCM).

**Methods:** The MC simulation was based on EGS4 code and was developed specifically for a 320 detector-row cone-beam CT scanner. The ICRP adult reference phantoms were used as patient models. Dose measurements were performed free-in-air and also in four CTDI phantoms: 150 mm and 350 mm long CT head and CT body phantoms. The MC program was validated by comparing simulations results with these actual measurements acquired under the same conditions. The measurements agreed with the simulations across all conditions within 5%. Patient dose assessment was performed for four clinical axial acquisitions using the ICRP adult reference phantoms, one of them using TCM.

**Results:** The results were nearly always lower than those obtained from other dose calculator tools or published in other studies, which were obtained using mathematical phantoms in different CT systems. For the protocol with TCM organ doses were reduced by between 28 and 36%, compared to the results obtained using a fixed mA value.

**Conclusions:** The developed simulation program provides a useful tool for assessing doses in a 320 detector-row cone-beam CT scanner using ICRP adult reference computational phantoms and is ready to be applied to more complex protocols.

© 2015 Associazione Italiana di Fisica Medica. Published by Elsevier Ltd. All rights reserved.

## Introduction

Technological developments and improved performance has led to an increase in the number of clinical indications for CT. Consequently, the collective radiation exposure of patients has considerably increased. Concerns regarding the potential radiation risks posed by CT imaging are reflected in the initiatives and actions of professional organizations and scientific societies and have prompted the search for methods to determine and control patient radiation exposure levels without compromising diagnostic efficacy.

The current practices for patient dose assessment in medical x-ray imaging should keep pace with advances in imaging technology and the most recent recommendations for radiation protection. This applies particularly to the so-called 'high-end' CT scanners, such as the 320 detector-row CT scanner (Aquilion ONE, Toshiba Medical Systems, Otawara-shi, Japan) that operates with a 160 mm wide cone beam coverage [1,2]. The cone beam design of this scanner already led to a revision of the classical dosimetric concept of Computed Tomography Dose Index (CTDI) [3,4].

The specific design of the CT scanner can be modeled within Monte Carlo (MC) simulation software for patient dose assessment while accounting for all of the features that influence dose. MC simulations can be performed on voxelized anthropomorphic phantoms that realistically describe and reproduce human anatomy. To date, these voxelized anthropomorphic phantoms have not

\* Corresponding author.

E-mail address: [m.salvado@urv.cat](mailto:m.salvado@urv.cat) (M. Salvadó).

been implemented for CT, neither have methods been developed that accurately assess patient doses in the 320 detector-row cone-beam CT scanner.

The primary goal of this study was to devise a MC simulation software for dose assessment that reproduces the design of a 320 detector-row cone-beam CT scanner. Furthermore, our aim was to integrate International Commission on Radiation Protection (ICRP) computational voxel phantoms into the simulation program. The developed and validated MC simulation program was applied to assess the organ doses and effective doses of four clinical acquisition protocols with and without automatic tube current modulation (TCM).

## Materials and methods

### The CT scan

An Aquilion ONE CT scanner (Toshiba Medical Systems, Otawara, Japan) was used in this study. This scanner is a 3rd generation multi-detector CT scanner equipped with  $320 \times 0.5$  mm solid-state detector rows that produce a maximum Z axis coverage of 160 mm. The coverage allows for imaging of whole organs in a single axial rotation. The tube potential options are 80, 100, 120 and 135 kVp. The tube current can be set from 10 to 50 mA in 5 mA steps and from 50 to 580 mA in 10 mA steps. The rotation time is 0.35, 0.375, 0.4, 0.45, 0.5, 0.65, 0.75, 1.0, 1.5, 2.0 or 3.0 s. The unit has three beam shaping filters (i.e., small, medium and large bow tie filters) to modify the x-ray beam intensity inside the field of view (FOV) thus to reduce the dynamic range of detector dose by compensating for patient's cross-sectional shape. Each bow tie filter corresponds to a different FOV. The distance from focal spot to isocenter is 600 mm, and the distance from focal spot to detector is 1072 mm.

### Dose measurements

Dose measurements in standard CT dose phantoms and also free-in-air were required to characterize the scanner. Free-in-air dose measurements using a 100 mm long CT ionization chamber (Capintec Inc., Ramsey, New Jersey, USA) were performed as stationary scans at the isocenter and at varying vertical distances off-axis with the x-ray tube fixed in the gantry (lateral position) and the chamber aligned parallel to the Z-axis. Similarly, Z-axis dose measurements were performed by positioning the chamber at the isocenter parallel to Y-axis and moving it along the Z-axis.

Dose measurements were conducted in two standard CT dose phantoms (160 mm diameter for the head phantom and 320 mm diameter for the body phantom, both with a length of 150 mm) using a 100 mm long CT ionization chamber. Additionally two CT dose phantoms with an extended length of 350 mm (same diameters as the standard phantoms) were used with a 300 mm long CT pencil ionization chamber (CT-110, Applied Engineering Inc., Japan) [4].

The dose measurements were performed using a nominal beam width of 160 mm for all available combinations of tube voltages and bow tie filters. The ionization chambers were appropriately calibrated, and the readings were corrected for the actual air temperature and pressure during the measurements. The estimated uncertainties associated with the measurements of the ionization chambers were  $\pm 5\%$ .

The reference dose quantities  $CTDI_{100}$  and  $CTDI_{300}$  were adopted according to the definitions of the IEC [5] and the IAEA [3], which account for collimation widths larger than 100 mm:

$$CTDI_{length} = \frac{1}{\min\{N \times T, length\}} \int_{-length/2}^{+length/2} D(z) dz \quad (1)$$

where  $T$  is the nominal section thickness,  $N$  is the number of contiguous sections acquired in a single axial scan,  $N \times T$  is the nominal collimation width,  $length$  is the active length of the CT ionization chamber (100 mm and 300 mm),  $D(z)$  is the absorbed dose in air at position  $z$  in a single axial scan, and the denominator is the 'min operation' which provides the smallest of the two numbers  $N \times T$  (mm) or  $length$ . Following IAEA recommendations for a beam width of 160 mm, the  $CTDI_{100}$  dose quantity is referred to as average dose  $D_{100,avg}$ .

Weighted CT dose index values in both standard and extended CT dose phantoms, respectively  $D_{100w,avg}$  and  $CTDI_{300w}$ , were calculated using weighting factors of 1/3 for the center position and 2/3 for the average of four peripheral positions. The dose length product (DLP) was derived by multiplying  $D_{100w,avg}$  and the length of the scanned range.

### Monte Carlo simulation of radiation transport and CT system modeling

The software that was developed for MC calculations is based on Electron Gamma Shower V4 (EGS4) code [6] in combination with the Low Energy Photon Scattering Expansion (National Laboratory for High Energy Physics (KEK), Japan) [7]. The program simulates the radiation transport through voxelized objects or phantoms, and it is an adapted version of software that was used for dose calculation in another CT system [8–10] and for dental cone beam CT for oral and maxillofacial radiology purposes [11,12]. The simulation of photons transport in the energy range typical for CT scanners is based on processes of Rayleigh scattering, Compton scattering and photoelectric effect and the associated creation of fluorescent photons or Auger electrons. A cut-off energy of 5 keV was used for photon transport, and a cut-off energy of 30 keV was used for electrons.

The software was adapted according to the specifications of the Aquilion ONE CT scanner. The MC program simulates all aspects that influence dose distribution during a CT scan, including characteristics of the x-ray beam (tube voltage and primary filtration, bow tie filter, heel effect, beam width, penumbra, rotation and tube charge) and patient support table (shape, size and material).

A catalogue of x-ray spectra was used to generate spectra for different tube voltages (80, 100, 120 and 135 kV) and for the actual total equivalent filtration, anode material (tungsten), ripple (0%) and anode angle ( $15^\circ$ ) [13]. The total equivalent filtration at the central axis of the beam was derived from the measured half-value layers (HVL) at the isocenter for each combination of bow tie filter and tube voltage [4]. The energy spectrum was described in discrete values that were produced in intervals of 0.5 keV. The MC technique assigns a different initial energy to each photon based on the probabilities obtained from these spectra. For each simulated history (i.e., each photon), the initial position in the focal spot was randomly selected (focal spot sizes:  $0.9 \times 0.8$  or  $1.6 \times 1.4$  mm<sup>2</sup>). Furthermore, the initial angle of the photon was randomly selected within a restricted angular range that corresponded to the actual field dimensions.

A variance reduction technique was applied to model bow tie filters as relative attenuation profiles in axial plane and along the rotation axis [14,15]. Attenuation profiles were derived from free-in-air dose measurements in the axial plane and Z-axis. Dose

readings at each point were normalized to the value measured at the isocenter after correcting for distance. Finally, polynomial fits as a function of photon emission angle were calculated for the axial and Z-axis profiles.

The entire process was applied to four tube voltages and three different bow tie filters which corresponds to each FOV: large (500 mm), medium (320 mm) and small (240 mm). Thus, the simulation properly reproduced the x-ray beam including heel effect and penumbra. The actual beam width along the axis of rotation was measured with Gafchromic XR-QA Dosimetry Film (International Specialty Products Inc. (ISP), Wayne, New Jersey, USA).

Tube current modulation (TCM) compensates for differences in the attenuation under different acquisition angles by tailoring the tube current (mA) to the different projection angles. This process allows for the optimization of the acquisition with regard to the natural variations in size, shape and density across different regions of the body or between patients [16]. To reproduce the TCM, the simulation program obtained the tube current for each projection angle in steps of 1° from a numerical input file.

Radiation transport was simulated through voxelized 3D spaces that contain the CT dose phantoms or the ICRP male or female voxel phantoms. The patient support table was also included in the MC simulation. The appropriate properties, including density and chemical composition, were assigned to voxels. The calculated absorbed energy in each voxel was used to generate three-dimensional energy distributions. The total energy absorbed in the voxels was divided by the corresponding mass to calculate the (average) absorbed dose in the regions of interest such as ionization chambers, tissues and organs.

The simulations were performed in a supercomputing center (CSUC) that employed a Bull NovaScale computing cluster (Bull SAS, Les Clayes-sous-Bois, France) with 88 Xeon 4-core processors (Intel Corporation, Santa Clara, California, USA) in 22 nodes with 1.6 TB of primary memory and 52.6 TB of disk storage memory and a peak performance of 4.05 Tflop/s. Each simulation was performed using 20 million photon histories, and the average computation time was 20 min.

#### MC program adjustment and validation

The MC program was validated by comparing the simulations with the actual dose measurements in standard CT dose phantoms acquired under same conditions.

MC simulations were performed and absorbed doses were calculated within the central and peripheral cavities of four voxelized phantoms; i.e., two CT head dose phantoms and two CT body dose phantoms with lengths of 150 mm and 350 mm.

The pencil ionization chambers were modeled as two concentric cylinders consisting of air (inner cylinder, 7 mm in diameter) and C552 air-equivalent material (outer cylinder, up to 10 mm in diameter) with lengths of 100 and 300 mm, respectively. These cylinders represent the air cavity and the chamber wall. The relative uncertainties associated with the dose calculations were 4–5% [12].

For each tube voltage and bow tie filter combination, the ratios of measured to simulated values for the CTDI in the phantoms, under the same conditions, were used to convert the simulated relative energy distributions into absolute energy values.

#### ICRP adult reference voxel phantoms

Anthropomorphic voxel phantoms of the ICRP [17] were derived from CT scans of humans. In fact, these phantoms are an evolution of two voxel phantoms known as Laura and Golem [18,19]. ICRP recommendation provides the mass, spatial distribution and

composition of each organ and tissue for the standard adult male (AM) and adult female (AF). The whole body phantoms are represented by three-dimensional arrays of voxels. Table 1 provides the main anatomical information and data related to the ICRP phantoms.

Each voxel phantom was incorporated into the simulation program as three 3D matrices; one matrix had labels for the 141 organs or tissues, one had labels for the 53 materials (including air outside the body and the patient support table), and one had labels for the 29 organs that contribute to the effective dose. Figure 1 shows the coronal and sagittal views for the different materials and the different organs of the AF and AM voxel phantoms and the corresponding 3D surface view.

Specific considerations are required for dose calculations for tissues with red bone marrow (RBM) or endosteum (bone surface) because the dimensions of the trabeculae (the cavities containing bone marrow and endosteum) have a microscopic structure that is smaller than the size of a voxel. Because these volumes could not be correctly segmented in the voxel phantoms [20], 44 categories of skeletal tissue composed of 20 different materials were implemented according to their specific mass fractions of RBM, yellow bone marrow (YBM) and endosteum. To obtain the doses in the organs with spongiosa, the program calculates the absorbed energy fractions in the RBM and endosteum. For this purpose, when a photon transfers energy in one of these skeletal voxels (with homogeneous compositions of different mixtures of endosteum, RBM and YBM), the program calculates the contribution to the absorbed energy in the RBM by multiplying the absorbed energy in this voxel by the RBM attenuation fraction (which depends on the mass fraction and the mass energy-absorption coefficients) [21]. The contributions to the absorbed energy in the endosteum were calculated following the same procedure. To compute the energy in the whole RBM (or endosteum), the contributions of all of the simulated interactions in all voxels were considered.

Additionally, the implementation of bone dosimetry also required special care because secondary particles that are released from mineral bone components (i.e., cortical bone and trabecular bone) can deposit their energies into the RBM and endosteum. This energy effect is implemented in the simulation program by an enhancement factor, which depends on the energy of the interacting photon and the bone category according to the trabecular or RBM content of the bone in each voxel [22]. During the simulation, the enhancement factors were derived from polynomial equations, and the energy absorbed by the bone was corrected for in terms of excess doses from secondary particles by multiplying the absorbed energy and the enhancement factor.

#### Clinical acquisition protocols and tube current modulation (TCM)

The MC program was used to simulate volumetric axial CT scans. Table 2 shows the corresponding acquisition parameters for four

**Table 1**  
Main characteristics of the standard adult male and female voxel phantoms of the ICRP Publication 110 [16].

	AM phantom	AF phantom
Gender	Male	Female
Age (years)	38	43
Height (cm)	178	168
Mass (kg)	73	60
Number of voxels per slab	254 × 127	299 × 137
Number of slabs	222	348
Voxel size (mm <sup>3</sup> )	2.137 × 2.137 × 8	1.775 × 1.775 × 4.84

AM, adult male; AF, adult female.

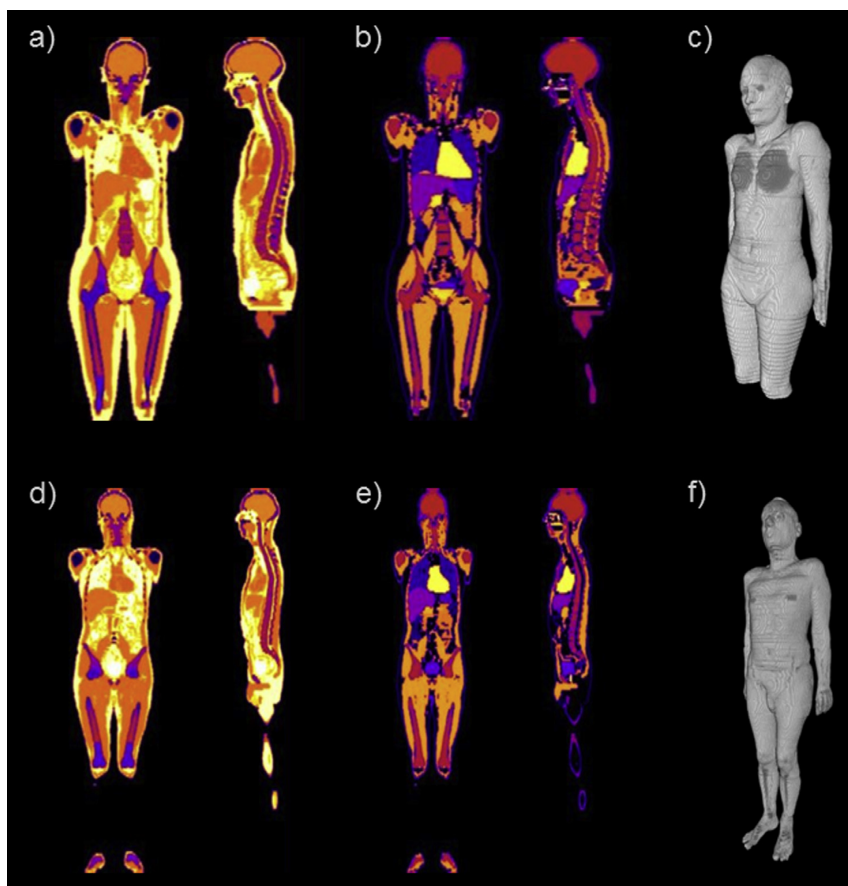


**Figure 1.** Top: the adult female phantom (AF); bottom: the adult male phantom (AM). From left to right: coronal (a) and sagittal (d) views showing the different materials in different colors, coronal (b) and sagittal (e) views showing the different organs with weighting factors that contribute to the effective dose, and 3D surface views (c and f). Phantoms have been arbitrarily colored for illustration purposes.

clinical CT examinations. All protocols used one full rotation. The ICRP voxel phantoms were centered at the isocenter, and as in clinical practice, the arms were removed from the scan range for the renal arteries CTA protocol and for the shoulder and hip CT protocols.

The acquisition protocol for the CTA renal arteries was performed with TCM. The minimum and maximum tube current values for this protocol were determined by performing an actual scan on the Aquilion ONE CT of an anthropomorphic phantom (Rando phantom, manufactured in one piece, The Phantom Laboratory, New York, USA). The anthropomorphic phantom represents the trunk and head of an average-sized male.

The appropriate tube current for each projection angle was estimated based on the assumption that the dose on the detector should remain constant under different projections for an elliptical PMMA phantom. This phantom was a cylinder with an elliptical

cross section with lateral and antero-posterior diameters of 32 and 20 cm, respectively.

To determine the tube current for each projection angle, an axial acquisition with a constant tube current of an elliptical PMMA phantom was simulated. The inverse of the absorbed energy on the detector was normalized and adjusted to match the minimum and maximum tube current values determined by the CT system.

The organ and effective doses for the CTA renal arteries acquisitions were also calculated with simulations with constant tube current ( $mA_{MAX}$ ) to compare these results with those obtained using TCM.

#### Conversion factors from dose length product to effective dose

The MC simulation generates three-dimensional (3D) dose distributions from which the mean absorbed dose in each organ or

**Table 2**

Acquisition parameters for the four selected CT examinations according to the manufacturer's recommendations.

	kVp	mAs	Bow tie filter	AF nominal scan length (cm) and slices interval	AM nominal scan length (cm) and slices interval
CT vascular – CTA head	120	225	Small	15.5 (317–348)	16.0 (203–222)
CT vascular – CTA renal arteries	100	37.5	Medium	16.0 (211–243)	16.0 (131–150)
CT musculoskeletal – shoulder	120	37.5	Medium	13.6 (276–303)	12.8 (173–188)
CT musculoskeletal – hip	135	45	Medium	16.0 (166–198)	16.0 (101–120)

tissue can be derived. Effective doses were calculated using the tissue weighting factors of the ICRP Publication 103 [23]. Gender-specific calculations of effective dose ( $E$ ) were performed for the AM and AF voxel phantoms. The calculations of the effective doses for males were performed without a tissue weighting factor for the breast, and a breast tissue weighting factor of 0.24 was used for the females. Additionally, the gender-averaged effective dose was normalized to the tube charge for each protocol. The gender-averaged effective dose conversion factors (also known as  $k$ -factors) were derived as the quotients of the calculated effective doses and the calculated DLPs.

## Results

### Free-in-air dose profiles

The free-in-air attenuation profiles along the Y- and Z-axes employing the medium bow tie filter and for all the possible tube voltages are shown in Figs. 2 and 3, respectively. The figures also show the polynomial fits ( $R^2 > 0.99$  in all cases) that were used as input to the MC simulation to reproduce the bow tie filter (Fig. 2) and the heel effect (Fig. 3). The output of the MC simulation is expressed as normalized absorbed dose values. These simulated values corresponded very well with the actual measured dose values (differences lower than 6%).

The similar dose profiles that were measured free-in-air and calculated along the Y-axis for small, medium and large bow tie filters at a tube voltage of 120 kV are shown in Fig. 4.

### Doses in CT dose phantoms

To validate the scanner model and the MC simulation, the dose measurements and calculated values for the CT dose phantoms were compared. Good agreements (i.e., within a range of  $\pm 8\%$ ) between the measured and simulated values of the absorbed doses at the center and at the four peripheral positions in the head or body phantoms were found for the twelve acquisition combinations of three bow tie filters and four tube voltages. Table 3 provides a comparison of the experimental and simulated dose values

within the CT body and head phantoms using 120 kV and a medium bow tie filter. The results are expressed as  $D_{100,avg}$  and  $CTDI_{300}$ .

A more general overview of the measured and simulated weighted values of  $D_{100,avg}$  and  $CTDI_{300w}$  is presented in Table 4. These results confirm that the dose calculations obtained using the MC simulation corresponded with the actual exposure conditions.

### Tube current modulation

The minimum and maximum tube current values of the TCM function described in section 2.6 were 80 and 140 mA, respectively. The function presented in Fig. 5 provides the tube current values, normalized to the maximum value ( $mA_{Max}$ ), that were used in the simulations of each projection angle for the acquisitions of the CTA renal arteries in the AF and AM phantoms.

### Doses in the ICRP adult reference voxel phantoms

Figure 6 provides an overview of seven selected organ doses for the CTAs of the head and renal arteries and CTs of the shoulder and CT hip scans. These organs are the seven that receive the highest equivalent dose in each protocol. The percentage contributions to the effective doses, according to ICRP Publication 103 weighting factors, are also provided for each organ in the figures.

Table 5 shows the dose length products (DLP), the gender-averaged effective doses ( $E$ ), the effective doses normalized to the tube charge ( $E/mAs$ ), and the effective doses normalized to the dose length product ( $E/DLP$ ).

## Discussion

A Monte Carlo simulation has been developed for radiation exposure that results from a volumetric 320 detector-row cone-beam CT scanner and that accounts for realistic x-ray spectra, filtration, device geometry and TCM. The program has been validated by comparing simulated and measured dose profiles free-in-air and dose quantities from the PMMA CT dose phantoms. Additionally, two anthropomorphic ICRP adult reference computational voxel phantoms were utilized in the simulation model to calculate the organ and effective doses for clinical acquisition protocols.

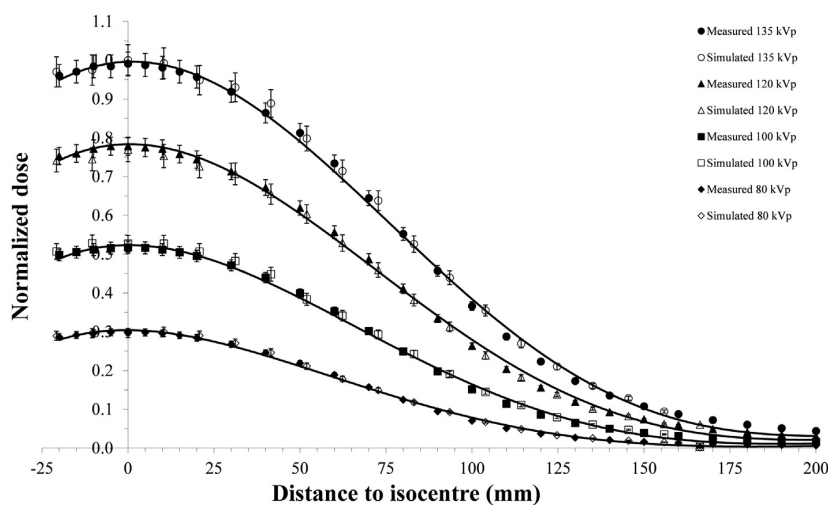
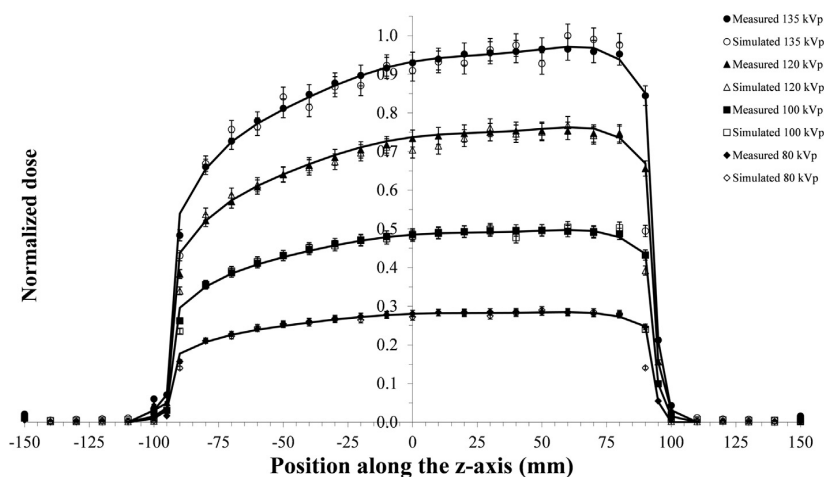
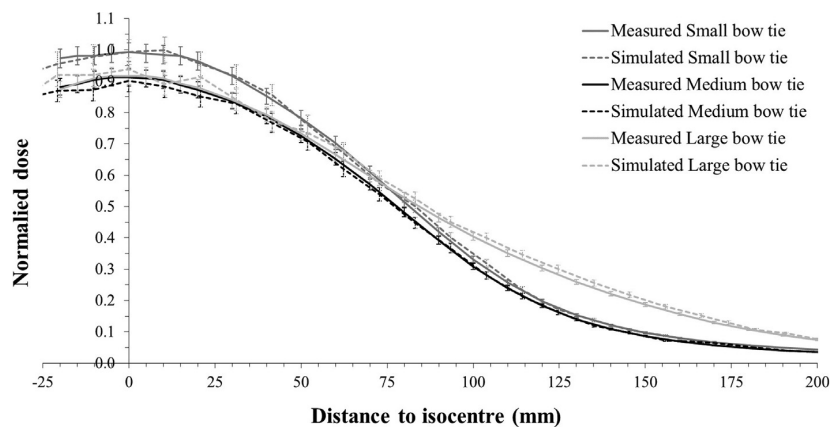


Figure 2. Measured (closed markers) and calculated (open markers) normalized axial free-in-air dose profiles (along the patient's AP direction) for the medium bow tie at 80 kV (diamonds), 100 kV (squares), 120 kV (triangles) and 135 kV (circles). The effect of the bow tie filter can be observed.



**Figure 3.** Measured (closed markers) and calculated (open markers) free-in-air dose profiles along the Z-axis (rotation axis) for the medium bow tie at 80 kV (diamonds), 100 kV (squares), 120 kV (triangles) and 135 kV (circles). The heel effect can be observed.



**Figure 4.** Measured (continuous line) and calculated (dashed line) normalized axial free-in-air dose profiles (AP direction of the patient) for small, medium and large bow tie filters (in gray, black and light gray, respectively) at a tube voltage of 120 kV.

**Table 3**

Results of the MC simulations and dose measurements for the Aquilion ONE CT scanner ( $320 \times 0.5$  mm acquisition configuration) for the CT doses of the head and body phantoms (120 kV, medium bow tie). Two dose descriptors ( $D_{100,avg}$ ,  $CTDI_{100}$ ) were derived from the calculated and measured dose distributions in the CT dose phantoms. Doses are provided for the center and each peripheral position in the phantom (N, E, S and W correspond to 12, 3, 6 and 9 o'clock positions, respectively). The weighted doses are also listed in the table.

$D_{100,avg}$ (mGy/mAs), 100 mm pencil chamber and 150 mm phantom length			$CTDI_{300}$ (mGy/mAs), 300 mm pencil chamber and 350 mm phantom length			
Measured (ionization chambers)	Calculated (Monte Carlo simulations)	$\Delta$ (%) <sup>a</sup>	Measured (ionization chambers)	Calculated (Monte Carlo simulations)	$\Delta$ (%) <sup>a</sup>	
<b>Body phantom</b>						
Position N	0.118	0.117	-1.0	0.111	0.113	1.8
Position E	0.117	0.114	-2.5	0.109	0.111	1.5
Position S	0.096	0.092	-3.6	0.102	0.099	-3.0
Position W	0.117	0.118	1.3	0.109	0.117	7.5
Center	0.058	0.055	-6.4	0.078	0.080	2.9
Weighted	0.094	0.092	-2.4	0.098	0.100	2.3
<b>Head phantom</b>						
Position N	0.201	0.199	-1.3	0.214	0.221	3.2
Position E	0.189	0.186	-1.9	0.202	0.208	2.9
Position S	0.174	0.166	-4.2	0.187	0.199	6.4
Position W	0.189	0.181	-4.7	0.202	0.208	3.0
Center	0.173	0.163	-6.1	0.205	0.207	1.2
Weighted	0.183	0.176	-4.0	0.202	0.208	2.9

<sup>a</sup>  $\Delta$  (%) =  $\frac{\text{Calculated} - \text{Measured}}{\text{Measured}} \times 100$

**Table 4**  
Results of the MC simulations and the dose measurements for the Aquilion ONE CT scanner ( $320 \times 0.5$  mm acquisition configuration) for the CT doses of the head and body phantoms. Two dose descriptors ( $D_{100w,avg}$ ,  $CTDI_{100w}$ ) were derived from the calculated and measured dose distributions in the CT dose phantoms.

Tube voltage (kV)	Bow tie filter	$D_{100w,avg}$ (mGy/mAs), 100 mm pencil chamber and 150 mm phantom length			$CTDI_{300w}$ (mGy/mAs), 300 mm pencil chamber and 350 mm phantom length		
		Measured (ionization chambers)	Calculated (Monte Carlo simulations)	$\Delta$ (%) <sup>a</sup>	Measured (ionization chambers)	Calculated (Monte Carlo simulations)	$\Delta$ (%) <sup>a</sup>
80	S	0.032	0.031	-0.7	0.032	0.032	0.8
100	S	0.062	0.061	-1.4	0.064	0.065	1.5
120	S	0.099	0.097	-1.9	0.104	0.106	1.9
135	S	0.130	0.129	-1.3	0.140	0.143	1.6
80	M	0.029	0.028	-3.5	0.029	0.030	3.2
100	M	0.058	0.056	-2.1	0.059	0.060	1.6
120	M	0.094	0.092	-2.4	0.098	0.100	2.3
135	M	0.125	0.122	-2.2	0.132	0.134	2.2
80	L	0.032	0.032	-1.8	0.033	0.033	1.9
100	L	0.064	0.063	-0.9	0.066	0.067	0.8
120	L	0.103	0.102	-0.6	0.111	0.111	0.6
135	L	0.141	0.138	-2.2	0.149	0.152	2.3
80	S	0.067	0.065	-3.6	0.072	0.075	3.1
100	S	0.125	0.120	-3.7	0.136	0.141	3.0
120	S	0.194	0.188	-3.1	0.215	0.220	2.5
135	S	0.254	0.244	-3.8	0.281	0.289	2.9
80	M	0.061	0.059	-4.3	0.066	0.068	2.7
100	M	0.115	0.110	-4.2	0.126	0.129	2.5
120	M	0.183	0.176	-4.0	0.202	0.208	2.9
135	M	0.239	0.229	-4.2	0.265	0.272	2.7

<sup>a</sup>  $\Delta$  (%) =  $\frac{\text{Calculated} - \text{Measured}}{\text{Measured}} \times 100$ .



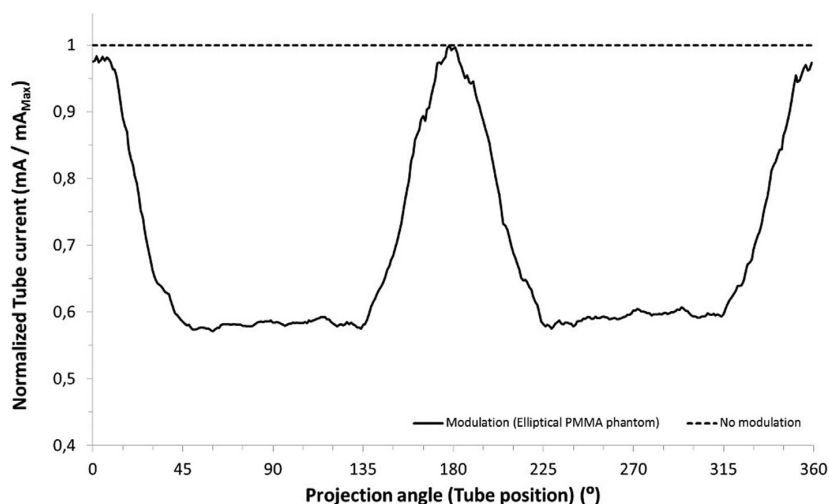


**Figure 5.** Tube current modulation (TCM) function normalized to the maximum tube current ( $\text{mA}_{\text{Max}}$ ) values. The projection angle indicates the tube position in a clockwise rotation where  $0^\circ$  corresponds to W (9 o'clock position) and  $90^\circ$  to N (12 o'clock position).

The CTDI values obtained by simulation exhibited good agreement with the ionization chamber measurements within the cavities of phantoms for both lengths of the ionization chambers (100 and 300 mm) and the phantoms (150 and 350 mm). The differences between the measured and simulated values, either in terms of  $D_{100\text{w, avg}}$  or  $\text{CTDI}_{300\text{w}}$ , were below 5% in the head and body phantoms. These differences might have been due to uncertainty in measurements with the ionization chamber. Other sources of error might have been due to uncertainties in the simulation model implementation (e.g., filtration, spectra, geometry of the scanner or voxelized objects) and to a lesser extent, the statistical errors that depend on the number of simulated histories. Similar errors have been reported for MC simulations by other authors [14,24,25]. The good correspondence between the measured and simulated results provides and guarantees the correct validation of the program and the CT scanner model.

A comparison between these measured values, using 120 kV and a large bow tie filter (500 mm FOV), and those obtained by Gomà et al. [26] from measurements on the same scanner model and using a Gaussian model to fit measured dose profiles, shows negative differences, less than  $-20\%$  for  $\text{CTDI}_{\text{w}}$  vs.  $\text{CTDI}_{300\text{w}}$ ; of about  $-8\%$  for  $\text{CTDI}_{100\text{w}}$  vs.  $D_{100\text{w, avg}}$  comparison, and  $-13\%$  for  $\text{CTDI}_{100}$  vs.  $D_{100, \text{avg}}$  at the center of the body phantom. This systematic underestimation can be explained by both the shorter phantom length and measurement range used in this study compared with the phantom length (450 mm) and measurement range (600 mm), used by Gomà et al. The former provides a more complete contribution from scattered radiation, the latter includes a large portion of the tails of the dose profile in the calculation. Since the authors did not provide information about the FOV or the bow tie filter selected to perform the measurements, the same comparison was also done using our dose measurements with

medium bow tie filter. All the differences described above become slightly larger ( $-29\%$ ,  $-12\%$  and  $-17\%$  respectively). Differences between the organ doses in the male and female ICRP phantoms were observed in all protocols. The doses to the female phantom were predominantly higher due to differences in body masses and organ shapes and locations between the AF and AM phantoms and to a lesser extent to, differences in scan lengths of some protocols. Although Fig. 6 shows the seven organs that received the highest equivalent doses in each protocol, other organs with low equivalent doses might make non-negligible contributions (between 1% and 6%) to the effective dose. The gender-averaged effective doses shown in Table 5 are valid for standard patients and for the specific protocols reproduced in this study and were compared with those calculated with the ImPACT CT Dosimetry Calculator [27]. Because this tool performs calculations for the Aquilion 16 CT scanner and not the Aquilion ONE CT scanner, the effective doses obtained from the CT Dosimetry Calculator were 40 and 23% higher for the head and hip explorations, respectively. For the renal arteries studies, similar effective doses were obtained; however, the equivalent organ doses were different depending on their positions in the phantom. For example, the equivalent dose in the lung was higher for the ImPACT (1 mSv for ImPACT and 0.09 mSv for gender-averaged equivalent dose in this study), and the equivalent dose in the colon was higher in this study (0.11 mSv for the ImPACT and 2.1 mSv for gender-averaged equivalent dose in this study). For the shoulder protocol, the effective dose obtained by the ImPACT was 40% lower than the effective dose value obtained in the present study. The main differences in these results might be due to the use of different phantoms (the ImPACT CT Dosimetry Calculator uses mathematical phantoms). Particularly in the shoulder acquisition, the lower dose values obtained with mathematical phantoms compared to those obtained with ICRP phantoms can be explained

**Table 5**

Dose-length products, sex-averaged effective dose ( $E$ ), the  $E$  normalized to the mAs, and the  $E/\text{DLP}$  for the four studied acquisitions.

	DLP (mGy·cm)	$E$ (mSv)	$E/\text{mAs}$ ( $10^{-3}$ mSv/mAs)	$E_{\text{DLP}}$ ( $10^{-3}$ mSv/mGy·cm)
CT vascular – CTA head	733	1.07	4.74	1.46
CT vascular – CTA renal arteries	47.2	0.64	13.2	13.5
CT musculoskeletal – shoulder	50.0	0.83	22.2	16.7
CT musculoskeletal – hip	95.3	0.97	21.6	10.2

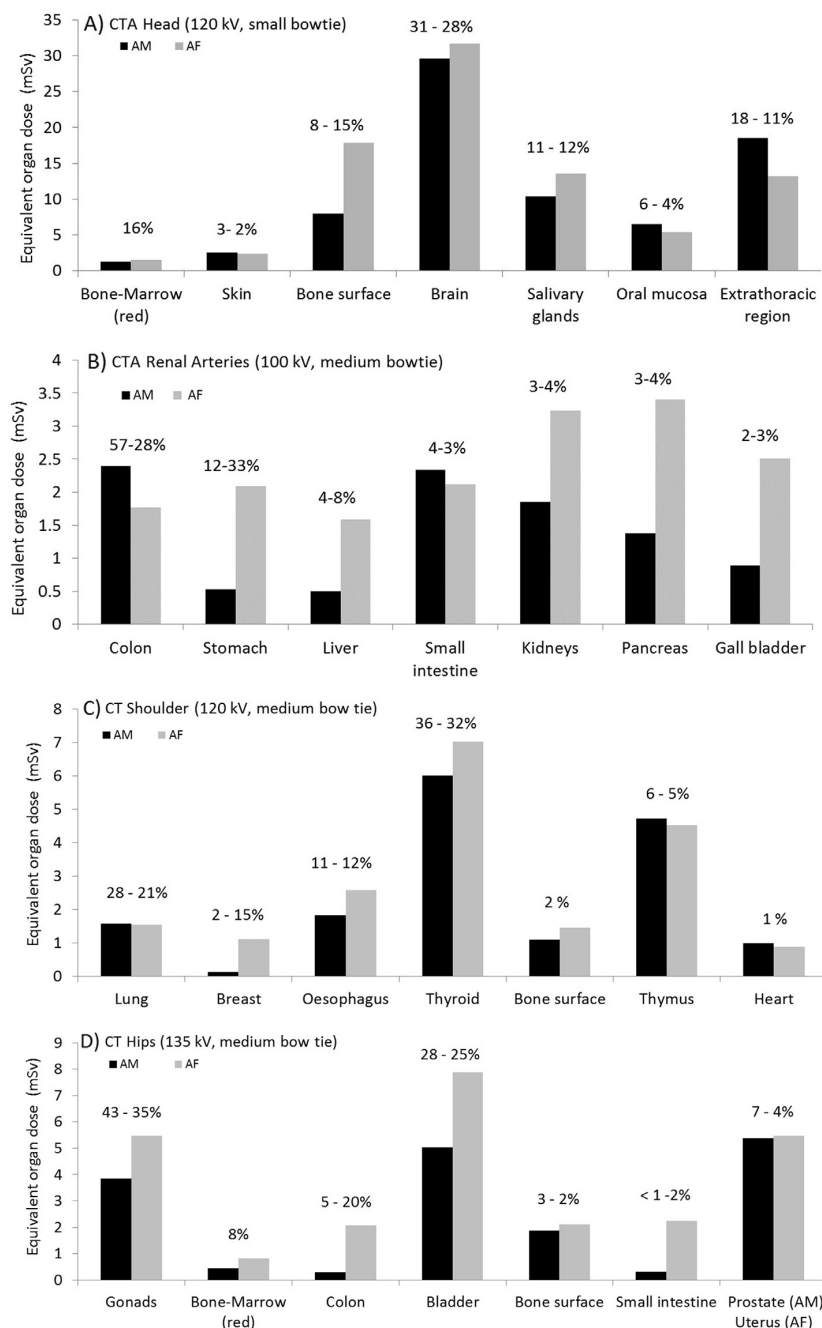


**Figure 6.** Equivalent doses (mSv) for the organs or tissues for the CTAs of the head (A) and renal arteries (B) and the shoulder (C) and hip (D) examinations using the adult male (AM, in black) and adult female (AF, in gray) anthropomorphic phantoms. The percentages indicate the contributions of each organ to the effective doses according to the ICRP Publication 103 [22].

by the significantly different distances between the thyroid and the breast in both phantoms. Additionally some parameters, which have been taken into account for the Aquilion ONE scanner like large beam cone width and heel effect, cannot be taken into account with the Aquilion 16 CT scanner.

The results presented in Table 5 and in Fig. 6 for the CTA renal arteries examinations were obtained using the previously calculated TCM functions. The same quantities were also calculated in

simulations involving constant tube current ( $mA_{Max}$ ) to compare both techniques. The variations observed in the dose distributions were due to implication of the TCM: first, the decreases in the tube charge, and second, the greater uniformity of the dose distributions. The reduction of the mean tube charge in a full rotation compared with the constant tube charge at  $mA_{Max}$  was 31% (see Fig. 5). As could be expected, this value equaled the reduction of the effective dose compared to the result calculated with the constant

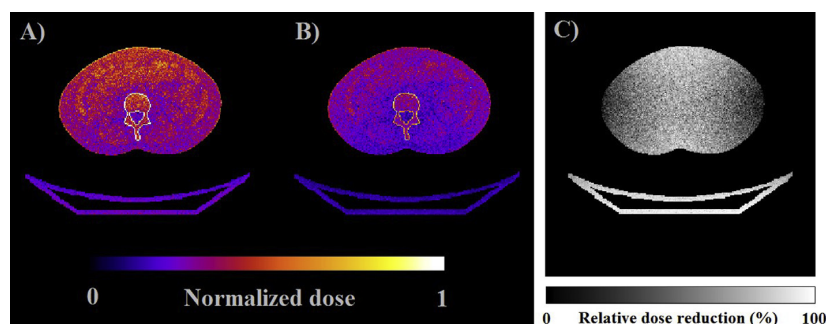


**Figure 7.** Calculated dose distributions in the AF phantom reproducing the CTA renal arteries exploration with constant tube current ( $mA_{Max}$ ) (image A) and employing mA modulation (image B). The relative dose differences were calculated as reduction percentages (image C =  $100 \cdot (\text{image A} - \text{image B}) / \text{image A}$ ).

tube current. The organ doses were reduced by between 28 and 36% depending on the organ location. Despite the uniformity in the organ dose variations, the changes in the dose distributions can be appreciated if the entrance skin dose (ESD) values in the W position (lateral, LAT) and N position (anterior-posterior, AP) are compared to the same results obtained using a constant tube current. The ESD values in the AF phantom, as measured as the quotient of the absorbed energy in the skin voxels (with  $1 \text{ cm}^2$  surfaces) and their respective masses, were reduced by 37% in AP and 20% in LAT positions. The quotients of the ESD values obtained for AP and LAT positions were 30% when no modulation was simulated and 11% when modulation was applied. These latter results indicate that the dose distribution uniformity was greater when TCM was employed. For example, Fig. 7 shows the obtained dose distributions in the AF during the CTA renal arteries scans in the axial sections located in the central beam for both the conditions of constant tube current and TCM. The relative differences between these dose distributions revealed a higher variation in AP axis than in the LAT axis.

Because the DLP values are displayed on the console of Aquilion ONE CT scanner and can be used as a primary estimator of effective dose, the conversion factors (i.e., DLP to effective dose) were calculated for each CT exam. The obtained results were compared with the values that have been reported in the literature. In particular, there are some authors who have calculated these factors using mathematical phantoms in Aquilion 16 CT scanners [28,29]. For the head protocol, the conversion factors reported in the present study were between 23 and 39% lower than those reported by these authors. Regarding the renal arteries and the shoulder and hip protocols, no similar studies have been published. However, the conversion factors from our study were nearly always lower than those obtained by the same authors using generic protocols; e.g., differences between  $-31$  and  $11\%$  in the abdomen explorations (renal arteries),  $-15$  and  $18\%$  in the chest (shoulder) scans, and  $22$  and  $29\%$  in the pelvis (hips) scans were found. These discrepancies can be explained by the significant differences in the CT scanner systems and by the more realistic and accurate representations of human anatomy provided by the voxel phantoms used in this study. Other authors reported E/DLP conversion factors for axial coronary CT angiography studies with Aquilion ONE CT scanners [26,30,31]. Differences between reported values and those obtained in this study, for the shoulder scan, are in the range  $2-30\%$ . Such differences are hard to analyze, because neither the anatomical area scanned nor the protocols applied are the same.

One limitation of this study is that the data from the performed simulations were only used to estimate organ and effective doses in standard patients and thus did not account for large variations in size or morphology. Dose variations due to patient miscentering in vertical or horizontal direction within the gantry [32] have not been

considered. Finally, although this paper refers only to a specific CT scanner model for which all necessary information was available, the developed MC simulation program exhibited great flexibility and should be adaptable to new x-ray diagnostic systems. Additionally, the availability of the ICRP adult reference computational phantoms makes this simulation program a suitable tool for assessing realistic doses from a 320 detector-row volumetric CT scanner.

## Conclusions

An MC method for estimating the doses from 320-slice CT scanning protocols was developed and validated. The good agreements between the CTDI values obtained from the simulations and the measurements of the head and body PMMA phantoms demonstrate that the developed scanner model is an accurate tool for purposes of dose estimation. The MC code was adapted to be capable of accounting for any arbitrary scan protocol, including those with TCM, for 320 detector-row cone-beam CT scanners. The anthropomorphic voxel phantoms from the ICRP were also successfully implemented in the simulation program. As an initial application, these phantoms were used to estimate the organ and effective doses for standard patients obtained from general protocols of the Aquilion ONE CT system. Results utilizing both TCM and constant tube current conditions were obtained and compared to evaluate the dose reductions and variations in dose distributions. While the explorations simulated in this study were not of the protocols that are actually the most commonly performed with this scanner model, future research will be focused on specific studies performed with the Aquilion ONE CT scanner, such as angiography and perfusion CT protocols.

## Acknowledgments

Part of this research was performed using the resources of the *Sonorsi de Serveis Universitaris de Catalunya* (CSUC).

## References

- [1] Dewey M, Zimmermann E, Laule M, Rutsch W, Hamm B. Three-vessel coronary artery disease examined with 320-slice computed tomography coronary angiography. *Eur Heart J* 2008;29:1669. <http://dx.doi.org/10.1093/eurheartj/ehm626>.
- [2] Rybicki FJ, Otero HJ, Steigner ML, Vorobiof G, Nallamshetty L, Mitsouras D, et al. Initial evaluation of coronary images from 320-detector row computed tomography. *Int J Cardiovasc Imaging* 2008;24:535–46. <http://dx.doi.org/10.1007/s10554-008-9308-2>.
- [3] IAEA. Status of computed tomography dosimetry for wide cone beam scanners. IAEA Hum Heal Ser No 5, ISBN 978-92-0-120610-7. doi:STI/PUB/1528.

- [4] Geleijns J, Salvadó Artells M, de Bruin PW, Matter R, Muramatsu Y, McNitt-Gray MF. Computed tomography dose assessment for a 160 mm wide, 320 detector row, cone beam CT scanner. *Phys Med Biol* 2009;54:3141–59. <http://dx.doi.org/10.1088/0031-9155/54/10/012>.
- [5] IEC. Medical electrical equipment: Part 2-44. Particular requirements for the basic safety and essential performance of x-ray equipment for computed tomography. IEC 60601-2-44 ed30 2009.
- [6] Nelson WR, Hirayama H, Rogers DW. The EGS4 code system. 1985.
- [7] Hirayama H, Namito Y, Ban S. Implementation of a general treatment of photoelectric-related phenomena for compounds or mixtures in EGS4. KEK Internal Report 2000-3; 2000.
- [8] Geleijns J, Salvadó Artells M, Veldkamp WJH, López Tortosa M, Calzado Cantera A. Quantitative assessment of selective in-plane shielding of tissues in computed tomography through evaluation of absorbed dose and image quality. *Eur Radiol* 2006;16:2334–40. <http://dx.doi.org/10.1007/s00330-006-0217-2>.
- [9] Salvadó M, López M, Morant JJ, Calzado A. Monte Carlo calculation of radiation dose in CT examinations using phantom and patient tomographic models. *Radiat Prot Dosim* 2005;114:364–8. <http://dx.doi.org/10.1093/rpd/nch516>.
- [10] Geleijns J, Joemai RMS, Dewey M, De Roos A, Zankl M, Cantera AC, et al. Radiation exposure to patients in a multicenter coronary angiography trial (CORE 64). *Am J Roentgenol* 2011;196:1126–32. <http://dx.doi.org/10.2214/AJR.09.3983>.
- [11] Morant JJ, Salvadó M, Casanovas R, Hernández-Girón I, Velasco E, Calzado A. Validation of a Monte Carlo simulation for dose assessment in dental cone beam CT examinations. *Phys Med* 2012;28:200–9. <http://dx.doi.org/10.1016/j.ejmp.2011.06.047>.
- [12] Morant JJ, Salvadó M, Hernández-Girón I, Casanovas R, Ortega R, Calzado A. Dosimetry of a cone beam CT device for oral and maxillofacial radiology using Monte Carlo techniques and ICRP adult reference computational phantoms. *Dentomaxillofac Radiol* 2013;42:92555893. <http://dx.doi.org/10.1259/dmfr/92555893>.
- [13] Cranley K, Gilmore B, Fogarty G, Desponds L. Catalogue of diagnostic x-ray spectra and other data. IPEM Rep No 78; 1997.
- [14] Jarry G, DeMarco JJ, Beifuss U, Cagnon CH, McNitt-Gray MF. A Monte Carlo-based method to estimate radiation dose from spiral CT: from phantom testing to patient-specific models. *Phys Med Biol* 2003;48:2645–63. <http://dx.doi.org/10.1088/0031-9155/48/16/306>.
- [15] Skrzyński W. Measurement-based model of a wide-bore CT scanner for Monte Carlo dosimetric calculations with GMCTdospp software. *Phys Med* 2014. <http://dx.doi.org/10.1016/j.ejmp.2014.06.045>.
- [16] Schlattl H, Zankl M, Becker J, Hoeschen C. Dose conversion coefficients for CT examinations of adults with automatic tube current modulation. *Phys Med Biol* 2010;55:6243–61. <http://dx.doi.org/10.1088/0031-9155/55/20/013>.
- [17] ICRP. Adult reference computational phantoms. ICRP publication 110. *Ann ICRP* 2009;39(2). <http://dx.doi.org/10.1016/j.icrp.2009.07.004>.
- [18] Zankl M, Wittmann A. The adult male voxel model “Golem” segmented from whole-body CT patient data. *Radiat Environ Biophys* 2001;40:153–62. <http://dx.doi.org/10.1007/s004110100094>.
- [19] Zankl M, Becker J, Fill U, Petoussi-Hens N. GSF male and female adult voxel models representing ICRP Reference Man - the present status. The Monte Carlo Method: Versatility Unbounded in a Dynamic Computing World. *Am Nucl Soc* 2005. LaGrange Park, IL.
- [20] Zankl M, Eckerman KF, Bolch WE. Voxel-based models representing the male and female ICRP reference adult - the skeleton. *Radiat Prot Dosim* 2007;127:174–86. <http://dx.doi.org/10.1093/rpd/ncm269>.
- [21] Zankl M, Fill U, Petoussi-Hens N, Regulla D. Organ dose conversion coefficients for external photon irradiation of male and female voxel models. *Phys Med Biol* 2002;47:2367–85. <http://dx.doi.org/10.1088/0031-9155/47/14/301>.
- [22] King SD, Spiers FW. Photoelectron enhancement of the absorbed Dose from X Rays to human bone marrow: experimental and theoretical studies. *Br J Radiol* 1985;58:345–56. <http://dx.doi.org/10.1259/0007-1285-58-688-345>.
- [23] ICRP. The 2007 recommendations of the international commission on radiological protection. ICRP Publication 103 *Ann ICRP* 2007;37(2–4). <http://dx.doi.org/10.1016/j.icrp.2007.10.001>.
- [24] DeMarco JJ, Cagnon CH, Cody DD, Stevens DM, McCollough CH, O'Daniel J, et al. A Monte Carlo based method to estimate radiation dose from multi-detector CT (MDCT): cylindrical and anthropomorphic phantoms. *Phys Med Biol* 2005;50:3989–4004. <http://dx.doi.org/10.1088/0031-9155/50/17/005>.
- [25] Deak P, van Straten M, Shrimpton PC, Zankl M, Kalender WA. Validation of a Monte Carlo tool for patient-specific dose simulations in multi-slice computed tomography. *Eur Radiol* 2008;18:759–72. <http://dx.doi.org/10.1007/s00330-007-0815-7>.
- [26] Gomà C, Ruiz A, Jornet N, Latorre A, Pallerol RM, Carrasco P, et al. Radiation dose assessment in a 320-detector-row CT scanner used in cardiac imaging. *Med Phys* 2011;38:1473–80. <http://dx.doi.org/10.1118/1.3558020>.
- [27] Shrimpton PC, Edyvean S. CT scanner dosimetry. *Br J Radiol* 1998;71:1–3. <http://dx.doi.org/10.1259/bjr.71.841.9534691>.
- [28] Huda W, Magill D, He W. CT effective dose per dose length product using ICRP 103 weighting factors. *Med Phys* 2011;38:1261–5. <http://dx.doi.org/10.1118/1.3544350>.
- [29] Deak PD, Smal Y, Kalender WA. Multisession CT protocols: sex- and age-specific conversion factors used to determine effective dose from dose-length product. *Radiology* 2010;257:158–66. <http://dx.doi.org/10.1148/radiol.10100047>.
- [30] Einstein AJ, Elliston CD, Arai AE, Chen MY, Mather R, Pearson GDN, et al. Radiation dose from single-heartbeat coronary CT angiography performed with a 320-detector row volume scanner. *Radiology* 2010;254:698–706. <http://dx.doi.org/10.1148/radiol.09090779>.
- [31] Seguchi S, Aoyama T, Koyama S, Fujii K, Yamauchi-Kawaura C. Patient radiation dose in prospectively gated axial CT coronary angiography and retrospectively gated helical technique with a 320-detector row CT scanner. *Med Phys* 2010;37:5579–85. <http://dx.doi.org/10.1118/1.3496985>.
- [32] Habibzadeh MA, Ay MR, Asl ARK, Ghadiri H, Zaidi H. Impact of miscentering on patient dose and image noise in x-ray CT imaging: phantom and clinical studies. *Phys Med* 2012;28:191–9. <http://dx.doi.org/10.1016/j.ejmp.2011.06.002>.



## 4.2 Dose assessment in specific studies

### 4.2.1 Dose assessment in cardiac CT

- [II] Geleijns J, Joemai RMS, Cros M, Hernandez-Giron I, Calzado A, Dewey M, Salvadó M. A Monte Carlo simulation for the estimation of patient dose in rest and stress cardiac computed tomography with a 320-detector row CT scanner. *Phys Med* 2015;31:1029-34 (DOI: 10.1016/j.ejmp.2015.08.008)

#### Abstract

*Purpose:* To estimate organ dose and effective dose for patients for cardiac CT as applied in an international multicenter study (CORE320) with a 320-Detector row CT scanner using Monte Carlo (MC) simulations and voxelized phantoms. The effect of positioning of the arms, off-centering the patient and heart rate on patient dose was analyzed.

*Methods:* A MC code was tailored to simulate the geometry and characteristics of the CT scanner. The phantoms representing the adult reference male and female were implemented according to ICRP 110. Effective dose and organ doses were obtained for CT acquisition protocols for calcium scoring, coronary angiography and myocardial perfusion.

*Results:* For low heart rate, the normalized effective dose (E) for cardiac CT was higher for female (5.6 mSv/100 mAs) compared to male (2.2 mSv/100 mAs) due to the contribution of female breast tissue. Averaged E for female and male was 11.3 mSv for the comprehensive cardiac protocol consisting of calcium scoring (1.9 mSv); coronary angiography including rest cardiac perfusion (5.1 mSv) and stress cardiac perfusion (4.3 mSv). These values almost doubled at higher heart rates (20.1 mSv). Excluding the arms increased effective dose by 6–8%, centering the patient showed no significant effect. The k-factor (0.028 mSv/ mGy·cm) derived from this study leads to effective doses up to 2–3 times higher than the values obtained using now outdated methodologies.

*Conclusion:* MC modeling of cardiac CT examinations on realistic voxelized phantoms allowed us to assess patient doses accurately and we derived k-factors that are well above those published previously.





## Original Paper

# A Monte Carlo simulation for the estimation of patient dose in rest and stress cardiac computed tomography with a 320-detector row CT scanner



Jacob Geleijns<sup>a,\*</sup>, Raoul M.S. Joemai<sup>a</sup>, Maria Cros<sup>b</sup>, Irene Hernandez-Giron<sup>a</sup>, Alfonso Calzado<sup>c</sup>, Marc Dewey<sup>d</sup>, Marçal Salvado<sup>b</sup>

<sup>a</sup> Radiology Department, Leiden University Medical Center, Albinusdreef 2, Leiden 2333 ZA, Netherlands

<sup>b</sup> Faculty of Medicine and Health Sciences, Universitat Rovira i Virgili, Sant Llorenç 21, Reus 43201, Spain

<sup>c</sup> Radiology Department, Universidad Complutense, Madrid 28040, Spain

<sup>d</sup> Charité Centrum für diagnostische und interventionelle Radiologie und Nuklearmedizin Institut für Radiologie CCM, Charitéplatz 1, Berlin 10117, Germany

## ARTICLE INFO

## Article history:

Received 3 April 2015

Received in revised form 17 July 2015

Accepted 22 August 2015

Available online 4 October 2015

## Keywords:

Rest and stress cardiac computed

tomography

CT dosimetry

Monte Carlo simulation

ICRP voxel phantoms

Effective dose to the patient

## ABSTRACT

**Purpose:** To estimate organ dose and effective dose for patients for cardiac CT as applied in an international multicenter study (CORE320) with a 320-Detector row CT scanner using Monte Carlo (MC) simulations and voxelized phantoms. The effect of positioning of the arms, off-centering the patient and heart rate on patient dose was analyzed.

**Methods:** A MC code was tailored to simulate the geometry and characteristics of the CT scanner. The phantoms representing the adult reference male and female were implemented according to ICRP 110. Effective dose and organ doses were obtained for CT acquisition protocols for calcium scoring, coronary angiography and myocardial perfusion.

**Results:** For low heart rate, the normalized effective dose (E) for cardiac CT was higher for female (5.6 mSv/100 mAs) compared to male (2.2 mSv/100 mAs) due to the contribution of female breast tissue. Averaged E for female and male was 11.3 mSv for the comprehensive cardiac protocol consisting of calcium scoring (1.9 mSv); coronary angiography including rest cardiac perfusion (5.1 mSv) and stress cardiac perfusion (4.3 mSv). These values almost doubled at higher heart rates (20.1 mSv). Excluding the arms increased effective dose by 6–8%, centering the patient showed no significant effect. The k-factor (0.028 mSv/mGy.cm) derived from this study leads to effective doses up to 2–3 times higher than the values obtained using now outdated methodologies.

**Conclusion:** MC modeling of cardiac CT examinations on realistic voxelized phantoms allowed us to assess patient doses accurately and we derived k-factors that are well above those published previously.

© 2015 Associazione Italiana di Fisica Medica. Published by Elsevier Ltd. All rights reserved.

## Introduction

The application of cardiovascular imaging with computed tomography (CT) is well integrated in routine clinical practice. CT scanners allowing axial single heart beat imaging with 320 detector rows have advanced the field of cardiac CT [1,2]. With single-beat cardiac CT, image quality improves whereas acquisition time, patient dose, and image artifacts are reduced [3]. Such new technologies for cardiovascular CT imaging demand an accurate assessment of radiation exposure to patients. Reliable patient dose assessment is also required for the calculation of radiation risks that are associated to cardiac CT.

Proper estimation of organ doses and effective dose in cardiac CT is a challenging task. The development of methodologies for accurate and practical assessment of patient dose in cardiac CT is lagging behind the developments in CT technology and applications. The latest generic recommendations were introduced in 2007 by the ICRP (International Commission on Radiological Protection) to estimate the effective dose for radiation protection purposes [4]. Besides, the ICRP standardized voxel phantoms were introduced in 2009 [5]. It is generally acknowledged that the latest recommendation for the calculation of effective dose is associated with an increase of the effective dose for cardiac CT, but little in depth information is available. According to the ICRP, the standard adult voxel phantoms are now state of the art in dose assessment and thus, organ dose values for both internal and external radiation sources should be derived for such phantoms. The ICRP published a detailed description of the two voxel phantoms, representing the reference adult male (AM) and female (AF) [5]. These phantoms are

\* Corresponding author. Radiology Department, Leiden University Medical Center, Albinusdreef 2, Leiden 2333 ZA, Netherlands. Tel.: +31 71 5262049; fax: +31 (0)71 524 8256.

E-mail address: [J.Geleijns@lumc.nl](mailto:J.Geleijns@lumc.nl) (J. Geleijns).



the international standard for the calculation of radiation exposure of adults. These two concepts, the latest recommendation for effective dose and the ICRP voxel phantoms, have not yet been implemented for patient dosimetry in radiology in general and for cardiac CT with modern CT scanners and the latest acquisition protocols in particular.

The primary goal of this study was to calculate organ doses and effective dose for the cardiac CT acquisition protocol applied in an international multicenter study (CORE320), with a 320 detector row volumetric CT scanner, according to the internationally recognized standards in dosimetry [6]. The cardiac CT protocol included CT calcium scoring, CT coronary angiography and CT myocardial perfusion. For this task, Monte Carlo simulation software was used to calculate the dose distribution in two ICRP anthropomorphic voxel phantoms for this specific scanner and these acquisition protocols [7].

In clinical cardiac CT it is common practice to use an offset in the positioning of the patient so that the heart is centered relative to the axis of rotation of the scanner, and the arms of the patient are generally removed from the scanned range by positioning them along the head. However, most generic models for patient dosimetry assume that the CT scan is performed with the patient's body, not the heart, centered along the axis of rotation. The arms of the ICRP voxel phantoms are positioned along the body, which is also not according to clinical practice in cardiac CT. Therefore, a secondary goal of this study was to investigate the effect of the positioning of the patient and the arms on the assessment of effective dose. Dose calculations were thus performed for acquisition geometries in which the patient's body or heart is placed in the center of rotation of the scanner and for phantom configurations with the arms along the body and with the arms removed from the scanned range. These different configurations for the simulations were investigated to enable the comparison of the results of this study with those based in other existing generic models for patient dosimetry in the literature. Finally, the third goal was a comparison between the dose values obtained in this study based on dedicated MC simulations and those existing in the literature based on k-factors [8–14] and also with results obtained with the ImPACT CT Patient Dosimetry Calculator [15].

## Materials and methods

### Voxel phantoms of an average female and male adult

Two voxel phantoms representing the female (AF) and male (AM) standard adults were prepared for use in combination with the Monte Carlo (MC) dose simulation algorithm [16]. The voxel phantoms are a more realistic representation of a human compared to the MIRD type mathematical reference phantoms (based on the ICRP publication from 1975), which were used until recently [17]. Two complementary representations of each of the ICRP voxel phantoms had to be created to implement them in the simulations. One representation defines the spatial distribution and identification number for 141 organs and tissues; the other provides the 53 different atomic compositions of the different materials in the phantoms plus the atomic composition of the air outside body and CT table. The voxel phantoms represent an average female (height 163 cm, weight 60 kg, body mass index (BMI) 22.6 kg/m<sup>2</sup>) and an average male (height 176 cm, weight 73 kg, BMI 23.6 kg/m<sup>2</sup>). The voxel size is respectively 1.78 × 1.78 × 4.8 mm<sup>3</sup> (AF) and 2.14 × 2.14 × 8 mm<sup>3</sup> (AM). In addition, the phantoms were customized without the upper extremities (arms) to reproduce the clinical setting in cardiac CT. When removing upper extremities, the mass of the tissues in these volumes was taken into account for the calculation of absorbed dose. Figure 1 shows the two AF and AM voxel phantoms in two depictions, one showing sagittal and lateral views with the different

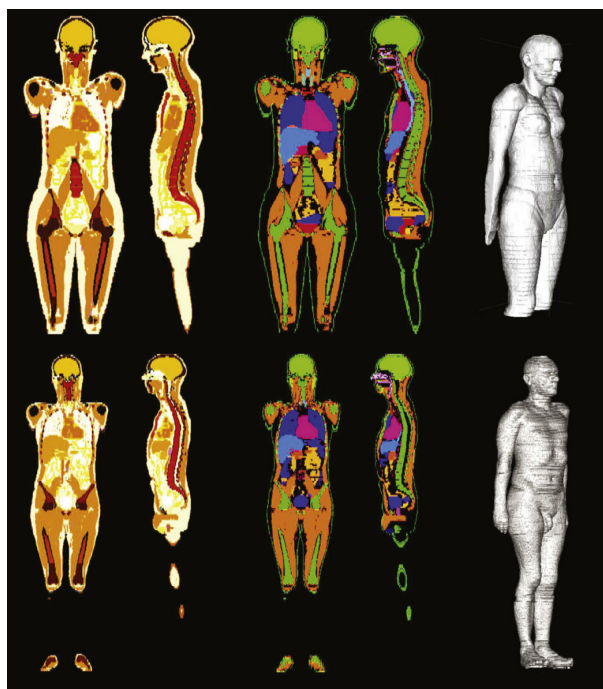


**Figure 1.** From left to right: coronal and sagittal images showing in different colors the different organs and materials (left) and the tissue weighting factors assigned to these organs (middle); and a 3D surface rendering (right). Above the female phantoms, below the male phantom. Note, in this configuration of the phantom, the arms are present, and aligned along the body.

materials and tissue weighting factors in different colors, and one surface rendering.

### Monte Carlo dose simulations of the Aquilion ONE CT scanner

The MC code used to estimate the radiation exposure resulting from a CT scan simulates the radiation transport in a voxelized space. For this study, the simulation takes into account specific characteristics of the technical design of the Aquilion ONE CT scanner. The MC algorithm is a modified version of a previously validated one that was used for dose calculations in CT examinations with other Aquilion CT scanners [8,18] and in another cone beam CT for oral and maxillofacial radiology [16,19]. For the Aquilion ONE CT scanner special attention was paid to accurately modeling of the beam geometry (including the penumbra), the X-ray spectrum, the bow tie filter, and the heel effect. A benchmarked Electron Gamma Shower V4 (EGS4) application [20] in combination with a Low Energy Photon Scattering Expansion [21] was used for the calculation of radiation transport. The program was developed and validated for the Aquilion ONE CT scanner in a previous study, comparing results from MC simulations with the actual measurements acquired under the same conditions in standard CT dose phantoms [7]. The measurements agreed with the MC results across all conditions with relative differences up to 6%. MC simulations were performed in a cluster computer (CSUC), composed by 14 Bull Nova Scale R422E1 servers with 28 nodes and 56 Xeon 4 core processors running at 3.0 GHz with 896 GB as total memory. For the simulations 2•10<sup>7</sup> photon histories were used. Thus absorbed doses by all tissues included in ICRP publication 103 were calculated and subsequently used to assess effective dose [4]. Special attention was paid to estimate the absorbed dose in the skeleton. To calculate the absorbed dose in bone

**Table 1**

Acquisition protocol for the CORE320 multicenter study. Acquisitions were performed with a tube voltage of 120 kV, a range of 140 mm, and a field of view of 400 mm. The acquisition settings correspond with a standard sized patient.

	Gender Male/female	Heart rate bpm	Tube current mA	No. of beats #	Rotation time s	Tube charge mAs
Coronary CS	Female	All rates	140	1	0.35	49
Without contrast	Male	All rates	140	1	0.35	49
Coronary CTA and rest cardiac perfusion	Female	≤ 65	370	1	0.35	129.5
	Male	≤ 65	400	1	0.35	140
With contrast	Female	≥ 66	340	2	0.35	238
	Male	≥ 66	400	2	0.35	280
Stress cardiac perfusion	Female	≤ 65	300	1	0.35	105
	Male	≤ 65	370	1	0.35	129.5
	Female	≥ 66	300	2	0.35	210
	Male	≥ 66	350	2	0.35	245

marrow and bone endosteum, the fraction of the mass of bone marrow relative to the fraction of endosteum in each voxel and their energy absorption coefficients was used to calculate the average energy imparted in the entire voxel. Additionally, a correction was made for the increased imparted energy by enhancement that occurs in bone marrow and endosteum due to the interface effects between these tissues and the cortical bone or trabeculae. This dose enhancement is related to the creation of secondary electrons due to photoelectric interactions in cortical bone or trabeculae, and the posterior energy release by the photoelectrons in the adjacent bone marrow. The relative uncertainties associated with the dose calculations in the MC simulations were in the range 4–5% [7,16].

#### CORE320 cardiac CT acquisition protocol

Dose calculations were performed for the cardiac CT acquisition protocol that was used in the CORE320 multicenter study for calcium scoring, coronary angiography (also used for rest perfusion imaging), and stress perfusion imaging [3]. Technical details of the acquisition protocols for patients with an average size (BMI between 20 and 24.9 kg/m<sup>2</sup>) are listed in Table 1. The AF and AM voxel phantoms BMI values fall into this category.

The CORE320 acquisition protocols provide additional settings for five categories of smaller or larger patients that were not analyzed in this study. The acquisition of the coronary arteries is also used for assessment of rest perfusion. This acquisition was performed with intravenous iodinated contrast (ISOVUE®-370). Stress imaging was preceded by intravenous adenosine infusion (0.14 mg/kg/min) during 5 minutes, followed by administration of the intravenous iodinated contrast. The effect of the administration of iodine contrast was not simulated in this dosimetric study.

The simulations took into account the acquisitions parameters selected in the scanner depending on the gender and the heart rate of the patient. All acquisitions were performed as axial volumetric scans with coverage of the entire heart.

Gender specific calculations of effective dose (E) were performed for the AM and AF voxel phantoms. The calculations of the effective doses for males were performed without a tissue weighting factor for the breast, and a breast tissue weighting factor of 0.24 was used for the females [4].

#### Comparison with other dosimetric methods

The effective doses from the MC simulations performed in this study were compared to effective doses obtained using different approaches: the so-called k-factors, defined as the ratio of the effective dose and the dose length product for certain roughly defined body areas [8–14], and the dosimetric software such as the IMPACT CT Patient Dosimetry Calculator [15].

## Results

### Implementation of the voxel phantoms

The dosimetric characteristics of the Aquilion ONE scanner were modeled in a MC simulation algorithm and the ICRP voxel phantoms of the standard female (AF) and male (AM) were implemented as inputs for this model. Figure 2 shows a visualization of the dose distribution due to the volumetric cardiac CT acquisition for both phantoms.

### Normalized dose of cardiac CT acquisitions

The normalized organ doses (mGy/100 mAs) from a cardiac CT acquisition for the AF and AM voxel phantoms are listed in Table 2 for the clinical configuration (patient off centered and arms removed). Breast tissue and the heart were entirely covered by the X-ray beam, resulting in the highest normalized organ doses for these two tissues. Organ dose was intermediate (<10 mSv) for organs that were only partially covered by the X-ray beam, like lungs, stomach and esophagus. Negligible organ doses (<0.1 mSv) were observed for organs far outside the X-ray beam like brain, gonads, and uterus.

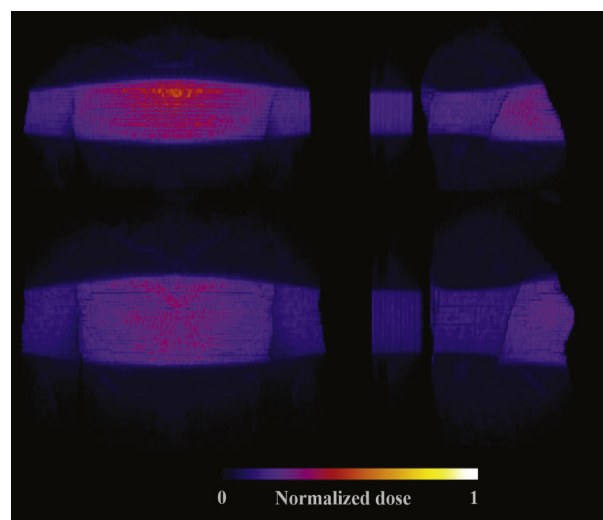


**Figure 2.** A visualization of the dose distribution due to the volumetric cardiac CT acquisition the standard female (AF, above) and male (AM, below) phantoms. The cone beam shape of the X-ray beam can be recognized. The phantoms were centered in the scanner and the arms were positioned along the body of the phantom.

1032

J. Geleijns et al./Physica Medica 31 (2015) 1029–1034

**Table 2**

Normalized organ doses for the adult female and male ICRP voxel phantoms (effective dose per 100 mAs) for the clinically most relevant configuration, with the heart positioned in the isocenter of the scanner, the arms were removed from the phantoms.

Organ or tissue	Normalized organ doses (mGy per 100 mAs)	
	Female	Male
Breast	12.6	11.5
Heart	12.8	10.2
Lung	9.3	7.2
Spleen	4.7	4.4
Stomach	4.2	4.4
Esophagus	5.5	4.3
Liver	4.2	3.4
Thymus	3.4	2.6
Bone surface	2.7	2.1
Lymphatic nodes	2.1	2.1
Adrenals	1.9	1.7
Gall bladder	1.6	1.3
Pancreas	1.0	1.3
Skin	1.3	1.1
Red bone marrow	1.5	0.97
Thyroid	1.1	0.91
Kidneys	0.94	0.90
Muscle	0.85	0.84
Small intestine	0.31	0.47
Colon	0.09	0.45
Salivary glands	0.23	0.15
Oral mucosa	0.28	0.13
Extra thoracic	0.21	0.13
Brain	0.05	0.04
Upper large intestine	0.02	0.02
Urinary bladder	0.01	0.01
Prostate	-	0.01
Gonads	0.02	0.00
Uterus	0.02	-

The normalized effective dose (mSv/100 mAs) is shown in Table 3. The effective dose for females was relatively high due to the high absorbed dose and high weighting factor for breast tissue. For a tube voltage of 120 kV, the normalized effective dose was 5.6 mSv per 100 mAs for the female phantom and 2.2 mSv per 100 mAs for the male phantom for the clinically most relevant configuration (with the body off-centered and the arms removed).

#### Effect of phantom positioning

Only subtle differences in effective dose assessment were observed when including or removing the arms from the scanned area. Excluding the arms resulted in an increase of the effective dose by about 6–8%. Only small differences in effective dose were observed for centering versus off-centering for both phantoms.

**Table 3**

Normalized effective dose (mSv per 100 mAs) according to ICRP 103 for a standard sized female and male patient, with the patient centered along the axis of rotation or off-centered with the heart along the axis of rotation, and the arms along the body and in the scanned range or arms removed.

	Female		Male	
	mSv per 100 mAs	% compared to off-centered without arms	mSv per 100 mAs	% compared to off-centered without arms
Centered with arms	5.2	-7%	2.0	-8%
Centered without arms	5.6	0%	2.2	1%
Off-centered with arms	5.2	-6%	2.0	-8%
Off-centered without arms	5.6	<sup>a</sup>	2.2	<sup>a</sup>

<sup>a</sup> This is the clinical reference condition (phantom off-centered without the arms in the scanned range).

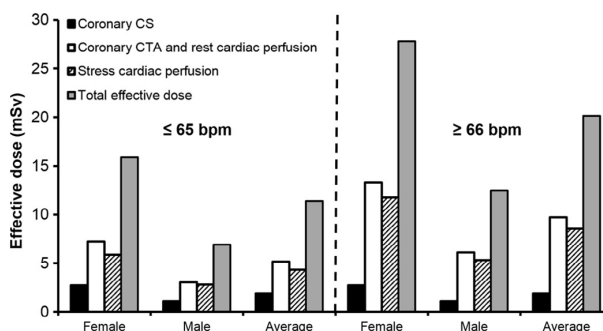


**Figure 3.** Absolute effective dose values for females and males, and gender averaged values, at low ( $\leq 65$  bpm) and high ( $\geq 66$  bpm) heart rates, and for coronary calcium score, coronary CTA including rest cardiac perfusion, and stress cardiac perfusion.

#### Effective dose of the CORE320 cardiac CT protocol

Figure 3 shows the effective dose values at high ( $\geq 66$  bpm, dual beat acquisition) and low heart rates ( $\leq 65$  bpm, single beat acquisition). Effective dose is shown separately for females and males and also gender averaged. Furthermore, the contribution of the three cardiac acquisitions (coronary calcium score, coronary CTA, stress myocardial perfusion) is shown. Effective doses for females were substantially higher compared to males. Effective doses were also substantially higher at high heart rates because in this case, a dual heart beat acquisition is performed, whereas for low heart rates, a single heart beat acquisition is feasible. Gender averaged effective dose was 1.9 mSv for coronary calcium score; 5.1 mSv for coronary CTA at low heart rates, and 9.7 mSv, at high heart rates. For stress myocardial perfusion, it was 4.3 mSv at low heart rates and 8.5 mSv at high heart rates.

#### Comparison with other dosimetric methods

The MC algorithm calculated organ doses (phantom off-centered, without arms) were compared with those obtained with the ImpACT CT patient dosimetry calculator (Fig. 4). The organ doses from this study are presented as an average for males and females. The relative differences between doses obtained from MC and doses from the ImpACT CT Patient Dosimetry Calculator are also indicated for each organ. There is reasonable agreement (differences lower than 15%) for some organs, like heart, lungs, esophagus; and large differences (between 60 and 90%) for other organs, particularly organs at the border between chest and abdomen, like spleen, stomach and liver; or between chest and neck, like thymus and thyroid.

Table 4 shows effective dose and k-factors for coronary CTA at low heart rates ( $\leq 65$  bpm). Three new k-factors were calculated in this study for a cardiac CT acquisition (for male, female and averaged) and a k-factor was derived from the ImpACT dosimetry application for the CORE320 cardiac CT acquisition. Additional effective doses were derived from k-factors that were published by several research groups and the European Commission (EC) [10,15–20]. Substantial differences in effective dose assessment, ranging from 2.6 to 5.6 for the average patient, and the associated k-factors (ranging from 0.014 to 0.030 for the average patient) were observed.

#### Discussion

The average effective dose for the standard sized female and male voxel phantoms (ICRP 110) is of the order of magnitude of 10 mSv

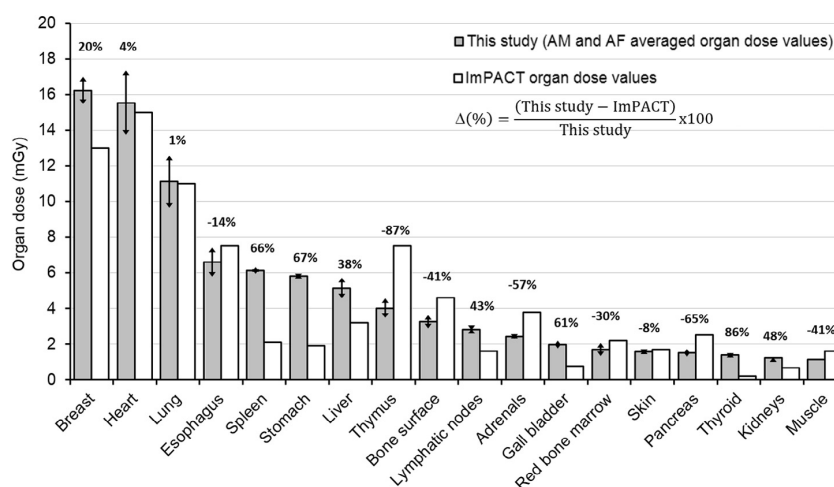


**Figure 4.** Absolute organ doses, averaged for females and males, for coronary CTA and rest cardiac perfusion, at a low heart rate ( $\leq 65$  bpm), results from this study (phantom off-centered, without arms) are compared with values that are calculated with the ImPACT CT patient dosimetry calculator. The relative differences on dose between the two approaches are also calculated, ( $\Delta$  (%)). The arrows represent the standard deviations of organ doses for AM and AF phantoms.

at low heart rates and 20 mSv at high heart rates for the comprehensive CORE320 cardiac CT protocol calculated according to the ICRP 103 recommendation [4,5]. This protocol includes coronary calcium scoring, combined coronary CT angiography that comprises rest myocardial perfusion, and stress myocardial perfusion. The effective dose is higher at high heart rates since in that case a dual heart beat acquisition is used in order to improve the temporal resolution, whereas at lower heart rates a single heart beat acquisition is selected. The effect of gender was substantial, effective dose for the female phantom was more than double compared to the dose for the male phantom which is mainly due to the high weighting factor for breast tissue.

To make the dose assessment for the cardiac CT acquisition more accurate, special attention was paid to the scanner geometry and patient positioning in clinical practice. X-ray beam characteristics of the Aquilion ONE CT scanner were incorporated in the MC algorithm. Furthermore, phantom positioning was performed according to the clinical practice by removing the arms from the two standard ICRP voxel phantoms from the scan region and the alignment of the phantoms with the heart along the axis of

rotation. Modifying the ICRP phantoms by removing the arms from the scan region had a noticeable effect on the dose estimation, leading to an increase of effective dose of about 6–8%. Removing the arms from the scan region increases the dose received by the trunk and since the organs and tissues in the trunk contribute more to the effective dose compared to those in the arms, its value is increased. It is recommended to modify the standard ICRP voxel phantoms accordingly for dose estimations of those CT acquisitions where the trunk of the patient is scanned with the arms positioned along the head. The effect on effective dose of the position of the patient, either centered or off-centered, was negligible.

There are three different approaches for patient dosimetry in CT that, arranged by increasing complexity and accuracy, are the following. The most basic strategy is the use of the so-called k-factors that are conversion factors for calculating effective dose from dose-length product [8–14]. The k-factors are neither specific for a certain type of CT scanner nor specific for the actual scan range and anatomy. These are serious drawbacks, since effective dose depends on the technical design of the CT scanner and the actual scanned anatomy. The use of dosimetric software such as the ImPACT CT Patient Dosimetry Calculator represents a step in increasing accuracy as it takes into account more details about the acquisition protocol and CT scanner. Monte Carlo (MC) simulations, which were used in this study, are the most advanced and versatile approach as the code can be adapted accurately to reproduce the specific dosimetric question and the actual exposure conditions.

Relatively low effective doses were derived from k-factors published by the EC and Deak, respectively 2.6 mSv and 2.7 mSv [11,22], an intermediate value of 4.1 mSv when applying the k-factor from Seguchi [14]. Higher effective dose values, similar to the 5.1 mSv derived from this study, were calculated with the k-factors published by Huda (4.8 mSv), Gosling (5.2 mSv), Einstein (5.4 mSv) and Geleijns (5.6 mSv), respectively [8,10,12,13]. Differences in the CT protocol, either general chest or dedicated cardiac CT, probably explain the biggest observed difference in k-factors. The rather low k-factors in the publications of the EC and Deak et al., are based on general chest CT. A k-factor specific for cardiac CT is expected to be higher, mainly because of the more prominent contribution of the breast tissue to effective dose in cardiac CT compared to general chest CT. The study of Seguchi et al. was performed with a relatively small phantom representing a standard Japanese adult male, this may

**Table 4**

The effective dose according to ICRP 103 and k-factors for the coronary CTA and rest cardiac perfusion acquisition protocol at low heart rates ( $\leq 65$  bpm).

Dosimetry	Effective dose mSv	k-factor mSv/mGy.cm
This study		
Female ( $\leq 65$ bpm)	7.2	0.041
Male ( $\leq 65$ bpm)	3.0	0.016
Average ( $\leq 65$ bpm)	5.1	0.028
Based on software		
ImPACT [21]	4.2	0.023
Based on k-factor <sup>a</sup>		
EC [17]	2.6 <sup>b</sup>	0.014
Deak et al. [15]	2.7	0.0145
Seguchi et al. [20]	4.1	0.022
Huda et al. [16]	4.8	0.026
Gosling et al. [19]	5.2	0.028
Einstein et al. [18]	5.4	0.029
Geleijns et al. [10]	5.6	0.030

<sup>a</sup> Effective dose calculated for the acquisition protocol of this study by using different k-factors.

<sup>b</sup> Effective dose calculation based on ICRP 60.

explain their intermediate result. Other differences in k-factors may be attributable to different definitions of effective dose, either effective dose according to ICRP60 or ICRP103, differences in dosimetry, either a simulation or actual measurements and differences in phantoms.

An alternative is to calculate organ doses and effective dose with readily available dosimetric tools. A widely used tool for this purpose is the ImpACT CT Patient Dosimetry Calculator. With such dosimetric tools the actual scan range can be defined accurately and the calculation of effective dose can be roughly adapted to the design of the CT scanner. A limitation of both the k-factors and the available dosimetric tools is that they do not allow patient positioning such as in cardiac CT, i.e. with an offset of the patient in order to align the axis of rotation of the scanner with the heart of the patient. Another limitation is that all currently available techniques for dose estimation in CT do not allow for calculation of organ dose and effective dose according to the latest recommended voxel phantoms. Shortcoming of these techniques is that they are outdated and inaccurate.

Some methodological differences between the MC algorithm and the ImpACT calculator that may explain the differences in organ dose, like the two voxel phantoms in the MC algorithm versus the hermaphrodite mathematical phantom in the ImpACT calculator; accurate modeling of the scanner versus 'scanner matching'; correct positioning of the patient (off-center, arms out of the scanned range) versus standard positioning of the patient (centered, arms along the body).

With the MC calculations that are presented in this study all these limitations can be overcome as they conveniently allowed for: 1. the implementation of the ICRP and ICRU jointly adopted concept of voxel or computational phantoms for adult humans; 2. the application of the updated ICRP tissue weighting factors that are recommended for the calculation of effective dose; and 3. accurately modeling of the cardiac CT acquisition protocol.

It should be concluded that effective dose is substantially underestimated with the ImpACT CT Patient Dosimetry Calculator and with some k-factors. K-factors lower than 0.025 mSv/mGy.cm should be regarded as inaccurate for cardiac CT and should not be used anymore. However, when comparing the results of this study with k-factors derived by Gosling, Einstein and Geleijns [8,12,13] they are very similar. This is surprising since the k-factors from these publications were obtained by applying dosimetric techniques that do not adequately fulfill the current recommendations of the ICRP Publication 110 for the calculation of the effective dose by using voxel phantoms that provide a more realistic and accurate representation of human anatomy [23].

Table 4 illustrates that special care is required when interpreting effective doses that are reported in other studies. Effective dose assessment may have been performed with a k-factor that is much too low, sometimes as low as 0.014 mSv/mGy.cm. According to current recommendations, such effective dose assessments lead to underestimation by a factor of 2 for the average patient (gender averaged), and underestimation by a factor of 3 for females.

In conclusion, MC simulations of organ dose and effective dose should be performed with two voxel phantoms, representing a reference adult male and female and serving as the international standard for dose calculations, dose assessment for a cardiac CT acquisition protocol used in a multicenter clinical trial was performed accordingly. Modifying the ICRP phantoms in accordance with clinical practice by removing the arms from the scan region had a noticeable effect on the dose estimation, leading to an increase of effective dose of about 6–8%. Previously published k-factors may lead

to underestimations of effective dose by a factor of 2 for an average patient and underestimation by a factor of 3 for a female patient. The results presented in this study could be considered as a frame of reference for effective dose assessment in cardiac CT.

## References

- [1] Dewey M, Zimmermann E, Deissenrieder F, Laule M, Dübel HP, Schlattmann P, et al. Noninvasive coronary angiography by 320-row computed tomography with lower radiation exposure and maintained diagnostic accuracy: comparison of results with cardiac catheterization in a head-to-head pilot investigation. *Circulation* 2009;120:867–75.
- [2] Kroft IJ, Roelofs JJ, Geleijns J. Scan time and patient dose for thoracic imaging in neonates and small children using axial volumetric 320-detector row CT compared to helical 64-, 32-, and 16- detector row CT acquisitions. *Pediatr Radiol* 2010;40:294–300.
- [3] George RT, Arab-Zadeh A, Cerci RJ, Vavere AL, Kitagawa K, Dewey M, et al. Diagnostic performance of combined noninvasive coronary angiography and myocardial perfusion imaging using 320-MDCT: the CT angiography and perfusion methods of the CORE320 multicenter multinational diagnostic study. *AJR Am J Roentgenol* 2011;197:829–37.
- [4] ICRP Publication 103. The 2007 recommendations of the International Commission on Radiological Protection. *Ann ICRP* 2007;37.
- [5] ICRP Publication 110. Adult reference computational phantoms. *Ann ICRP* 2009;39.
- [6] Rochitte CE, George RT, Chen MY, Arab-Zadeh A, Dewey M, Miller JM, et al. Computed tomography angiography and perfusion to assess coronary artery stenosis causing perfusion defects by single photon emission computed tomography: the CORE320 study. *Eur Heart J* 2014;35(17):1120–30.
- [7] Salvadó M, Cros M, Joemai RMS, Calzado A, Geleijns J. Monte Carlo simulation of the dose distribution of ICRP adult reference computational phantoms for acquisitions with a 320 detector-row cone-beam CT scanner. *Phys Med* 2015;31(5):452–62.
- [8] Geleijns J, Joemai RM, Dewey M, de Roos A, Zankl M, Cantera AC, et al. Radiation exposure to patients in a multicenter coronary angiography trial (CORE 64). *AJR Am J Roentgenol* 2011;196:1126–32.
- [9] Deak PD, Smal Y, Kalender WA. Multisection CT protocols: sex- and age-specific conversion factors used to determine effective dose from dose-length product. *Radiology* 2010;257:158–66.
- [10] Huda W, Tipnis S, Sterzik A, Schoepf UJ. Computing effective dose in cardiac CT. *Phys Med Biol* 2010;55:3675–84.
- [11] Bongartz G, Golding SJ, Jurik AG, et al. European guidelines on quality criteria for computed tomography. *EUR* 16262, ISBN 92-828-7478-8, ed, 1999.
- [12] Einstein AJ, Elliston CD, Arai AE, Chen MY, Mather R, Pearson GD, et al. Radiation dose from single-heartbeat coronary CT angiography performed with a 320-detector row volume scanner. *Radiology* 2010;254:698–706.
- [13] Gosling OE, Roobottom CA. Radiation exposure from cardiac computed tomography. *JACC Cardiovasc Imaging* 2010;3:1201–2.
- [14] Seguchi S, Aoyama T, Koyama S, Fujii K, Yamauchi-Kawaura C. Patient radiation dose in prospectively gated axial CT coronary angiography and retrospectively gated helical technique with a 320-detector row CT scanner. *Med Phys* 2010;37:5579–85.
- [15] Shrimpton PC, Edyvean S. CT scanner dosimetry. *Br J Radiol* 1998;71:1–3.
- [16] Morant JJ, Salvado M, Hernandez-Giron I, Casanovas R, Ortega R, Calzado A. Dosimetry of a cone beam CT device for oral and maxillofacial radiology using Monte Carlo techniques and ICRP adult reference computational phantoms. *Dentomaxillofac Radiol* 2013;42:92555893.
- [17] ICRP. Report of the Task Group on Reference Man, ICRP Publication 23, ICRP, 1975;23:1–480.
- [18] Geleijns J, Salvado AM, Veldkamp WJ, Lopez TM, Calzado CA. Quantitative assessment of selective in-plane shielding of tissues in computed tomography through evaluation of absorbed dose and image quality. *Eur Radiol* 2006;16:2334–40.
- [19] Morant JJ, Salvado M, Casanovas R, Hernandez-Giron I, Velasco E, Calzado A. Validation of a Monte Carlo simulation for dose assessment in dental cone beam CT examinations. *Phys Med* 2012;28:200–9.
- [20] Nelson WR, Hirayama H, Rogers DWO. The EGS code system. Report SLAC-265 ed: Stanford Linear Accelerator Center, 1985.
- [21] Hirayama H, Namito Y, Ban S. Implementation of a general treatment of photoelectric-related phenomena for compounds or mixtures in EGS4. KEK Internal Report 2000–3, 2000.
- [22] Deak P, van Straten M, Shrimpton PC, Zankl M, Kalender WA. Validation of a Monte Carlo tool for patient-specific dose simulations in multi-slice computed tomography. *Eur Radiol* 2007;18:759–72.
- [23] Zankl M, Petoussi-Hens N, Fill U, Regulla D. The application of voxel phantoms to the internal dosimetry of radionuclides. *Radiat Prot Dosimetry* 2003;105:539–48.

### 4.2.2 Dose assessment in perfusion CT

- [III] Cros M, Geleijns J, Joemai RMS, Salvadó M. Perfusion CT of the brain and liver and of lung tumors: Use of Monte Carlo simulation for patient dose estimation for examinations with a cone-beam 320-MDCT scanner. *Am Jour Roentgenol* 2016;206:129-35 (DOI: 10.2214/AJR.15.14913)

#### Abstract

*Objective:* The purpose of this study was to estimate the patient dose from perfusion CT examinations of the brain, lung tumors, and the liver on a cone-beam 320-MDCT scanner using a Monte Carlo simulation and the recommendations of the International Commission on Radiological Protection (ICRP).

*Materials and methods:* A Monte Carlo simulation based on the Electron Gamma Shower Version 4 package code was used to calculate organ doses and the effective dose in the reference computational phantoms for an adult man and adult woman as published by the ICRP. Three perfusion CT acquisition protocols – brain, lung tumor, and liver perfusion – were evaluated. Additionally, dose assessments were performed for the skin and for the eye lens. Conversion factors were obtained to estimate effective doses and organ doses from the volume CT dose index and dose-length product.

*Results:* The sex-averaged effective doses were approximately 4 mSv for perfusion CT of the brain and were between 23 and 26 mSv for the perfusion CT body protocols. The eye lens dose from the brain perfusion CT examination was approximately 153 mGy. The sex-averaged peak entrance skin dose (ESD) was 255 mGy for the brain perfusion CT studies, 157 mGy for the lung tumor perfusion CT studies, and 172 mGy for the liver perfusion CT studies.

*Conclusion:* The perfusion CT protocols for imaging the brain, lung tumors, and the liver performed on a 320-MDCT scanner yielded patient doses that are safely below the threshold doses for deterministic effects. The eye lens dose, peak ESD, and effective doses can be estimated for other clinical perfusion CT examinations from the conversion factors that were derived in this study.



## Perfusion CT of the Brain and Liver and of Lung Tumors: Use of Monte Carlo Simulation for Patient Dose Estimation for Examinations With a Cone-Beam 320-MDCT Scanner

Maria Cros<sup>1</sup>  
Jacob Geleijns<sup>2</sup>  
Raoul M. S. Joemai<sup>2</sup>  
Marçal Salvadó<sup>1</sup>

**OBJECTIVE.** The purpose of this study was to estimate the patient dose from perfusion CT examinations of the brain, lung tumors, and the liver on a cone-beam 320-MDCT scanner using a Monte Carlo simulation and the recommendations of the International Commission on Radiological Protection (ICRP).

**MATERIALS AND METHODS.** A Monte Carlo simulation based on the Electron Gamma Shower Version 4 package code was used to calculate organ doses and the effective dose in the reference computational phantoms for an adult man and adult woman as published by the ICRP. Three perfusion CT acquisition protocols—brain, lung tumor, and liver perfusion—were evaluated. Additionally, dose assessments were performed for the skin and for the eye lens. Conversion factors were obtained to estimate effective doses and organ doses from the volume CT dose index and dose-length product.

**RESULTS.** The sex-averaged effective doses were approximately 4 mSv for perfusion CT of the brain and were between 23 and 26 mSv for the perfusion CT body protocols. The eye lens dose from the brain perfusion CT examination was approximately 153 mGy. The sex-averaged peak entrance skin dose (ESD) was 255 mGy for the brain perfusion CT studies, 157 mGy for the lung tumor perfusion CT studies, and 172 mGy for the liver perfusion CT studies.

**CONCLUSION.** The perfusion CT protocols for imaging the brain, lung tumors, and the liver performed on a 320-MDCT scanner yielded patient doses that are safely below the threshold doses for deterministic effects. The eye lens dose, peak ESD, and effective doses can be estimated for other clinical perfusion CT examinations from the conversion factors that were derived in this study.

**Keywords:** cone-beam 320-MDCT scanner, International Commission on Radiological Protection (ICRP) computational phantoms, Monte Carlo simulation, patient dose assessment, perfusion CT

DOI:10.2214/AJR.15.14913

Received April 27, 2015; accepted after revision July 21, 2015.

<sup>1</sup>Medical Physics Unit, Faculty of Medicine and Health Sciences, Universitat Rovira i Virgili, C/Sant Llorenç 21, 43201 Reus, Tarragona, Spain. Address correspondence to M. Cros (maria.cros@urv.cat).

<sup>2</sup>Department of Radiology, Leiden University Medical Center, Leiden, The Netherlands.

AJR 2016; 206:129–135

0361–803X/16/2061–129

© American Roentgen Ray Society

**T**here is a growing interest in the use of perfusion CT of a wide variety of organs for either research or clinical applications; however, there is also growing concern with regard to radiation exposure of patients from CT in general and from perfusion CT studies in particular [1]. This study addresses the radiation exposure from perfusion CT studies of the brain, lung, and liver with a volumetric 320-MDCT scanner and a 160-mm-wide cone beam.

During perfusion CT studies, IV administration of iodine is performed. Perfusion CT studies require repeated acquisitions of the volume of interest during the first pass of the contrast material, lasting approximately 1 minute, but may also include delayed phases, lasting from 2 to 10 minutes. The dynamic perfusion CT study thus involves a series of continuous or intermittent acquisitions for which the timing of each acquisition, the tube voltage, the tube current, and the rota-

tion time are optimized to achieve the required quality of the study with an optimized radiation exposure of the patient. Various models are being used to derive quantitative information from perfusion CT studies, such as deconvolution or maximum-slope models. Functional hemodynamic parameters, such as blood flow, blood volume, mean transit time, and time to peak enhancement, can be derived from perfusion CT studies.

Particular advantages of perfusion CT are that CT scanners are available for acute patients both during and after working hours and that the perfusion CT examinations are relatively easy to perform. Moreover, perfusion CT results are well suited for quantitative analysis because the voxel values are expressed as Hounsfield units that are related to the linear attenuation coefficient of the tissue, which is sensitive to the concentration of iodine.

The primary application of perfusion CT of the brain is for the diagnosis and assess-



Cros et al.

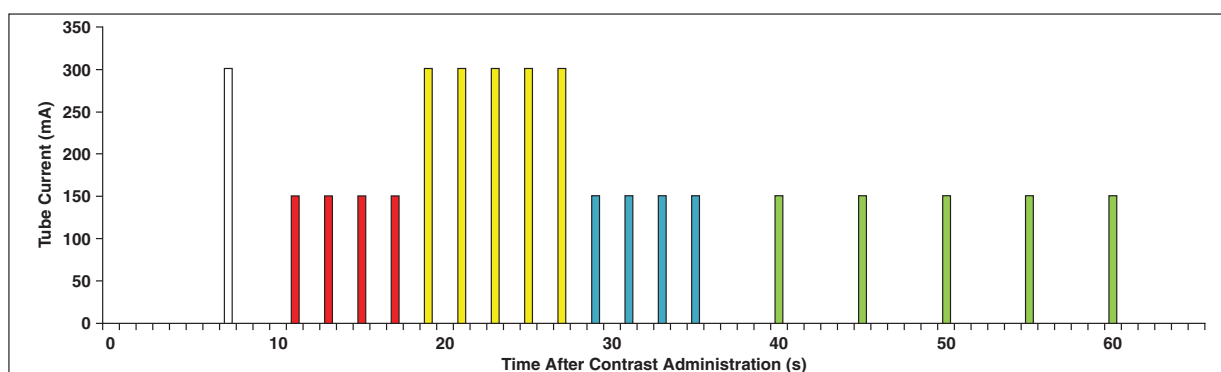


Fig. 1—Bar graph shows tube current values for dynamic acquisition sequences performed for brain perfusion CT examinations. White = mask, red = early arterial phase, yellow = peak arterial phase, blue = late arterial phase, green = venous phase.

ment of stroke [2]. Since the introduction of dynamic volumetric CT of the entire brain, this use of perfusion CT has become a relatively common clinical application. For perfusion CT of the body, the primary application is in oncology—for example, for lesion characterization and for assessment of tumor response to medication or radiation [3, 4]. Perfusion CT studies are still performed primarily as research applications.

Radiation protection in perfusion CT studies is particularly relevant because patient dose rises substantially during the dynamic study when the volume of interest is scanned repeatedly. In perfusion CT studies, it is of interest to assess organ dose and effective dose. With the recent insight that the eye lens is sensitive for radiation-induced cataract [5], it is also of importance to assess the dose to the eye lens during perfusion CT of the brain. It is also necessary to assess the peak entrance skin dose (ESD) accurately for perfusion CT acquisitions because the threshold dose for induction of deterministic skin effects is relatively low, and the skin dose accumulates significantly during the study. The sensitivity of skin is different at different body parts. The mildest deterministic effect that will be observed for the skin of the skull is epilation, but for the body, the mildest effect is skin erythema [6]. Deterministic skin effects are not expected at a peak ESD of less than 2000 mGy. In the past, incorrectly designed acquisition protocols caused an excessively high skin dose for perfusion CT studies of the brain and led to epilation of the skin in certain patients [7]; these cases stress the importance of assessment of skin dose for perfusion CT studies [7].

Patient dosimetry in perfusion CT studies should be performed according to the

latest international standards. This requirement means that the effective dose should be calculated according to the latest definitions of the International Commission on Radiological Protection (ICRP) [8]. Moreover, the ICRP has recently published voxel models for the standard adult man and standard adult woman that realistically reproduce human anatomy for dose assessments [9]. Dose assessments for these voxel phantoms can be performed with Monte Carlo simulations.

The purpose of this study was to evaluate patient dose for clinical perfusion CT protocols for imaging the body and the brain. The dosimetric characteristics of the volumetric scanner that was used for the perfusion CT examinations in this study (Aquilion ONE, Toshiba Medical Systems) were modeled in an algorithm for Monte Carlo simulations, and the two ICRP voxel phantoms were included in these simulations. Organ dose (including dose to the eye lens), effective dose, and ESD were assessed. The results are correlated with well-established standards in CT dosimetry, the volume CT dose index ( $CTDI_{vol}$ ), and dose-length product (DLP) to determine the corresponding conversion factors.

## Materials and Methods

### Monte Carlo Simulation

A Monte Carlo simulation-based code was used to perform the simulations. The program was developed and validated for a cone-beam 320-MDCT scanner (Aquilion ONE) in a previous study [10]. For the calculation of radiation transport, the Electron Gamma Shower Version 4 (EGS4) package (Stanford Linear Accelerator Center) [11] in combination with low-energy photon scattering expansion (National Laboratory for High Energy Physics) [12] was used. The developed Monte Carlo tool takes into account all as-

pects that have an effect on dose during a CT study, such as x-ray spectrum, x-ray collimation characteristics (including the penumbra), bowtie filtration (related to field size), and heel effect. Additionally, CT acquisition protocol parameters, such as tube voltage, tube current, pitch, tube position, and scanning range, are introduced as inputs. According to the given parameters, the program calculates the absorbed energy in each voxel of the volume, and 3D dose distributions are generated.

The Monte Carlo simulations were performed at a supercomputing center and were performed using  $20 \times 10^6$  photon histories. The computation time for one acquisition—that is, one full rotation for a volumetric acquisition—was 20 minutes on average.

### Voxel Phantoms

The adult reference computational phantoms for an adult man and an adult woman published by the ICRP [9] were used in this study. These phantoms were constructed from CT images of patients and represent an average adult man (average height, 178 cm; average weight, 73 kg) and an average adult woman (average height, 168 cm; average weight, 60 kg). The voxel size is  $2.137 \times 2.137 \times 8.000 \text{ mm}^3$  for the male phantom and  $1.775 \times 1.775 \times 4.840 \text{ mm}^3$  for the female phantom. The implementation of adult male and adult female phantoms in the simulation program was performed using the information (mass, spatial distribution, and composition) of each organ or tissue provided in an ICRP report [9]. Each voxel phantom was implemented as three different representations: one concerning the 53 materials to define their chemical properties used during the radiation transport, one to classify the 141 organs or tissues, and one to label the 29 organs that contribute to the effective dose calculation. This type of classification is useful to calculate the dose of each organ or tissue when the simulation is finished. Because microscopic structures of the skeleton are smaller

## Patient Dose From Perfusion CT

than the size of a voxel, a specific subsegmentation was implemented for tissues containing red bone marrow or endosteum (bone surface). In addition, the energy of the secondary particles released from mineral bone components was taken into account through an enhancement factor.

## Perfusion CT Acquisition Protocols

The Monte Carlo simulations were performed using three different perfusion CT acquisition protocols: brain, lung tumor, and liver. The parameters for the three protocols are provided in Table 1. In the brain perfusion CT protocol, a series of intermittent volume scans were obtained over a 60-second period. The first volume was used as the mask for dynamic subtraction, and the next series are performed every 2 seconds during the arterial phase (early arterial, peak arterial, and late arterial); the tube current was increased in the peak arterial phase to ensure that the appropriate image quality was achieved. The last series acquires volumes every 5 seconds to capture the slower venous flow. Figure 1 shows a schematic representation of the dynamic acquisition sequence for the brain perfusion CT protocol.

All of the acquisitions were obtained as axial volumetric scans with a nominal beam width of 160 mm. The nominal scanning length was 160

**TABLE 1: Acquisition Parameters for the Three Perfusion CT Examinations According to the Manufacturer's Recommendations<sup>a</sup>**

Perfusion CT Examinations	Peak Tube Voltage (kVp)	Rotation Time (s)	Tube Current (mA)	No. of Scans	Total Tube Current-Exposure Time Product (mAs)	FOV
Brain						
Mask	80	0.75	300	1	225	S
Early arterial phase	80	0.75	150	4	450	S
Peak arterial phase	80	0.75	300	5	1125	S
Late arterial phase	80	0.75	150	4	450	S
Venous phase	80	0.75	150	5	562.5	S
Lung tumor	100	0.5	60	36	1080	M
Liver	100	0.5	100	23	1150	L

Note—S = small bow-tie filter, M = medium bow-tie filter, L = large bow-tie filter.  
<sup>a</sup>Aquilion ONE, Toshiba Medical Systems.

mm in all cases, and the actual exposed length was 170 mm, considering overbeaming. The arms of the phantoms were removed for the lung tumor and liver perfusion CT protocols, thus taking into account that the arms are not positioned alongside the body but are positioned above the head during these clinical perfusion CT examinations.

The lung tumor perfusion CT protocol is performed with 40–60 mL of IV contrast medium administered at a flow rate of 5–7 mL/s, the liver

perfusion CT protocol is performed with 30–80 mL of contrast medium administered at a flow rate of 6–10 mL/s, and the brain perfusion CT protocol is performed with 50 mL of contrast medium administered at a flow rate of 5–6 mL/s depending on patient weight. All the protocols are performed with a contrast medium with a concentration of 370 mg I/mL.

## Dose Calculations

Monte Carlo simulations using the acquisition parameters shown in Table 1 for the three perfusion CT protocols were performed with two standard CT dose phantoms (150 mm-long; head phantom: 160 mm diameter; body phantom: 320 mm diameter) using a 100-mm-long CT ionization chamber and following the same methods used in previous studies [10, 13]. The  $CTDI_{vol}$  values were obtained from the simulations for each perfusion CT study, which corresponds to the average dose in the 100-cm-long CT ionizing chamber according to the definition published by the International Electrotechnical Commission [14]. The results were compared with the  $CTDI_{vol}$  value that appeared in the console of the Aquilion ONE scanner for each perfusion CT protocol. The differences between the results and the values on the console were approximately 1%.

The mean absorbed dose in each organ or tissue was computed as the total absorbed energy in the voxels corresponding to the organ or tissue divided by the total mass. Sex-specific calculations of effective doses were performed using the tissue-weighting factors from ICRP Report 103 [8] for each protocol. Additionally, sex-averaged effective doses were calculated considering a tissue-weighting factor of 0.24 for breast tissue of the adult female phantom and no tissue-weighting factor for breast of the adult male phantom. These averaged effective dose results were also normalized to the total tube charge (i.e.,

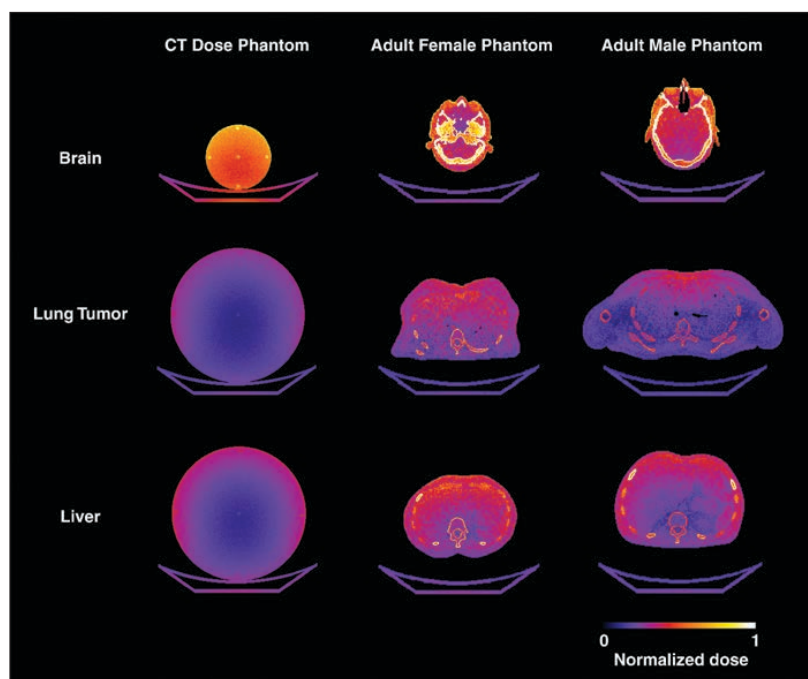


**Fig. 2—**Normalized dose distributions in CT dose phantom (left), adult female phantom (middle), and adult male phantom (right) for brain perfusion CT examinations (top row), lung tumor perfusion CT examinations (middle row), and liver perfusion CT examinations (bottom row).

Cros et al.

**TABLE 2: Dose-Length Product (DLP), Effective Dose, and Conversion Factors for Estimating Effective Dose From DLP for the Three Perfusion CT Examinations**

Perfusion CT Examinations	DLP (mGy × cm)	Effective Dose (mSv)			Sex-Averaged Effective Dose Normalized to Total Tube Current–Exposure Time Product (× 10 <sup>-3</sup> mSv/mAs)	Conversion Factors for Estimating Effective Dose From DLP (× 10 <sup>-3</sup> mSv/mGy × cm)
		Adult Male Phantom	Adult Female Phantom	Sex-Averaged		
Brain	3016	3.5	4.6	4.1	1.5	1.4
Lung tumor	995	17.0	25.0	23.4	21.7	23.5
Liver	1175	27.3	26.3	25.7	22.3	21.9

total tube current–exposure time product). For each protocol, the DLP was derived from the CTDI<sub>vol</sub> obtained from the simulations with the CT dose phantoms and taking into account the nominal scanning length. Additionally, conversion factors for estimating the effective dose from DLP were calculated.

**Eye Lens Dose and Peak Entrance Skin Dose Estimations**

Although not required for the effective dose calculation, the absorbed dose of the eye lens in the adult male phantom and adult female phantom was reported for the brain perfusion CT protocol. Moreover, the sex-averaged eye lens dose was calculated. For the peak ESD estimation, dose distributions in voxels identified as skin were generated for each protocol (brain, lung tumor, and liver). The peak ESD was computed by selecting the region with the highest value of absorbed dose and by averaging the dose values of the voxels in this region equivalent to 1 cm<sup>2</sup> of skin surface. The sex-averaged peak ESD was calculated. Conversion factors to estimate the eye lens dose and the peak ESD from CTDI<sub>vol</sub> were also obtained.

**Results**

The Monte Carlo program used to perform the simulations, which reproduce accurately the dosimetric characteristics of the Aquilion ONE scanner, enabled the dose assessments in the ICRP voxel phantoms (adult male and adult female phantoms) for the perfusion CT brain, lung tumor, and liver acquisitions.

Figure 2 shows the normalized dose distributions of one axial section in three phan-

toms—the CT dose phantom, the adult male phantom, and the adult female phantom—for the three perfusion CT protocols. The regions with the highest absorbed dose can be identified, such as the skeleton for all perfusion CT acquisitions. Absorbed doses for the adult male and adult female phantoms are presented in Figure 3 for the three perfusion CT protocols. Selection was based on either an exceeded limit of 10 mGy or a total percentage contribution to the effective dose of greater than 90%. The corresponding CTDI<sub>vol</sub> is indicated for comparison with the organ doses.

Table 2 shows the DLPs and the effective doses for the brain, lung tumor, and liver perfusion CT protocols. Effective doses are presented separately for adult male and adult female phantoms and are also sex-averaged and normalized to the total tube charge. The DLP-to-effective dose conversion factors are also shown for the three perfusion CT acquisitions. For the brain perfusion CT protocol, the total effective dose was computed by the sum of the contribution of the five series performed with different acquisition parameters (Fig. 4).

The eye lens dose for the brain perfusion CT protocol and the peak ESD for all perfusion CT studies are presented in Table 3 and are compared with the CTDI<sub>vol</sub> values. The absorbed dose distribution in the voxels identified as skin in the adult female phantom derived from a brain perfusion CT acquisition is presented as a cumulative dose-

volume histogram (Fig. 5). This histogram relates radiation dose, which is represented along the horizontal axis, to the volume of skin receiving radiation greater than or equal to the corresponding dose.

**Discussion**

This study used a Monte Carlo simulation tool to estimate the radiation dose from brain, lung tumor, and liver perfusion CT protocols using the adult male and adult female voxel phantoms from the ICRP and a cone-beam 320-MDCT scanner. Conversion factors were obtained to estimate effective doses from values that are indicated on the scanner console, such as CTDI<sub>vol</sub> and DLP. Moreover, dose assessment was performed for the skin and eye lens.

Dose distributions in the three phantoms used (CT dose phantom, adult male phantom, and adult female phantom) can be compared using the calculation of the average dose volume. The average dose volume, computed as the total energy in the directly irradiated volume divided by the total mass in the same volume and averaged for male and female phantoms, was 182.8 mGy for brain perfusion CT studies and 58.7 and 73.6 mGy for lung tumor and liver perfusion CT studies, respectively. These results were close to the corresponding CTDI<sub>vol</sub>, representing 97%, 94%, and 100% of the respective CTDI<sub>vol</sub> values.

A similar relationship can be observed in Figure 3. The organ doses were higher for

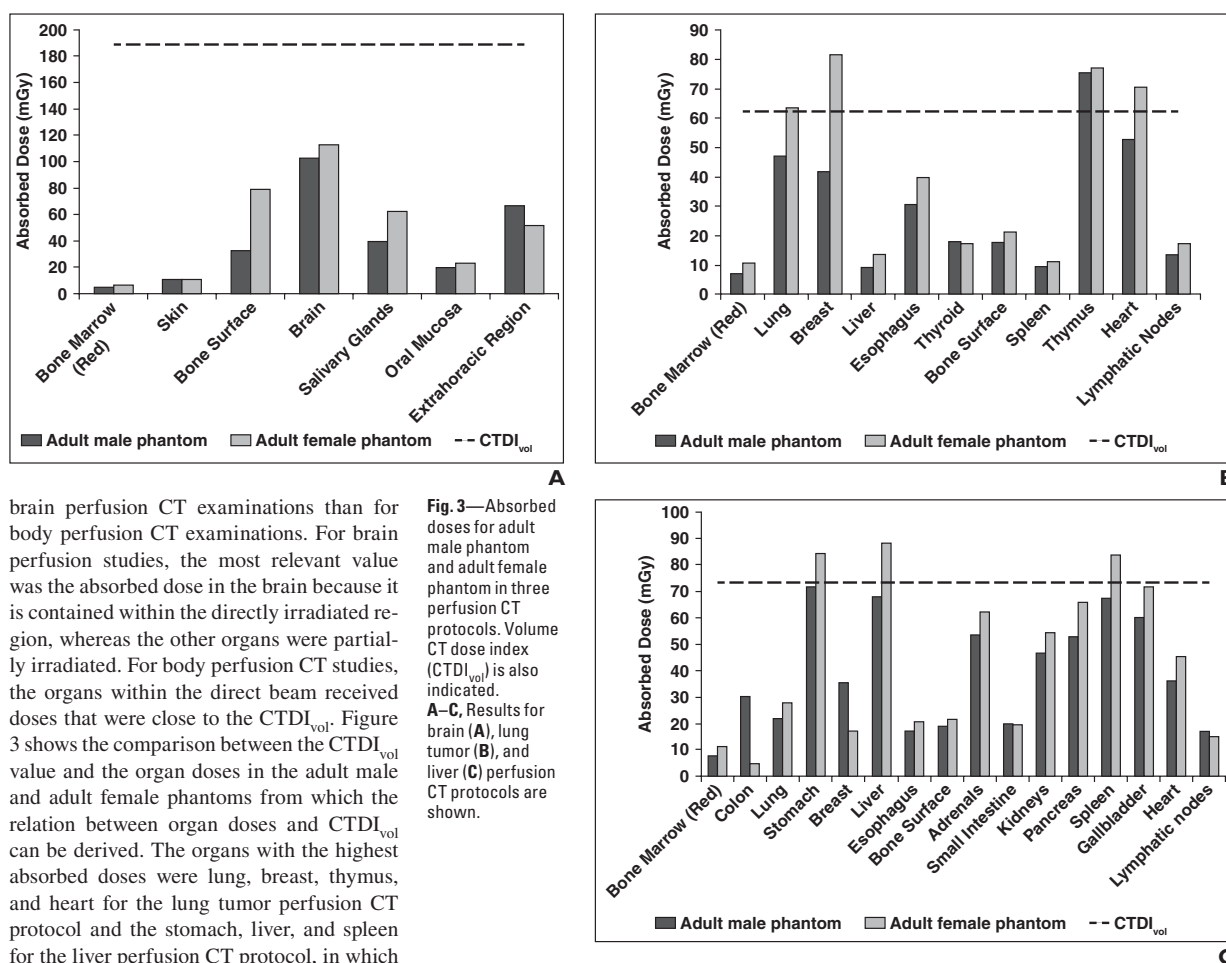
**TABLE 3: Eye Lens Dose for Brain Perfusion CT and Peak Entrance Skin Dose (ESD) for the Three Perfusion CT Examinations**

Perfusion CT Examination	CTDI <sub>vol</sub> (mGy)	Eye Lens				Peak ESD	
		Absorbed Dose (mGy)			% of CTDI <sub>vol</sub>	Sex-Averaged Absorbed Dose (mGy)	% of CTDI <sub>vol</sub>
		Adult Male Phantom	Adult Female Phantom	Sex-Averaged			
Brain	188.5	168.1	137.7	152.9	81.1	255	135
Lung tumor	62.3					157	252
Liver	73.6					172	234

Note—CTDI<sub>vol</sub> = volume CT dose index.

Downloaded from www.ajronline.org by Univ Rovira I Virgili on 01/18/16 from IP address 193.147.222.244. Copyright ARRS. For personal use only; all rights reserved

## Patient Dose From Perfusion CT



brain perfusion CT examinations than for body perfusion CT examinations. For brain perfusion studies, the most relevant value was the absorbed dose in the brain because it is contained within the directly irradiated region, whereas the other organs were partially irradiated. For body perfusion CT studies, the organs within the direct beam received doses that were close to the CTDI<sub>vol</sub>. Figure 3 shows the comparison between the CTDI<sub>vol</sub> value and the organ doses in the adult male and adult female phantoms from which the relation between organ doses and CTDI<sub>vol</sub> can be derived. The organs with the highest absorbed doses were lung, breast, thymus, and heart for the lung tumor perfusion CT protocol and the stomach, liver, and spleen for the liver perfusion CT protocol, in which the partially irradiated organs, such as adrenals, kidneys, pancreas, and gallbladder, also received a substantial absorbed dose.

Several relevant differences between organ doses in the adult male and adult female phantoms can be observed. For the brain perfusion CT protocol, the quotient between bone surface dose in the adult female phantom and adult male phantom was 2.4. These differences can be explained because bone surface mass in men is twice the mass in women and the absorbed energy in women is 30% higher than in men. For the perfusion CT liver examinations, doses in the colon and breast in the adult male phantom were higher than these organ doses in the adult female phantom. This difference can be explained because the directly irradiated volume proportions of colon and breast are larger in the adult male phantom than in the adult female phantom: 69.3% of the breast volume is irradiated in the adult male phan-

**Fig. 3**—Absorbed doses for adult male phantom and adult female phantom in three perfusion CT protocols. Volume CT dose index (CTDI<sub>vol</sub>) is also indicated. **A–C**, Results for brain (A), lung tumor (B), and liver (C) perfusion CT protocols are shown.

tom and 11.0% in the adult female phantom and 44.7% of the colon volume is irradiated in the adult male phantom and 0.5% in the adult female phantom.

The sex-averaged effective doses from the brain perfusion CT studies were approximately 4 mSv. As can be observed in Figure 4, the maximum contribution was from the peak arterial series because of the total tube current used in it. The effective dose for the adult female phantom was higher than that for the adult male phantom for all five series, even though a proportional contribution can be observed in each series of the protocol. For the lung tumor and liver perfusion CT studies, the sex-averaged effective doses were 5.8 and 6.3 times higher than the effective dose from the brain perfusion CT studies, respectively. For the liver examinations, the effective dose in the adult male phantom was slightly higher than that in the adult female phantom because of the large contribu-

tion of colon and breast organ doses. In this case, because no tissue-weighting factor for breast in adult men was used, the sex-averaged effective dose was lower than the same sex-specific values.

The DLPs for the liver and lung tumor examinations were of the order of magnitude of 1000 mGy × cm, whereas for the brain examinations, the DLP was 3 times higher. These results reflect the differences in the total tube current used in the brain perfusion CT studies compared with the body perfusion CT studies. Additionally, these values are influenced by the size differences (i.e., attenuation differences) between the head and the body of the phantoms.

The effective doses obtained in this study are consistent with the results reported by other authors (3.6 mSv) for a similar brain perfusion CT protocol on a 320-MDCT scanner using thermoluminescent dosimeters (TLDs) in a Rando phantom (The Phan-

Cros et al.

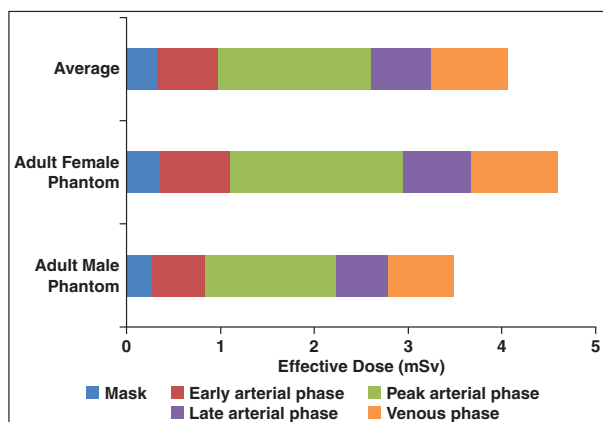


Fig. 4—Schematic shows contribution to effective dose of each series in brain perfusion CT protocol.

172 mGy for the liver perfusion CT studies. Thus, the maximum ESDs from brain, lung tumor, and liver perfusion CT studies in an Aquilion ONE unit were lower than these thresholds, representing 8–13% of the lowest dose threshold.

Conversion factors to estimate the peak ESD from  $CTDI_{vol}$  for the three perfusion CT protocols were provided from the data provided in Table 3. These values, which can be a useful tool in clinical practice, were 1.4, 2.5, and 2.3 mSv/mGy for the brain, lung tumor, and liver perfusion CT protocols, respectively.

In the case of a brain perfusion CT examination, which presents higher skin doses, Figure 5 shows a detailed analysis of the dose in all the voxels identified as skin in an adult female phantom. The percentage of skin voxels that received each absorbed dose (presented in milligrays) can be read from the skin dose–volume histogram: 16% of the skin voxels received some part of the dose, from which approximately 60% received doses lower than 110 mGy. From the dose distribution map, voxels with values greater than 110 mGy were identified as those that are directly irradiated. The noncumulative dose–volume histogram in the directly irradiated area corresponds to a gaussian function, where the maximum is 192 mGy (mean dose in voxels within the scanning area). This mean skin dose corresponds to 75% of the peak ESD, but it is closer to the  $CTDI_{vol}$ . The results presented in this study were higher than those published by other authors for a 320-MDCT scanner [15]; in that study, the authors measured skin dose in a scanned area (92 mGy) using a located TLD's measurement, but they were not able to determine the peak ESD [15].

tom Laboratory) [15]. Other studies use k factors, obtained from 64-MDCT scanners [16, 17], to quantify the effective dose associated with head or body perfusion 320-MDCT protocols. In comparison with the results of the current study, these k factors overestimated the effective dose by approximately 63% in the brain perfusion CT protocol and underestimated it by approximately 34% in the body perfusion CT acquisitions. To our knowledge, studies on effective doses for body perfusion CT protocols using simulations or measurements in anthropomorphic phantoms have not been published.

The sex-averaged eye lens dose from the brain perfusion CT examinations was approximately 153 mGy, which is 81% of the  $CTDI_{vol}$ . The eye lens dose in the adult female phantom was lower than that in the adult male phantom due to the position of the eyes in the head. The fraction of bone in the same slice of eye lens in the adult female phantom is larger than that in the adult male phantom, leading to a higher attenuation of radiation in the adult female phantom. The organ doses do not exceed the thresholds suggested by ICRP guidelines for the deterministic effects in the lens of the eyes [18]. The lowest threshold is 500 mGy for a posterior subcapsular cataract with a period of latency of 8 years. Because sensitivity to radiation can differ depending on patient age and patient disease, eye lens dose must be taken into account on a patient-by-patient basis. Moreover, radiation can accelerate cataracts caused by other factors (e.g., ultraviolet B radiation, diabetes, corticosteroid use). The results from the current study are higher than those published by other authors for similar brain protocols with a volumetric 320-MDCT scanner but using TLD

measurements in a Rando phantom [15]. This discrepancy in results can be explained by the differences in the phantoms used.

Although skin doses were on the order of magnitude of 10 mGy in the three perfusion CT studies, the peak ESDs in the directly irradiated region were more relevant and must be evaluated. The thresholds in a single brief exposure for early transient erythema and temporary epilation are 2000 and 3000 mGy, respectively [18]. These values represent a dose average for the entire population; as a consequence, possible variations in patients must be considered. The sensitivity to radiation differs depending on factors such as the dose rate or the irradiated area; for example, the skin of the head is more resistant to radiation than the irradiated skin in a lung examination. However, in the current study, the peak ESD was 255 mGy for the brain perfusion CT protocol, 157 mGy for the lung tumor perfusion CT studies, and

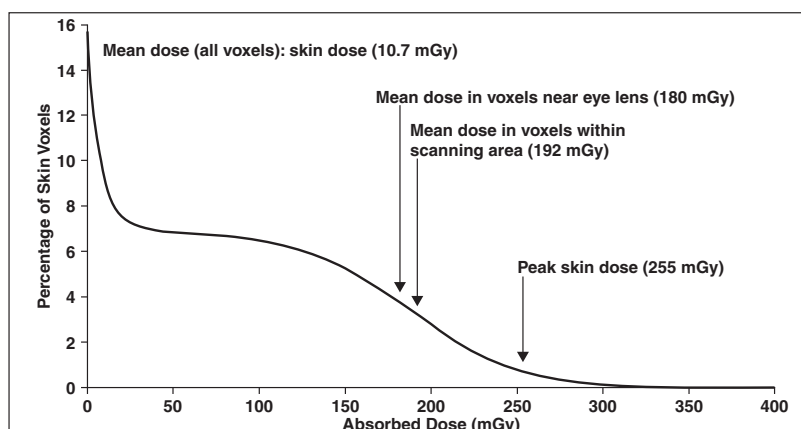


Fig. 5—Cumulative dose–volume histogram for skin derived from brain perfusion CT examination of adult female phantom. Normalized number of voxels for each absorbed dose value (in milligrays) is shown.

### Patient Dose From Perfusion CT

In clinical practice, the results of the current study can be useful to estimate dose for patients from the data shown in the console of the Aquilion ONE unit. However, a limitation is that this study focuses on “standard” adult patients. Because the sizes of adult heads have small individual differences, the results obtained for the brain perfusion CT studies can be a good estimation of patient doses. For the body perfusion CT studies, size changes significantly depending on the patient. Thus, the effect of patient size on dose from body perfusion CT protocols needs to be analyzed in future studies.

The radiation dose from perfusion CT studies must be controlled to establish efficient, optimized, and safe protocols without losing relevant diagnostic imaging information. In this study, a Monte Carlo method was used to estimate organ and effective doses from perfusion CT studies of the brain, lung tumors, and liver using a 320-MDCT scanner and computational phantoms from the ICRP. The dose assessments in the eye lens and skin showed that thresholds for deterministic effects were not exceeded in the studied protocols. Clinically, the results presented in this study can be used to estimate eye lens dose, peak ESD, and effective doses from the data ( $CTDI_{vol}$  and DLP) that appear in the console of a 320-MDCT scanner (Aquilion ONE) and to ensure that the established protocol is operating below the deterministic effects dose limits.

In conclusion, although  $CTDI_{vol}$  is a good conservative estimator of organ doses in the directly irradiated area in a brain perfusion CT examination, including eye lens dose,  $CTDI_{vol}$  underestimates several organ doses in body perfusion CT studies. The results indicate that contrary to the eye lens doses,  $CTDI_{vol}$  underestimates the peak ESD in all the body perfusion CT examinations. There-

fore, the skin dose conversion factors can be useful to estimate peak ESD to optimize the protocols to avoid radiation skin injuries.

### References

1. Brix G, Lechel U, Nekolla E, Griebel J, Becker C. Radiation protection issues in dynamic contrast-enhanced (perfusion) computed tomography. *Eur J Radiol* 2014 Nov 20 [Epub ahead of print]
2. Dababneh H, Bashir A, Guerrero WR, et al. Mean transit time on Aquilion ONE and its utilization in patients undergoing acute stroke intervention. *J Vasc Interv Neurol* 2014; 7:73–81
3. Kim SH, Kamaya A, Willmann JK. CT perfusion of the liver: principles and applications in oncology. *Radiology* 2014; 272:322–344
4. Li XS, Fan HX, Fang H, Huang H, Song YL, Zhou CW. Value of whole-tumor dual-input perfusion CT in predicting the effect of multiarterial infusion chemotherapy on advanced non-small cell lung cancer. *AJR* 2014; 203:(web)W497–W505
5. International Commission on Radiological Protection. Statement on tissue reactions. Ottawa, ON, Canada: ICRP, 2011; report no. 4825-3093-1464
6. Geleijns J, Wondergem J. X-ray imaging and the skin: radiation biology, patient dosimetry and observed effects. *Radiat Prot Dosimetry* 2005; 114:121–125
7. Imanishi Y, Fukui A, Niimi H, et al. Radiation-induced temporary hair loss as a radiation damage only occurring in patients who had the combination of MDCT and DSA. *Eur Radiol* 2005; 15:41–46
8. [No authors listed]. The 2007 recommendations of the International Commission on Radiological Protection: ICRP publication 103. *Ann ICRP* 2007; 37:1–332
9. Menzel HG, Clement C, DeLuca P. ICRP publication 110: realistic reference phantoms: an ICRP/ICRU joint effort—a report of adult reference computational phantoms. *Ann ICRP* 2009; 39:1–164
10. Salvadó M, Cros M, Joemai RMS, Calzado A, Geleijns J. Monte Carlo simulation of the dose distribution of ICRP adult reference computational phantoms for acquisitions with a 320 detector-row cone-beam CT scanner. *Phys Med* 2015; 31:452–462
11. Nelson WR, Hirayama H, Rogers DW. The EGS4 code system. Stanford, CA: Stanford Linear Accelerator Center, 1985; report SLAC-265
12. Hirayama H, Namito Y, Ban S. Implementation of a general treatment of photoelectric-related phenomena for compounds or mixtures in EGS4: KEK internal report 2000-3. National Laboratory for High Energy Physics [www.kek.jp/research/egs/kek/egs4/photo.pdf](http://www.kek.jp/research/egs/kek/egs4/photo.pdf). Published May 2000. Accessed July 15, 2015
13. Geleijns J, Salvadó Artells M, de Bruin PW, Matter R, Muramatsu Y, McNitt-Gray MF. Computed tomography dose assessment for a 160 mm wide, 320 detector row, cone beam CT scanner. *Phys Med Biol* 2009; 54:3141–3159
14. International Electrotechnical Commission. Medical electrical equipment: part 2-44—particular requirements for the basic safety and essential performance of x-ray equipment for computed tomography. Geneva, Switzerland: IEC, 2009; report no. IEC 60601-2-44-ed30
15. Diekmann S, Siebert E, Juran R, et al. Dose exposure of patients undergoing comprehensive stroke imaging by multidetector-row CT: comparison of 320-detector row and 64-detector row CT scanners. *AJNR* 2010; 31:1003–1009
16. Bongartz G, Golding SJ, Jurik AG, et al. European Guidelines on Quality Criteria for Computed Tomography Luxembourg: European Commission; 2000:EUR 16262
17. Valentin J; International Commission on Radiological Protection. Managing patient dose in multi-detector computed tomography (MDCT): ICRP publication 102. *Ann ICRP* 2007; 37:1–79, iii
18. Stewart FA, Akleyev AV, Hauer-Jensen M, et al. ICRP publication 118: ICRP statement on tissue reactions and early and late effects of radiation in normal tissues and organs—threshold doses for tissue reactions in a radiation protection context. *Ann ICRP* 2012; 41:1–322



### 4.3 Development of software for dose assessment

- [IV] Cros M, Joemai RMS, Geleijns J, Molina D, Salvadó M. SimDoseCT: dose reporting software based on Monte Carlo simulation for a 320 detector-row cone-beam CT scanner and ICRP computational adult phantoms. *Phys Med Biol* 2017 (DOI: [doi.org/10.1088/1361-6560/aa77ea](https://doi.org/10.1088/1361-6560/aa77ea))

#### Abstract

This study aims to develop and test software for assessing and reporting doses for standard patients undergoing computed tomography (CT) examinations in a 320 detector-row cone-beam scanner. The software, called SimDoseCT, is based on Monte Carlo (MC) simulation code, which was developed to calculate organ and effective doses in ICRP anthropomorphic adult reference computational phantoms for acquisitions with the Aquilion ONE CT scanner (Toshiba). SimDoseCT consists of a graphical user interface connected to a MySQL database, which contains the look-up-tables that were generated with MC simulations for volumetric acquisitions at different scan positions along the phantom using any tube voltage, bow tie filter, focal spot and nine different beam widths. Two different methods were developed to estimate doses from acquisitions using other available beam widths in the scanner. A correction factor was used to estimate doses in helical acquisitions. Hence, the user can select any available protocol in the Aquilion ONE scanner for a standard adult male or female and obtain the dose results through the SimDoseCT interface. The program was validated by comparing dose results with those obtained from dedicated MC simulations for three volumetric acquisitions (head, thorax and abdomen). The comparison was repeated using eight different collimations and also for another collimation in a helical abdomen examination. The results showed differences of 0.1 mSv or less for absolute dose values in most organs and also in the effective dose calculation. The software provides a suitable tool for dose assessment in standard adult patients undergoing CT examinations in a 320 detector-row cone-beam scanner.





## **SimDoseCT: dose reporting software based on Monte Carlo simulation for a 320 detector-row cone-beam CT scanner and ICRP computational adult phantoms**

**Maria Cros<sup>1</sup>, Raoul M S Joemai<sup>2</sup>, Jacob Geleijns<sup>2</sup>, Diego Molina<sup>3</sup> and Marçal Salvadó<sup>1</sup>**

<sup>1</sup> Faculty of Medicine and Health Sciences, Universitat Rovira i Virgili, C/Sant Llorenç, 21, 43201 Reus, Spain.

<sup>2</sup> Radiology Department, Leiden University Medical Center, Albinusdreef 2, 2333 ZA Leiden, The Netherlands

<sup>3</sup> Freelance computer analyst/programmer in collaboration with Universitat Rovira i Virgili, C/Sant Llorenç, 21, 43201 Reus, Spain.

E-mail: maria.cros@urv.cat

### **Abstract**

This study aims to develop and test software for assessing and reporting doses for standard patients undergoing computed tomography (CT) examinations in a 320 detector-row cone-beam scanner. The software, called SimDoseCT, is based on Monte Carlo (MC) simulation code, which was developed to calculate organ- and effective doses in ICRP anthropomorphic adult reference computational phantoms for acquisitions with the Aquilion ONE CT scanner (Toshiba). MC simulation was validated by comparing CTDI measurements within standard CT dose phantoms with results from simulation under the same conditions. SimDoseCT consists of a graphical user interface connected to a MySQL database, which contains the look-up-tables that were generated with MC simulations for volumetric acquisitions at different scan positions along the phantom using any tube voltage, bow tie filter, focal spot and nine different beam widths. Two different methods were developed to estimate organ- and effective doses from acquisitions using other available beam widths in the scanner. A correction factor was used to estimate doses in helical acquisitions. Hence, the user can select any available protocol in the Aquilion ONE scanner for a standard adult male or female and obtain the dose results through the software interface. Agreement within 9% between CTDI measurements and simulations allowed the validation of the MC program. Additionally, the algorithm for dose reporting in SimDoseCT was validated by comparing dose results from this tool with those obtained from MC simulations for three volumetric acquisitions (head, thorax and abdomen). The comparison was repeated using eight different collimations and also for another collimation in a helical abdomen examination. The results showed differences of 0.1 mSv or less for absolute dose in most organs and also in the effective dose calculation. The software provides a suitable tool for dose assessment in standard adult patients undergoing CT examinations in a 320 detector-row cone-beam scanner.

## 1. Introduction

The number of computed tomography (CT) examinations increased in recent years due to technological advances and new acquisition techniques. The National Council on Radiation Protection and Measurements reported on the high contribution of CT in the annual radiation exposure of the population in the United States, which represents the 24% of the dose thus becoming the most significant contribution after natural background radiation (Schauer and Linton 2009). A study published by the European Commission demonstrated that CT was associated with more than half of the medical radiation exposure of the European population in 2007-2010 (European Commission 2013). Considering the current interest in radiation exposure from CT examinations, there is a need to develop methods for patient doses assessment in CT examinations that are up to date with current scanner technology and design, current acquisition protocols and the latest reference in computational phantoms. Awareness about radiation exposure in CT contributes to the optimization of the clinical application of CT and the reduction of radiation risks.

Currently, CT scanners display dose information based on operational dosimetric quantities such as the volume CT dose index ( $CTDI_{vol}$ ), which provides the average absorbed dose in a transection of a standard cylindrical CT dose phantom, and the dose-length product (DLP), which also considers the scan length. According to the ICRP (ICRP 1977, ICRP 1991), in radiation protection organ- and tissue doses are the preferred dose descriptors since they can be correlated with radiation risks. The effective dose (E) is calculated from organ- and tissue doses and takes into account the overall radiation-induced health effects and it also allows for practical comparison between radiation exposure from different techniques in diagnostic radiology and beyond.

There are different methods to estimate the organ- and tissue doses or effective dose from CT examinations such as laborious studies with dosimeters embedded in anthropomorphic phantoms or advanced Monte Carlo (MC) simulations. These complex MC studies usually provide numerous and large look-up-tables from which useful dosimetric information can be retrieved, like organ- and tissue doses, with software tools that consist of a relatively simple algorithm and a user interface. From these software tools simple k-factors can be derived that convert the DLP for broadly defined body regions into effective dose or dose in a few organs, which are useful for rough assessment of radiation exposure (ICRP 2007a, Kobayashi *et al.* 2016).

Several dosimetric software tools have been developed to facilitate the retrieval of organ- and tissue dose and effective dose from look-up-tables that were generated with MC simulations, i.e. ImpactDose (Kalender *et al.* 1999), CT-Expo (Stamm and Nagel 2002), Waza-Ari (Ban *et al.* 2011a, Takahashi *et al.* 2011), ImPACT (ImPACT 2012) and VirtualDose (Ding *et al.* 2015). These tools are often used for clinical dose assessment, but also for dose assessment in scientific studies involving CT. Differences between the software tools are significant and the user has to be aware of the limitations (Abdullah *et al.* 2012). Many of the software tools, such as CT-Expo or ImPACT, provide limited functionality due to the use of nowadays outdated mathematical phantoms. In addition, they use outdated look-up-tables, some dating back to the late 1980s and early 1990s. Jansen and Shrimpton (2016) demonstrated for recent scanners potential deviations by up to around 30% when comparing new dedicated MC simulations with results from the ImPACT calculator. A limitation of the Waza-Ari program is that it uses only phantoms based on relatively small Japanese patients and doses can differ around 20% for the same examination compared to ICRP phantoms (Ban *et al.* 2011b). VirtualDose uses anatomically realistic phantoms but not the standard male and female from

ICRP110 (ICRP 2009) and only allows dose estimation for 16-slices scanners at the moment. These disadvantages were overcome with ImpactDose since it has gradually incorporated many scanners and phantoms, even those published by ICRP110. The ImPACT calculator is kept up-to-date by scanner matching, this means that current CT scanners are matched with scanners from the late 1980s based on dosimetric characteristics, but the look-up-tables are calculated for scanners from the late 1980s.

In conclusion, contemporary CT scanners, like the 320 multi-slice CT scanner (Aquilion ONE Vision, Toshiba), are not implemented appropriately in currently available dose assessment programs, and they are often based on outdated mathematical phantoms. For example, for the Aquilion ONE current, the cone beam shape and the use of the adequate beam width with its associated overbeaming is not adequately taken into account (McCullough and Zink 1999).

This study aimed at developing and testing software for accurate dose assessment in CT with the Aquilion ONE scanner. The software, called SimDoseCT, is based on look-up tables generated from MC simulation. The dose assessment should take into account all relevant technical characteristics of the scanner, like focal spot size, overbeaming, overranging, beam shaping filter, the cone beam geometry and the heel effect. Dose assessment was performed for the current standard phantoms, namely the ICRP computational adult male and female phantom. The software should also take into account all possible acquisitions within the Aquilion ONE CT scanner, like axial (volumetric), helical and scanogram acquisitions. Selecting the appropriate acquisition technique in the software was facilitated by using a graphical user interface that accurately resembles the user interface of the actual CT scanner.

Hence, a tool for an accurately organ- and effective doses estimation in a 320 detector-row cone-beam scanner was offered with the aim of improving the easily dose evaluation for standard adult patients in CT contemporary scanners.

## 2. Materials and methods

### 2.1 CT scanner model

The Aquilion ONE CT scanner (Toshiba Medical Systems, Otawara, Japan, software version 4.74ER001) was modelled in great detail for this study. This 320 detector-row cone-beam CT scanner operates at sixteen different beam collimations allowing a z-axis coverage of the beam between 2 and 160 mm (i.e. 160, 140, 128, 120, 100, 80, 60, 50, 40, 32, 20, 16, 12, 8, 4 and 2 mm) and at different tube voltages (i.e. 80, 100, 120 and 135 kVp). Three beam shaping filters (i.e., small, medium and large bow tie filters) can be selected to optimize the x-ray beam intensity inside the field of view (FOV).

The tube current can be selected from 10 to 50 mA in 5 mA steps and from 50 to 580 mA in 10 mA steps. The scanner allows eleven rotation times: 0.35, 0.375, 0.4, 0.45, 0.5, 0.65, 0.75, 1.0, 1.5, 2.0 or 3.0 s. The focal spot size, either large or small, is automatically chosen by the scanner depending on the selected acquisition parameters.

The Aquilion ONE CT scanner has two scan modes for cross-sectional imaging with a rotating x-ray tube, i.e. an axial (volumetric) acquisition or a helical acquisition. In addition the scanner is also able to perform projection imaging with a static x-ray tube for planning purposes, which is referred to as a scanogram.

## 2.2 ICRP computational phantoms

The two adult computational phantoms, the anthropomorphic male (AM) and anthropomorphic female (AF) phantoms, were published by the ICRP (ICRP 2009) and they were used in this study for dose estimation. These two phantoms are regarded as the current international standard for dosimetry. They were constructed from CT images of humans and they represent an average male (length 178 cm, weight 73 kg) and an average female (length 168 cm, weight 60 kg). The voxel size is  $2.1 \times 2.1 \times 8.0 \text{ mm}^3$  for the male and  $1.8 \times 1.8 \times 4.8 \text{ mm}^3$  for the female. The ICRP provides detailed information for the two phantoms, including mass, spatial distribution and composition of each organ or tissue. Each phantom was implemented in a MC simulation program (Salvadó *et al.* 2015), through three representations for each voxel concerning respectively the 141 organs or tissues, the 53 materials and the 29 organs that contribute to the effective dose calculation. A specific subsegmentation was required for tissues containing red bone marrow (RBM) or endosteum (bone surface) because the microscopic structures of the skeleton are smaller than the size of a voxel (Zankl *et al.* 2007). Additionally, for the mentioned tissues, the energy increase due to the secondary particles that are released from mineral bone components was implemented in the simulation program through an enhancement factor (King and Spiers 1985). Figure 1 shows a surface rendering of the adult phantoms used and different views showing the organs that contribute to the effective dose calculation.

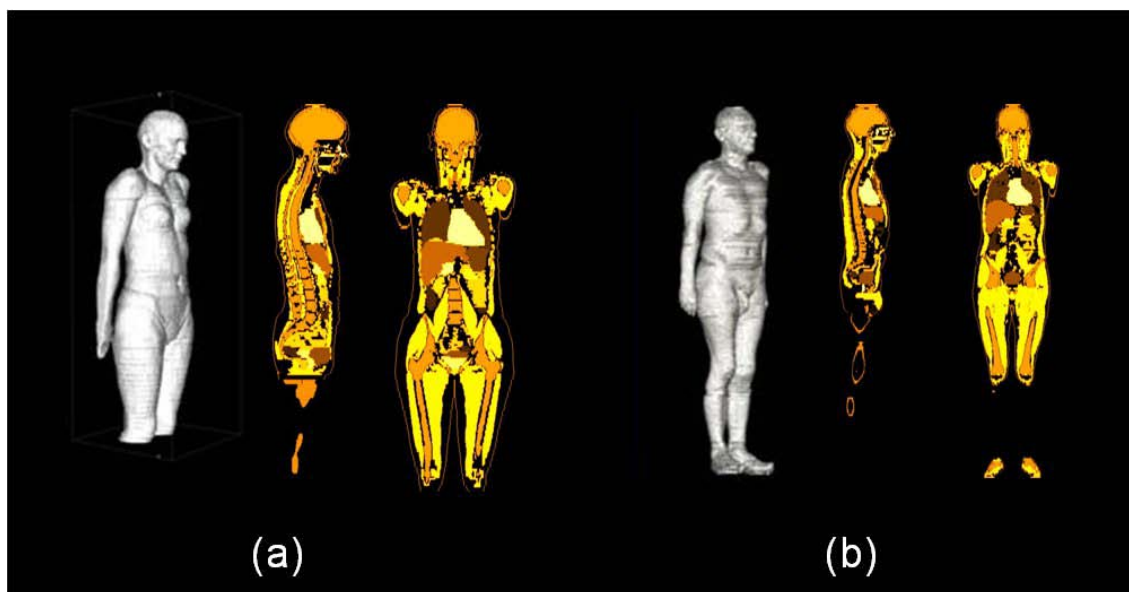


**Figure 1.** From left to right, 3D surface views and sagittal and coronal views showing the different organs with weighting factors that contribute to the effective dose in different colours for (a) adult female phantom and (b) adult male phantom.

## 2.3 Monte Carlo simulation

The Aquilion ONE CT scanner was modelled in a MC program according to the specific technical characteristics of this scanner. The MC code simulates all aspects that influence the dose distribution in the phantoms during a CT scan, including the characteristics of the

interaction (attenuation and scatter), the x-ray spectrum and x-ray beam (tube voltage and primary filtration, bow tie filter, cone beam geometry, heel effect, beam width, penumbra, rotation and tube charge) and the patient support table (shape, size and material). The CT acquisition parameters can be introduced as an input to the MC code (i.e. tube voltage, tube current, pitch, scan position and scan range). For the calculation of radiation transport, the Electron Gamma Shower V4 (EGS4) code (Nelson *et al.* 1985) in combination with the Low Energy Photon Scattering Expansion (National Laboratory for High Energy Physics (KEK) Japan) (Hirayama *et al.* 2000) was used. The simulation of photons transport in the energy range typical for CT scanners is based on processes of Rayleigh scattering, Compton scattering and photoelectric effect and the associated creation of fluorescent photons or Auger electrons. A cut-off energy of 5 keV was used for photon transport, and a cut-off energy of 30 keV was used for electrons.

The MC program was developed and validated for a beam collimation of 160 mm in a previous study (Salvadó *et al.* 2015). In this prior work, the validation was performed with a set of CTDI measurements and the corresponding simulations within two standard CT dose phantoms (150 mm long, 160 mm diameter for the head phantom and 320 mm diameter for the body phantom) and using a 100 mm long CT ionization chamber. Agreement between measurements and MC results was within 5%. Similar procedure was used in this study to validate the MC program for all the available collimations in the scanner by comparing the results from simulations in standard CT dose phantoms with the CTDI measurements provided by Toshiba's manufacturer under the same conditions. The CTDI was calculated according to the definitions of the IEC (IEC 2009) and the IAEA (IAEA 2011) at the centre position and as average at the peripheral positions of the CT dose phantoms. The validation was performed for each available collimation, tube voltage, FOV and focal spot size. Once validated, the MC code calculates the absorbed energy in each voxel of the phantom. The mean absorbed dose in each organ or tissue was computed as the total absorbed energy in the voxels corresponding to this organ or tissue divided by the total mass. The mean absorbed dose in each material was also calculated.

MC simulations were performed for cross-sectional imaging of the two anthropomorphic adult reference computational phantoms concerning all possible combinations of the following acquisition parameters: tube voltage (i.e. 80, 100, 120 and 135 kVp), FOV (small, medium and large; this is associated with the beam shaping filter), focal spot size (small or large) and nominal beam width (160, 128, 60, 50, 40, 16, 8, 4 and 2 mm). The simulations were performed as separate axial scans of one rotation (360 different angles) at different positions each 4 mm along the phantom from head to feet for all collimations except for narrowest beams. Simulations were performed each 2 mm for 4 mm-collimation and each 1 mm for 2 mm-collimation. Thus, the overlap in the simulations ranges from a 2-fold overlap for the 2, 4 and 8 mm beam widths to a 40-fold overlap for the 160 mm beam width.

Additionally, simulations were performed for the projection imaging of the two phantoms (scanogram) using contiguous simulations, each 1 mm along the phantom, for a beam width of 2 mm, for all tube voltages and FOV sizes, a large focal spot size and four tube angles (0, 90, 180 and 270°). MC simulations provided doses in all organs and doses in all different materials in the phantom, normalized per mAs.

In most CT acquisition protocols of the body, the arms of the patient are positioned along the head and in CT scans of the head, along the body. Accordingly, the arms were removed from the phantoms during all the simulations. The mass of the arms was taken into account for the calculation of the absorbed dose.

The MC simulations were performed in a supercomputing center (CSUC, Consorci de Serveis Universitaris de Catalunya) and were carried out using  $2.0 \times 10^7$  photon histories for each cross-sectional simulation and  $2.0 \times 10^6$  for each projection simulation (scanograms). The computation times for a complete cross-sectional simulation, e.g. one full rotation in each scan position along the phantom, were on average 5 days for all the collimations, except for narrowest beams that were 10 days for 4mm-collimation and 20 days for 2mm-collimation. The computation time for the scanograms was on average 2 days.

#### 2.4 *SimDoseCT software*

SimDoseCT consists of a graphical user interface connected to a MySQL database. The application runs on a PC and shows the same interface as the scan console of the Aquilion ONE CT scanner (software version 4.74). The user can design an acquisition protocol with the same options and user interface as on the scanner console. Once the acquisition protocol is designed the user has the option to visualize the dose values either by selecting a dose tab in the interface or by generating a PDF dose report. Both options will trigger the application to retrieve dose values from the database. The database can either be stored local or accessed as an online database by performing a secure query. The graphical user interface has read-only privileges in the database for security reasons. The user can change any acquisition parameter and the dose will be updated in real-time to show how it affects the organ dose and effective dose. This software is coded using the object-oriented programming language C# (Microsoft, USA).

#### 2.5 *Dose calculation algorithm in SimDoseCT*

Doses were stored, for specific scan positions along the phantom, in the database (each 4, 2 mm and 1 mm for the narrowest beam widths). Doses at other scan positions can be linearly interpolated by SimDoseCT in steps of 0.5 mm. Since MC simulations were performed only for nine of the sixteen available beam widths of the Aquilion ONE scanner, two methods were used to estimate doses from acquisitions using other available beam widths. Table 1 shows the method used for each beam width.

**Table 1.** Nominal beam width of reference and method used to estimate the absorbed dose for the seven collimations not included in database.

b (mm)	b <sub>ref</sub> (mm)	Method used
140	128	1
120	60	2
100	50	2
80	40	2
32	16	2
20	16	1
12	16	1

For beam widths close to one of the sixteen available beam widths in the database, the following correction factor based on actual beam widths was used to calculate absorbed doses (*method 1*):

$$D = D_{\text{ref}} \cdot \frac{b_{\text{actual}}}{b_{\text{ref,actual}}} \quad (1)$$

where  $D$  is the absorbed dose to be estimated for beam width  $b$  and  $b_{\text{ref}}$  is the beam width corresponding to dose values,  $D_{\text{ref}}$ . The subscript *actual* indicates that the overbeaming was also considered in the beam width. The overbeaming was calculated from the actual shape of the x-ray beam profile along the axis of rotation from the scanner. For beam widths equal to or below 80 mm, overbeaming was measured using the Gafchromic XR-QA Dosimetry Film (International Specialty Products Inc. (ISP), Wayne, NJ, USA) and for larger beam widths, the Piranha 657 dose profiler (RTI Electronics, Fairfield, NJ, USA) was used.

For beam widths that are substantially smaller or wider compared to beam widths available in the database, a different method was used. The dose values were calculated using a reference beam width that is twice as small as the beam width of interest. The sum of the absorbed doses from two scan positions with an interval equal to the beam width of reference was used together with a correction factor to take into account the effect of overbeaming (*method 2*):

$$D = D_{\text{ref}} \cdot \frac{b_{\text{actual}}}{2b_{\text{ref,actual}}} \quad (2)$$

where  $D$  is the absorbed dose to be estimated for beam width  $b$ , and  $D_{\text{ref}}$  is the absorbed dose for the beam width  $b_{\text{ref}}$ . The subscript *actual* indicates that the overbeaming was also considered in the beam width.

The dose from the scanogram acquisition is calculated by directly summing the dose from contiguous positions within the range of the scanogram, using a beam width of 2 mm.

For the axial mode with a single rotation, the program provides the doses from the database according to the CT input parameters and concerning the scan position to cover the scan range with the selected beam collimation. When contiguous axial scans are required to cover the scan range with the selected collimation, the program obtains the organ doses by summing the dose corresponding to the actual positions and actual beam width.

The dose values that are stored in database are normalized to mAs per rotation. These values have to be corrected for the nominal mAs ( $Q_{\text{nom}}$ ), the pitch ( $p$ ) and the overlap between the successive positions taking into account the distance between the successive positions ( $d_s$ ) and the beam width ( $b$ ). The corresponding correction factor is  $Q_{\text{eff}}$ .

$$Q_{\text{eff}} = \frac{1}{p} \cdot \frac{d_s}{b} \cdot Q_{\text{nom}} \quad (3)$$

The extra rotations at the start and the end of the helical acquisition (overranging) were also considered and added to the planned scan range. The overranging was assessed as one entire extra rotation at the start and the end of the acquisition following the same procedure described in previous works (van der Molen and Geleijns 2007).

In addition to organ doses, the software also calculates the effective dose for the male and female phantom using tissues weighting factors from ICRP Report 103 (ICRP 2007b). For the



gender-specific calculation, the weighting factor for female breast tissue was taken 0.24 and no tissue weighting factor was applied for male breast tissue. SimDoseCT also provides the  $CTDI_{vol}$  that corresponds to the designed acquisition protocol, for all combinations of tube voltage, FOV and beam collimation. The dose length product (DLP) was calculated by multiplying the  $CTDI_{vol}$  with the nominal scan length. SimDoseCT shows the dose results (i.e. organ doses, effective dose,  $CTDI_{vol}$  and DLP) in real time for the whole protocol as well as for each individual scan.

### 2.6 Validation of SimDoseCT algorithm

Validation of the software algorithm was achieved by comparing the dose estimation from the SimDoseCT tool with dose results obtained from dedicated MC simulations for specific acquisitions. The dose values taken into account in the validation were the effective dose and the absorbed doses in organs that contribute to the effective dose. In addition, the absorbed dose in other relevant organs such as eye lens, testis and ovaries were also evaluated. The testing was performed using three different axial volumetric protocols for head, thorax and abdomen. The reported doses for the axial acquisitions are associated with only one rotation. For each protocol, the validation was performed for six collimations for which the look-up-table was not included in the database (140, 120, 100, 80, 20 and 12 mm) and for the maximum and minimum available beam widths of the scanner (160 and 2 mm). A 64 slice, 32 mm-collimation, abdomen protocol was used to validate the helical mode. The CT acquisition parameters of the protocols that were used for the validation are provided in Table 2.

**Table 2.** Acquisition parameters of the CT protocols used for the SimDoseCT algorithm validation.

CT Examination	Tube voltage (kVp)	Rotation time (s)	Tube current (mA)	Pitch	Field of view (FOV)	Focal spot size	Beam width (mm)	Scan position from the top of the head (mm)	
								AM	AF
Volume - Head	80	0.5	200	–	Small	Small	160, 140,	80	80
Volume - Thorax	120	0.5	200	–	Medium	Large	120, 100, 80, 20,	436	402 <sup>a</sup>
Volume - Abdomen	100	0.5	200	–	Large	Large	12, 2	524	494 <sup>a</sup>
Helical - Abdomen	100	0.5	200	0.828	Large	Large	32	444-604	414-574 <sup>a</sup>

<sup>a</sup>Scan positions that required interpolation in SimDoseCT.

### 2.7 Dose comparison with results from other dosimetric software tools

Most of the existing dosimetric software tools today are based on pre-calculated tables with doses from outdated generic scanners from the late 1980s. Since SimDoseCT provides accurate organ dose reporting in a specific CT contemporary scanner, organ doses in SimDoseCT were compared with results from other CT patient dosimetry calculators, like ImPACT and ImpactDose, in order to demonstrate the functionality of the SimDoseCT tool for a 320 detector-row cone-beam scanner. ImPACT uses mathematical phantoms and Impactdose tool uses ICRP computational adult phantoms. Dose differences were calculated in the three volumetric examinations (head, thorax and abdomen) using a scan range of 160 mm.

### 3. Results

#### 3.1 Monte Carlo validation

To validate the MC simulation for all the available collimations in the 320 detector-row cone-beam scanner, differences in  $CTDI_{centre}$  and  $CTDI_{surface}$  from manufacturer measurements and from MC simulation were calculated. Differences were up to 9% for all the available collimations in the scanner and for all tube voltages and bow tie filters, confirming that dose calculations from MC simulation were in agreement with the actual exposure conditions. Table 3 provides the CTDI comparison for six different collimations using 80 kV for the head phantom with the small bow tie filter (S) and small focal spot size (SFS) and using 120 kV for the body with the medium filter (M) and large focal spot (LFS).

**Table 3.** CTDI measurements from manufacturer and CTDI results from MC simulation for six different collimations available in the Aquilion ONE scanner for a head and a body examination. Differences were also calculated.

Beam width (mm)	$CTDI_{centre}$ (mGy/mAs)			$CTDI_{surface}$ (mGy/mAs)		
	Measurements	MC simulation	$\Delta$ (%) <sup>a</sup>	Measurements	MC simulation	$\Delta$ (%) <sup>a</sup>
<b>HEAD 80kV,S,SFS</b>						
160	0.069	0.065	-6.7	0.075	0.077	3.1
80	0.063	0.058	-7.9	0.068	0.071	3.9
40	0.071	0.066	-5.9	0.076	0.079	3.0
32	0.079	0.074	-5.8	0.085	0.088	3.1
16	0.089	0.084	-5.1	0.096	0.098	2.2
2	0.224	0.212	-5.1	0.241	0.247	2.4
<b>BODY 120kV, M,LFS</b>						
160	0.061	0.056	-8.2	0.112	0.114	2.2
80	0.052	0.048	-8.5	0.092	0.095	2.9
40	0.059	0.055	-6.2	0.105	0.107	2.2
32	0.065	0.062	-5.0	0.116	0.118	1.4
16	0.078	0.073	-5.9	0.138	0.140	1.7
2	0.229	0.218	-4.9	0.406	0.412	1.4

$$^a \Delta(\%) = \frac{Simulated - Measured}{Measured} \times 100$$

#### 3.2 SimDoseCT

Look-up-tables were calculated for 445 scan positions along the AM phantom and 306 positions along the AF phantom for 264 combinations of scan parameters (kVp, FOV, focal spot size and collimation) available in the Aquilion ONE CT scanner. For the narrowest collimations (4 mm and 2 mm), the number of positions, and thus look-up-tables, is even two and four times higher respectively. The look-up-tables allow for dose calculation at any tube position through interpolation, even if the exact position is not included in the look-up-tables. At each scan position, and for all scan parameters the look-up-tables provide the normalised absorbed dose for 170 organs and tissues and for 54 materials. In total 378504 look-up-tables were calculated in almost  $1.0 \times 10^5$  hours of simulation time.

Consequently, by retrieving data from the look-up-tables the organ- and effective doses from any CT Aquilion ONE protocol (working with software version 4.74) and any scan range can be obtained for the male and female computational phantoms, for each scan mode (i.e.

volume, helical or scano) and for the CT acquisition parameters specified by the user in the SimDoseCT user interface (Table 4). The calculation takes into account the dose gradients in the beam e.g. due to the beam shaping filter, the heel effect and the penumbra due to the finite focal spot size. The effects of overbeaming and overranging are also taken into account.

**Table 4.** Available phantoms and CT scan parameters in SimDoseCT.

Scan mode	Phantom	Tube voltage (kVp)	Field of view (FOV)	Focus spot size	Beam width (mm)
Axial (Volumetric)	AM, AF	80, 100, 120, 135	Small, Medium, Large	Small, Large	160, 140 <sup>a</sup> , 128, 120 <sup>a</sup> , 100 <sup>a</sup> , 80 <sup>a</sup> , 60, 50, 40, 32 <sup>a</sup> , 20 <sup>a</sup> , 16, 12 <sup>a</sup> , 8, 4, 2
Helical	AM, AF	80, 100, 120, 135	Small, Medium, Large	Small, Large	80 <sup>a</sup> , 50, 40, 32 <sup>a</sup> , 20 <sup>a</sup> , 16, 8, 4, 2
Tube-fixed irradiation (Scanogram)	AM, AF	80, 100, 120, 135	Small, Medium, Large	Large	2

<sup>a</sup> Dose values based on calculation methods for dose estimation.

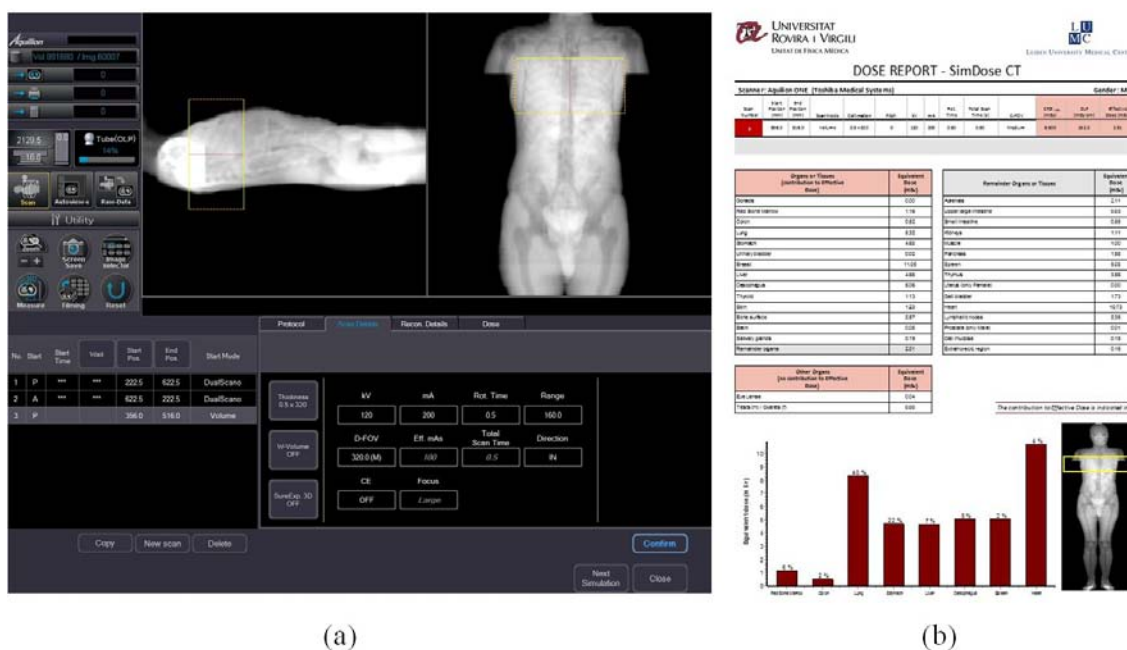


**Figure 2.** (a) User interface of SimDoseCT software and (b) an example of the dose report generated from SimDoseCT.

After entering the acquisition protocol in SimDoseCT, the dose results are displayed immediately in the user interface. A patient dose report can be generated and saved; an example is shown in Figure 2. The selected scan parameters for the protocol and the corresponding effective dose,  $CTDI_{vol}$  and DLP are reported in a table. The absorbed dose in all the organs that contribute to the effective dose, including the remainder organs, is listed in a table together with the absorbed dose of other organs or tissues of interest, such as eye lens and testis or ovaries. The report shows also a graph with the organ doses of the eight organs that have the highest contribution to the effective dose. A graphical representation of the scanned region in the phantom is shown to provide a visual control of the selected anatomical region for the scan. The described information is presented for the entire CT examination and also for each scanogram and each individual scan in the whole protocol.

### 3.3 Validation of SimDoseCT algorithm

Table 5 lists the  $CTDI_{vol}$ , the DLP and the effective doses in a head, a thorax and an abdomen CT examination for the eight selected collimations to validate the volumetric mode of the SimDoseCT software. The results are associated to only one rotation, so DLP and effective dose decrease with decreasing beam collimation. The differences between dose values obtained directly from dedicated MC simulations and SimDoseCT are presented. The results show that most differences in effective doses were below 6.5%, being negligible in most cases. For some protocols of thorax and abdomen the relative differences were slightly higher representing only absolute differences up to 0.1 mSv.

The differences in organ doses obtained from the comparison between both dose calculation tools were lower than 10% in most organs. In the case of using a beam width that used the method 1 or method 2 to estimate doses (i.e. 140, 120, 100, 80, 20 and 12 mm), the differences could represent more than 10% in some organs or tissues, such as eye lenses or extra thoracic region in head protocols; the thymus in thorax examinations or the breast in abdomen scans. In these organs, the differences were 0.5 mSv at the most and 1 mSv in the case of eye lenses (between 15 and 27%).

In the case of beam widths for which the dose data are included in look-up-tables, these differences were negligible in all organs. Dose differences of 0.1 mSv were found if the selected tube position involves an interpolation of the dose data in the SimDoseCT software.

For the abdomen CT protocol using a beam width of 32 mm in helical mode, the effective dose was 3.53 mSv in SimDoseCT and 3.64 mSv in the dedicated MC simulation for AM and 4.71 mSv and 4.74 mSv for AF, respectively. Hence, maximum differences of 3% were found. Figure 3 presents the organ absorbed doses in AM and AF phantoms for the abdomen study in helical mode obtained by SimDoseCT and MC simulation. The selection of organs was based on an exceeded limit of 1 mGy and their contribution to the effective dose is more than 99%. Differences in doses between both methods were below 5.5%, with maximum absolute differences of 0.3 mSv.

**Table 5.** Effective doses obtained using SimDoseCT tool and from a dedicated MC simulation program for the different volume CT examinations used for the SimDoseCT validation. The results are for one single axial rotation. The percentage dose differences between both methods were calculated. The CTDI<sub>vol</sub> and the DLP are also indicated in each case.

Beam width (mm)	CTDI <sub>vol</sub> (mGy)	DLP (mGy·cm)	E (mSv)					
			AM			AF		
			SimDoseCT	MC	$\Delta$ (%) <sup>a,b</sup>	SimDoseCT	MC	$\Delta$ (%) <sup>a,b</sup>
<b>Head</b>								
160	7.3	116.3	0.15	0.15	0.0	0.19	0.19	0.0
140	7.1	99.3	0.13	0.13	0.0	0.16	0.17	6.3
120	6.8	82.1	0.11	0.11	0.0	0.14	0.14	0.0
100	6.3	63.0	0.09	0.09	0.0	0.11	0.11	0.0
80	6.7	53.3	0.07	0.07	0.0	0.09	0.09	0.0
20	8.2	16.4	0.02	0.02	0.0	0.03	0.03	0.0
12	9.4	11.3	0.01	0.01	0.0	0.02	0.02	0.0
2	23.5	4.7	0.01	0.01	0.0	0.01	0.01	0.0
<b>Thorax</b>								
160	9.5	152.0	2.51	2.51	0.0	6.26	6.27	0.2
140	9.2	128.8	2.19	2.21	0.9	5.72	5.66	1.1
120	8.5	102.0	1.93	1.90	1.6	5.03	5.04	0.2
100	7.5	75.0	1.63	1.58	3.2	4.46	4.36	2.3
80	7.9	63.2	1.29	1.27	1.6	3.74	3.70	1.1
20	10.1	20.2	0.43	0.39	10.3	1.40	1.28	9.4
12	11.9	14.3	0.29	0.28	3.6	0.93	0.91	2.2
2	34.7	6.9	0.14	0.14	0.0	0.44	0.44	0.0
<b>Abdomen</b>								
160	6.6	105.1	2.10	2.10	0.0	2.60	2.59	0.4
140	6.3	87.6	1.90	1.89	0.5	2.22	2.24	0.9
120	5.8	70.0	1.68	1.66	1.2	1.96	1.93	1.6
100	5.2	51.6	1.47	1.43	2.8	1.68	1.62	3.7
80	5.4	43.2	1.22	1.21	0.8	1.36	1.34	1.5
20	6.9	13.9	0.41	0.38	7.9	0.44	0.41	7.3
12	8.2	9.8	0.28	0.27	3.7	0.30	0.29	3.5
2	23.8	4.8	0.13	0.13	0.0	0.14	0.14	0.0

$$^a \Delta(\%) = \frac{E_{\text{SimDoseCT}} - E_{\text{MC}}}{E_{\text{MC}}} \times 100$$

<sup>b</sup> Differences lower than 0.005 mSv were considered 0%.

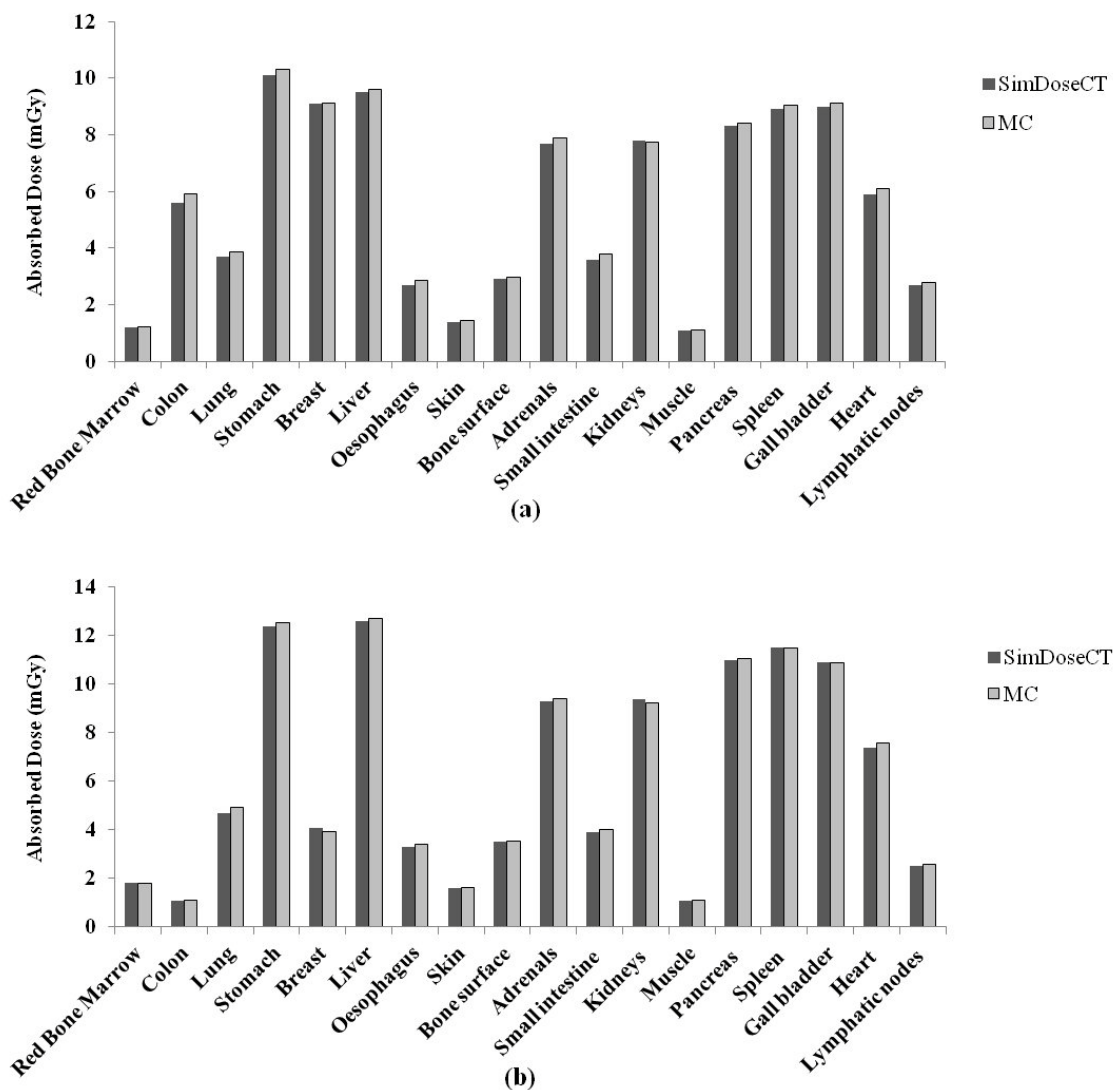


**Figure 3.** Absorbed doses for (a) adult male phantom and (b) adult female phantom in a helical abdomen protocol obtained from SimDoseCT tool and a dedicated MC simulation.

### 3.4 Comparison with other dosimetric software tools

The organ- and effective doses calculated in this study with SimDoseCT for a 160mm-volumetric acquisition were compared with results obtained from ImPACT and ImpactDose CT patient dosimetry calculators. Table 6 shows the absorbed doses in the eight organs that received the highest dose in each examination (head, thorax and abdomen) and the effective dose. The organ doses from SimDoseCT and ImpactDose are presented as an average for males and females. The relative differences between doses obtained from the different tools are also indicated.

**Table 6.** Absorbed doses in some organs and effective dose, averaged for males and females, obtained from SimDoseCT, ImPACT and ImpactDose dosimetry calculators for a head, thorax and abdomen examination. The relative differences on dose were also calculated.

	SimDoseCT	ImPACT		ImpactDose	
	Dose (mGy or mSv)	Dose (mGy or mSv)	$\Delta$ (%) <sup>a</sup>	Dose (mGy or mSv)	$\Delta$ (%) <sup>b</sup>
HEAD					
Eye lense	6.34	6.30	0.6	n.a <sup>b</sup>	n.a <sup>b</sup>
Brain	4.35	6.70	-54.2	4.53	-4.2
Extra thoracic region	2.49	0.48	80.7	n.a <sup>b</sup>	n.a <sup>b</sup>
Bone surface	2.26	1.90	15.7	2.36	-4.6
Salivary glands	2.24	6.70	-199.8	n.a <sup>b</sup>	n.a <sup>b</sup>
Oral mucosa	0.96	6.70	-601.6	2.03	-112.2
Red Bone Marrow	0.24	0.48	-100.0	0.19	20.0
Skin	0.44	0.48	-9.1	0.33	24.1
Effective Dose	0.17	0.31	-82.4	n.a <sup>b</sup>	n.a <sup>b</sup>
THORAX					
Breast	12.32	9.90	19.6	n.a <sup>b</sup>	n.a <sup>b</sup>
Heart	12.07	10.00	17.1	11.95	1.0
Lung	9.59	9.30	3.0	9.91	-3.3
Oesophagus	5.74	12.00	-109.1	6.34	-10.4
Liver	5.24	1.20	77.1	n.a <sup>b</sup>	n.a <sup>b</sup>
Spleen	5.17	0.89	82.8	7.24	-40.0
Stomach	4.59	0.77	83.2	5.42	-18.1
Thymus	4.39	12.00	-173.7	n.a <sup>b</sup>	n.a <sup>b</sup>
Effective Dose	4.39	3.50	20.2	n.a <sup>b</sup>	n.a <sup>b</sup>
ABDOMEN					
Stomach	7.15	4.80	32.9	8.02	-12.2
Liver	7.14	5.60	21.6	n.a <sup>b</sup>	n.a <sup>b</sup>
Spleen	6.92	5.40	21.9	6.67	3.5
Gall bladder	6.06	2.60	57.1	7.67	-26.6
Pancreas	5.44	6.50	-19.6	n.a <sup>b</sup>	n.a <sup>b</sup>
Adrenals	5.31	8.10	-52.5	n.a <sup>b</sup>	n.a <sup>b</sup>
Kidneys	4.62	3.30	28.5	6.21	-34.6
Heart	3.71	6.50	-75.2	3.19	13.9
Effective Dose	2.35	2.00	14.9	n.a <sup>b</sup>	n.a <sup>b</sup>

$$^a \Delta(\%) = \frac{\text{Dose}_{\text{ImPACT/ImpactDose}} - \text{Dose}_{\text{SimDoseCT}}}{\text{Dose}_{\text{SimDoseCT}}} \times 100$$

<sup>b</sup> Not available in Demo mode

The results showed that SimDoseCT doses in organs directly irradiated agreed with the values for ImpactDose within 13% such as brain in head examination, heart or lung in thorax study and stomach or spleen in abdomen protocol. However, significant discrepancies were observed between doses in organs partially irradiated due to their location at the border of the scan range. This was the case of oral mucosa in head study, spleen in thorax scan and kidneys in abdomen

examination. When results from SimDoseCT were compared with those from ImPACT, effective dose and absorbed dose in most organs showed large differences (between 15 and 85%) and even the dose was between two and six times higher in some organs, like salivary glands or oral mucosa in head scan and oesophagus and thymus in thorax examination.

#### 4. Discussion

A software tool, called SimDoseCT, has been developed for dose assessment in computed tomography based on Monte Carlo simulation of the radiation distribution for the Aquilion ONE 320 detector-row cone-beam scanner, in combination with two ICRP computational adult phantoms, one male and one female. The program consists of a graphical user interface, similar to the interface of the console of the Aquilion ONE scanner, and retrieves data from 378504 look-up-tables. With the software organ doses and effective dose can be accurately calculated for any acquisition protocol of the Aquilion ONE CT scanner. MC simulation was validated by comparing simulated and measured CTDI values for the CT dose phantoms using all the available collimations in the scanner. Additionally, a comparison between dose estimation from SimDoseCT and dose results obtained from dedicated MC simulations was performed to validate the methodology applied in the software.

The CTDI values obtained by simulations were on good agreement with those measured and provided by the manufacturer. The differences which were within 9% could be due to uncertainty in measurements and in the implementation of the scanner model for the simulation. Similar discrepancies were published in other studies (Jarry *et al.* 2003, DeMarco *et al.* 2005, Deak *et al.* 2008, Gu *et al.* 2009, Morant *et al.* 2012, Salvadó *et al.* 2015).

Good correspondence was found between the effective doses calculated using SimDoseCT and the results obtained from dedicated MC simulations. As can be observed in Table 5, the relative differences were 0.1 mSv or less for the absolute dose values. No relationship was observed between these small deviations and any beam width or method used to estimate the dose. Since the scan range selected in AF for thorax and abdomen protocols implied a tube position with interpolated dose data from different look-up-tables in SimDoseCT, most differences in Table 5 can be related to deviations caused by this interpolation.

A similar pattern was found for organ doses. The excellent agreement between SimDoseCT and dedicated MC simulations for acquisitions for which the look-up-tables were stored in the database demonstrated the correct general operation of the program. For acquisitions that required the use of calculation methods using the available look-up-tables, the minor differences in organ dose estimations demonstrated the good methodology of calculation employed by SimDoseCT. The organs that received the higher absorbed doses in each protocol, which were brain in head studies, breast, lung and heart in thorax examinations and stomach, liver and spleen in abdomen protocols, showed dose differences below 6% for collimations above 20 mm. The dose differences exceeding the 10% corresponded to the organs that absorbed a very low dose ( $< 0.5$  mSv), representing absolute dose deviations of only 0.1 mSv. This percentage was also surpassed in organs with very low mass but within the direct beam, such as eye lenses and thymus, or organs partially irradiated in the direct beam, such as extra thoracic region or salivary glands in head protocols and breast in abdomen protocols. In these cases, doses from SimDoseCT were always higher than results from MC simulations.

The results presented in Figure 3 for the helical abdomen scan further support the good concordance between results from SimDoseCT and MC program. This protocol implies the use of several calculation methods in SimDoseCT, i.e. beam width correction (method 2) and helical correction for both phantoms, and also interpolation in AF due to the tube position.



Consequently, the organ dose differences obtained in this case, below 5.5%, give an idea of the excellent consistency of the developed dose assessment methodology.

For the abdomen protocol in helical mode, it is important to take notice of the high doses received by the patient in comparison to the doses for a volume scan in the same range (160 mm-volume abdomen acquisition). The quotient between both effective doses were 1.7 and 1.8 for AM and AF respectively. This increase is due to the overlap caused by the pitch, the use of a narrower beam width (and the corresponding overbeaming) and the overranging, which was also implemented in the program for the helical mode. In this case, overranging resulted in an increase of 27.4% on sex-average effective dose and around 33% as average on organ doses. These results were in agreement with studies from other authors, who affirm that overranging may cause excess dose up to 30% (Kalender 2014). Regarding to the overbeaming, other authors (McNitt-Gray 2002, Smith *et al.* 2007) stated that narrower degree of collimation results in a greater penumbral effect, more overbeaming, and, therefore, an increase on the  $CTDI_w$  values by as much as 55% in a head phantom and 65% in a body phantom with the higher doses coming when narrower beam collimation is used. In the present study, MC simulations for the abdomen examination confirmed that differences on effective dose due to overbeaming were 5.8% when a collimation of 160 mm was used and 64.7% for the narrowest beam width (i.e. 2mm-collimation). Similar differences were found in organ doses, which were as average 7.5% and 64.8%, respectively.

Dose results from SimDoseCT showed relevant differences between AM and AF. The effective dose for female was between 1 and 2 times higher than that for adult male in head and abdomen examinations. These differences increased in thorax protocols, in which the ratio between effective dose in female and male was between 2.5 and 4 depending on collimation. Similar tendencies can be observed in organ doses, which were slightly higher in female than in male. This can be mainly explained because the smaller size of the women compared to men makes higher the absorbed dose in most organs or tissues under the same exposure conditions. It has to be also noted that no tissue-weighting factor for breast in men was used, while a weighting factor of 0.24 was used for breast in women. The SimDoseCT results for the collimation of 160 mm in volumetric mode were in agreement with those presented in previous studies (Salvadó *et al.* 2015, Geleijns *et al.* 2015, Cros *et al.* 2016) for head, thorax and abdomen protocols.

Several dosimetric software tools to report patient doses in CT examinations are available today. However, results obtained from comparison between organ- and effective doses obtained from SimDoseCT and with other dosimetry calculators showed significant discrepancies on dose due to the use of outdated scanner models and stylized phantoms. From results presented in Table 6, dose differences up to 40 % can be associated to the low specificity of the generic scanners available in most dosimetric software tools. The differences became larger in the comparison with ImPACT calculator because further than an unspecified scanner, hermaphrodite mathematical phantom is used. These results are consistent with those reported by other authors who confirm the significant differences due to anatomical variations between phantoms and deviations between scanner models (Ban *et al.* 2011b, Gu *et al.* 2013, Ding *et al.* 2015, Jansen and Shrimpton 2016). The results demonstrated that SimDoseCT represents a step in increasing accuracy in assessing doses from CT examinations with a 320 detector-row cone-beam scanner as it takes into account the specific technical characteristics about the CT scanner.

SimDoseCT extends the dose data that is shown on the clinical CT scanner console, being  $CTDI_{vol}$  and DLP, with organ- and tissue doses and effective dose. With SimDoseCT the goal was to allow for dose assessment that is tailor made for the Aquilion ONE scanner and that is

based on the ICRP computational phantoms. Of course the methodology can also be adapted to other CT scanners models. There are some limitations that must be taken into account. Firstly, the dose data provided by SimDoseCT apply only to standard adult patients, with no dose assessment in paediatric patients or patient with a physique that is not standard. Secondly, the angular and longitudinal tube current modulation employed by the scanner is not implemented in the program. However, the software presents a wide flexibility to overcome these limitations. Previously published studies (Salvadó *et al.* 2005, DeMarco *et al.* 2007) demonstrated that patient size has a significant impact on both effective dose and organ doses, leading to differences more than a factor of 2. In future research, size-specific dose estimates (SSDE) can be considered by including conversion factors in the database to calculate doses from  $CTDI_{vol}$ , such as conversion factors tabulated in AAPM Report 204 (AAPM 2011). Regarding to the tube current modulation, the tool could be adjusted to take into account a set of tube current values (mAs) depending on the z-tube position (longitudinal modulation). Unfortunately, the implementation of the x-y tube current variation (angular modulation) could introduce an uncertainty since the mAs per angle information is not provided in the DICOM files by the CT scanner. In summary, the current version of SimDoseCT becomes a suitable tool to estimate the organ- and effective doses in patients for Aquilion ONE CT examinations.

## 5. Conclusion

Software based on MC simulation for dose assessment in a 320 detector-row cone-beam CT scanner and ICRP adult phantoms was developed and validated. Through an interface, the user can select the acquisition parameters for any available protocol in the Aquilion ONE CT scanner to obtain the corresponding organ- and effective doses. MC code was validated by comparing dose measurements within standard CT dose phantoms with results from simulation. The good agreement between dose results from SimDoseCT for head, thorax and abdomen CT examinations and results from dedicated MC simulations for the same protocols demonstrates the accurate methodology of SimDoseCT and its usefulness and clinical application.

## Acknowledgments

Part of this research has been performed using the resources of CSUC (Consorci de Serveis Universitaris de Catalunya).

We thank Toshiba Medical Systems for providing information and CT dose index data from the scanner.

## References

- AAPM 2011 American Association of Physicists in Medicine AAPM report No.204: Size-Specific Dose Estimates (SSDE) in Pediatric and Adult Body CT Examinations ([www.aapm.org/pubs/reports/](http://www.aapm.org/pubs/reports/))
- Abdullah A, Sun Z, Pongnapang N and Ng K-H 2012 Comparison of Computed Tomography Dose Reporting Software *Radiat. Prot. Dosim.* **151** 153–7
- Ban N, Takahashi F, Ono K, Hasegawa T, Yoshitake T, Katsunuma Y, Sato K, Endo A and Kai M 2011a Waza-Ari: Computational Dosimetry System for X-Ray Ct Examinations II: Development of Web-Based System *Radiat. Prot. Dosim.* **146** 244–7
- Ban N, Takahashi F, Sato K, Endo A, Ono K, Hasegawa T, Yoshitake T, Katsunuma Y and Kai

- M 2011b Development of a web-based CT dose calculator: Waza-ARI *Radiat. Prot. Dosim.* **147** 333–7
- European Commission 2013. Radiation induced long-term health effects after medical exposure *Radiation Protection N.º 182* (<http://bookshop.europa.eu/en/eu-scientific-seminar-2013-radiation-induced-long-term-health-effects-after-medical-exposure-pbMJXA15001/>)
- Cros M, Geleijns J, Joemai R M S and Salvadó M 2016 Perfusion CT of the brain and liver and of lung tumors: Use of Monte Carlo simulation for patient dose estimation for examinations with a cone-beam 320-MDCT scanner *Am. Jour. Roentgenol.* **206** 129–35
- Deak P, van Straten M, Shrimpton P C, Zankl M and Kalender W A 2008 Validation of a Monte Carlo tool for patient-specific dose simulations in multi-slice computed tomography *Eur. Radiol.* **18** 759–72
- DeMarco J J, Cagnon C H, Cody D D, Stevens D M, McCollough C H, O'Daniel J and McNitt-Gray M F 2005 A Monte Carlo based method to estimate radiation dose from multidetector CT (MDCT): cylindrical and anthropomorphic phantoms *Phys.Med. Biol.* **50** 3989–4004
- DeMarco J J, Cagnon C H, Cody D D, Stevens D M, McCollough C H, Zankl M, Angel E and McNitt-Gray M F 2007 Estimating radiation doses from multidetector CT using Monte Carlo simulations: effects of different size voxelized patient models on magnitudes of organ and effective dose *Phys.Med. Biol.* **52** 2583–97
- Ding A, Gao Y, Liu H, Caracappa P F, Long D J, Bolch W E, Liu B and Xu X G 2015 VirtualDose: a software for reporting organ doses from CT for adult and pediatric patients *Phys.Med. Biol.* **60** 5601–25
- Geleijns J, Joemai R M S, Cros M, Hernandez-Giron I, Calzado A, Dewey M and Salvadó M 2015 A Monte Carlo simulation for the estimation of patient dose in rest and stress cardiac computed tomography with a 320-detector row CT scanner *Physica Medica* **31** 1029–34
- Gu J, Bednarz B, Caracappa P F and Xu X G 2009 The development, validation and application of a multi-detector CT (MDCT) scanner model for assessing organ doses to the pregnant patient and the fetus using Monte Carlo simulations *Phys.Med. Biol.* **54** 2699–717
- Gu J, Xu X G, Caracappa P F and Liu B 2013 Fetal doses to pregnant patients from CT with tube current modulation calculated using Monte Carlo simulations and realistic phantoms *Radiat. Prot. Dosim.* **155** 64–72
- Hirayama H, Namito Y and Ban S 2000 Implementation of a general treatment of photoelectric-related phenomena for compounds or mixtures in EGS4 *KEK Internal Report 2000-3* (<http://rcwww.kek.jp/research/egs/kek/egs4/photo.pdf>)
- IAEA 2011 Status of Computed Tomography dosimetry for wide cone beam scanners *IAEA Human Health Series 5*
- ICRP 1977 Recommendations of the ICRP *ICRP Publication 26 Ann. ICRP* **1**
- ICRP 1991 1990 Recommendations of the International Commission on Radiological Protection *ICRP Publication 60 Ann. ICRP* **21**
- ICRP 2009 Adult Reference Computational Phantoms *ICRP Publication 110 Ann. ICRP* **39**
- ICRP 2007a Managing Patient Dose in Multi-Detector Computed Tomography (MDCT) *ICRP Publication 102 Ann. ICRP* **37**
- ICRP 2007b. The 2007 Recommendations of the International Commission on Radiological Protection *ICRP Publication 103 Ann. ICRP* **37**

- IEC 2009 Medical electrical equipment: Part 2-44. Particular requirements for the basic safety and essential performance of x-ray equipment for computed tomography *IEC 60601-2-44 ed30*
- ImPACT 2012 ImPACT's CT dosimetry tool (<http://www.impactscan.org/>)
- Jansen J T M and Shrimpton P C 2016 Development of Monte Carlo simulations to provide scanner-specific organ dose coefficients for contemporary CT *Phys. Med. Biol.* **61** 5356–77
- Jarry G, DeMarco J J, Beifuss U, Cagnon C H and McNitt-Gray M F 2003 A Monte Carlo-based method to estimate radiation dose from spiral CT: from phantom testing to patient-specific models *Phys. Med. Biol.* **48** 2645–63
- Kalender W A , Schmidt B, Zankl M and Schmidt M 1999 A PC program for estimating organ dose and effective dose values in computed tomography *Eur. Radiol.* **9** 555–62
- Kalender W A 2014 Dose in x-ray computed tomography *Phys. Med. Biol.* **59** 129-50
- King S D and Spiers F W 1985 Photoelectron Enhancement of the Absorbed Dose from X Rays to Human Bone Marrow: Experimental and Theoretical Studies *Brit. J Radiol.* **58** 345–56
- Kobayashi M, Asada Y, Matsubara K, Susuki S, Matsunaga Y, Haba T, Kawaguchi A, Daioku T, Toyama H and Kato R 2016 Dose Estimating Application Software Modification: Additional Function of a Size-Specific Effective Dose Calculator and Auto Exposure Control *Radiat. Prot. Dosim.* 1–6
- McCollough C H and Zink F E 1999 Performance evaluation of a multi-slice CT system *Med. Phys.* **26** 2223–30
- McNitt-Gray M F 2002 AAPM/RSNA Physics Tutorial for Residents: Topics in CT. Radiation dose in CT *Radiographics : a review publication of the Radiological Society of North America Inc* **22** 1541–53
- van der Molen A J and Geleijns J 2007 Overranging in multisection CT: quantification and relative contribution to dose-comparison of four 16-section CT scanners *Radiology* **242** 208–16
- Morant J J, Salvadó M, Casanovas R, Hernández-Girón I, Velasco E and Calzado A 2012 Validation of a Monte Carlo simulation for dose assessment in dental cone beam CT examinations *Physica Medica* **28** 200–9
- Nelson W R, Hirayama H and Rogers D W 1985 The EGS4 Code System (<http://www.slac.stanford.edu/pubs/slacreports/slac-r-265.html>)
- Salvadó M , Lopez M, Morant J J and Calzado A 2005. Monte Carlo calculation of radiation dose in CT examinations using phantom and patient tomographic models *Radiat. Prot. Dosim.* **114** 364–8
- Salvadó M, Cros M, Joemai R M S, Calzado A and Geleijns J 2015 Monte Carlo simulation of the dose distribution of ICRP adult reference computational phantoms for acquisitions with a 320 detector-row cone-beam CT scanner *Physica Medica* **31** 452-62
- Schauer D A and Linton O W 2009 NCRP report no. 160 Ionizing radiation exposure of the population of the United States, medical exposure—are we doing less with more, and is there a role for health physicists? *Health Physics* **97** 1–5
- Smith A B, Dillon W P, Gould R and Wintermark M 2007 Radiation dose-reduction strategies for neuroradiology CT protocols *Am. J. Neuroradiol.* **28** 1628–32
- Stamm G and Nagel H D 2002 CT-Expo - a Novel Program for Dose Evaluation in CT *Fortschr Röntgenstr* **174** 1570–6

- Takahashi F, Sato K, Endo A, Ono K, Yoshitake T, Hasegawa T, Katsunuma Y, Ban N and Kai M 2011 WAZA-ARI: Computational dosimetry system for x-ray CT examinations. I. radiation transport calculation for organ and tissue doses evaluation using JM phantom *Radiat. Prot. Dosim.* **146** 241–3
- Zankl M, Eckerman K F and Bolch W E 2007 Voxel-based models representing the male and female ICRP reference adult - The skeleton *Radiat. Prot. Dosim.* **127** 174–86

## Chapter 5

# Discussion

### 5.1 Results discussion

The main contribution of this dissertation is the implementation of a tool based on MC simulation to assess organ absorbed doses and effective dose in patients undergoing CT examinations with a 320 detector-row cone-beam scanner and taking into account the latest recommendations of the ICRP. This was achieved by developing and validating a MC program to accurately reproduce the technical features of the scanner and by its application for patient dose estimates in specific clinical acquisitions that can be performed with this scanner such as cardiac CT protocol or perfusion CT studies. Besides, a dose reporting software based on MC simulation was developed with the aim of providing an useful tool for dose evaluation in CT contemporary scanners.

Due to the fast technical advances in x-ray imaging during last years and the increase in the number of CT examinations, there is a need to be aware about radiation exposure in current acquisition protocols in order to optimize the clinical application of CT and to reduce possible undesired radiation-induced health effects. At the beginning of this thesis, a large amount of scientific studies about dose assessment in CT examinations using MC simulation methods had been published. However, most of them were based on CT scanners with narrow geometries and mathematical phantoms. For this reason, these works became outdated with the publication of adult computational phantoms by the ICRP and the commercialization of the 320 multislice CT scanner (Aquilion ONE) by Toshiba Medical Systems. Hence, the significance of the tool developed in this thesis is related to the existence of very few studies focused on accurate dose assessment in latest technology CT scanners and reference anthropomorphic phantoms.

In order to achieve the goals of this dissertation, the first step was to develop a MC simulation tool for patient dose assessment for a 320 detector-row cone-beam scanner. The MC program was adapted according to the specifications of the Aquilion ONE CT scanner from a code previously developed for other CT systems [25–29]. The program takes into account all aspects that influence dose distribution such as the tube voltage, the primary filtration, the bow tie filter and the heel effect modelled as relative attenuation profiles, the beam width including the overbeaming, the focal spot size and the penumbra, rotation and tube charge, TCM and also the patient support table. Therefore, the MC program accurately simulates the cone-beam geometry of the 320 multislice scanner. The scanner implementation in the MC simulation code was described and validated in Paper [I]. For the validation, differences within 8% were found between measured and simulated values of the absorbed doses using a ionization chamber within a CT dose phantom. The good agreement demonstrated that the developed scanner model is an accurate tool for dose estimates. In addition, the ICRP

reference adult computational phantoms, which represents the standard male (AM) and female (AF), were also successfully implemented in the simulation program, as it was described in Paper [I]. Specific considerations were required in the implementation of tissues like red bone marrow (RBM) or endosteum because its microscopic structure was smaller than the size of a voxel.

Once validated, the MC program became an useful tool to assess absorbed doses in organs or tissues and to calculate the effective dose for standard adult patients. Hence, at this point, the next milestone was the application of the MC simulation for dose assessment in patients undergoing CT examinations in a 320 detector-row cone-beam scanner. This task was divided in different steps, all of them described in Papers [I], [II] and [III]. Firstly, dose assessment was performed for male and female anthropomorphic reference phantoms in four general clinical acquisition protocols from this scanner such as CTA head, CTA renal arteries, shoulder CT and hip CT. Secondly, the MC simulation tool was used for estimation of patient dose in specific CT studies performed in this scanner due to the advantages of its wide coverage in a single axial rotation. This is the case of rest and stress cardiac CT and the CTP examinations of the brain, liver and lung tumors.

For the CTA head, shoulder CT, hip CT and the CTP protocols, the sex-averaged effective doses were in the range of 0.1 and 0.5 mSv/100 mAs for head acquisitions and about 2.2 mSv/100 mAs for body examinations. All the acquisitions were performed in a volumetric mode using the maximum coverage (160 mm), except in shoulder CT that the coverage was about 130-140 mm. For cardiac CT protocol, which included CT coronary calcium scoring, CT coronary angiography and CT stress myocardial perfusion, effective doses were 5.6 mSv/100 mAs for female and 2.2 mSv/100 mAs for male. In this case, the dose values depend on the heart rate of the patient, since for high heart rates a dual heart beat acquisition is required instead of a single one. Thereby, effective doses were nearly doubled for patients with high heart rates.

Several relevant differences between organ doses in adult male and adult female can be appreciated in the performed CT examinations. Mostly, doses were approximately two times higher in female than male. Different factors influenced to these dose deviations, but the main reason was the difference between phantoms as far as body masses or organ locations are concerned. Differences on effective dose between male and female phantoms were mainly due to the high weighting factor used for breast tissue in female.

The effect on dose of the TCM was analysed in Paper [I], concretely for the CTA renal arteries examination. In the comparison between the acquisition using TCM and with a constant tube current ( $\text{mA}_{\text{Max}}$ ), results showed that TCM decreases organ- and effective doses in a factor proportional to the total tube current reduction and also leads to a greater uniformity of the dose distribution.

Although in clinical cardiac CT it is common practice to use an offset in positioning of the patient to center the heart to the axis of rotation of the scanner and the arms of the patient are positioned along the head instead of along the body, these considerations are not taken into account in most dosimetric studies. For this reason, Paper [II] analysed the influence on dose of the different configurations, i.e. patient centered and off-centered and arms removed or not removed from the scan range. The study demonstrated that the influence on effective dose of the positioning of the patient was negligible, but the effect of removing the arms from the scan range has to be taken into account because may lead to an increase of 6–8% on effective dose.

Perfusion CT examinations have become relevant in the radiation protection field because the volume of interest is scanned repeatedly in dynamic studies, and therefore, dose increases substantially during the CT scan. In addition, since eye lens is directly irradiated in brain acquisitions, it is necessary to assess doses in this organ. A similar relevance occurs in the skin dose, which is significantly accumulated during the study. For this reason, there is a need of assessing the peak entrance skin dose (ESD) to ensure that the threshold dose for induction deterministic effect is not exceeded. In Paper [III], absorbed doses in these organs or tissues of interest were also evaluated. Results showed that eye lens dose and ESD were lower than the dose thresholds published in ICRP guidelines for deterministic effects. In fact, they represented a 30% of the threshold for eye lens and between 8-14% for peak skin dose. However, because of the radiation risks depend on the patient and possible variations on dose may occur, conversion factors to estimate the eye lens dose and the peak ESD from the  $CTDI_{vol}$  were also calculated.

In addition to providing an accurate dose assessment for the different specific CT examinations, that are usually performed with the 320 detector-row cone-beam scanner due to its technical features, one of the milestones of this thesis was to provide tools for easy organ- and effective dose estimates in clinical practice. In order to achieve this goal, k-factors that allow the calculation of the effective dose from the dose quantities that appear in the console of the scanner, such as DLP, were derived in Papers [I], [II] and [III] for all the mentioned CT examinations, respectively.

However, it is important to remark that k-factors were only useful to roughly estimate effective dose or absorbed dose in a few organs. For this reason and to accomplish the last goal of this thesis, a software tool based on MC simulation was developed to facilitate the accurate dose assessment for standard patients undergoing CT examinations in a 320 multi-slice scanner. As it is described in Paper [IV], the software, called SimDoseCT (see Appendix A), calculates and reports the effective dose and the organ doses for any acquisition protocol available in the scanner from look-up-tables generated using MC simulation. Unlike the validation of the MC code performed in Paper [I] which was only for the collimation of 160 mm, in this case the validation was made for all the allowed collimations in the scanner in order to ensure the correct operation of the cone-beam geometry, including the overbeaming, in all the cases. Differences up to 9% between simulated and measured CTDI values allowed the validation of the MC program for all the collimations. Additionally, when dose estimation from SimDoseCT and dose results obtained from dedicated MC simulations were compared, the low differences (up to 0.1 mGy or mSv of absolute dose) demonstrated the correct functionality of the software.

## 5.2 Discussion on the state of the art

With the introduction of the 320 detector-row CT scanner, most research groups working in the field of x-ray dosimetry were aware about the new dosimetric concept introduced by the wide geometry of the scanner. From this moment, there was a need of researching about dose assessment in a 320 multislice scanner. Despite the publication of some studies about this topic, the latest recommendations of the ICRP such as the adult reference computational phantoms had not been taken into account yet.

In the meantime, and due to the large amount of studies published about dose assessment in scanners with narrower geometries, doses from a 320 multi-slice scanner



were estimated using the same methods. Therefore, k-factors derived from studies with other scanners were used for dose assessment in contemporary CT technologies, leading to significant deviations on dose estimation. In a similar way, the available dosimetric software tools at the moment [19–24] have been used to report patient doses in the new scanners, even if they were based on outdated scanner models and stylized phantoms.

In this framework, the combination of the latest generation of CT scanners and the most recent recommendations for radiation protection with a versatile tool such as MC simulation was the highlight of this dissertation. When dose results from the studies gathered in this thesis were compared with results from other authors who use outdated scanners or mathematical phantoms instead, relevant differences reinforced the significance of the developed tools.

A comparison between effective doses from clinical CT acquisitions included in Paper [I] and dose results given by ImPACT Dosimetry Calculator demonstrated that this tool overestimates doses in CTA head and hip CT examinations, and contrarily doses in shoulder CT were underestimated. ImPACT may lead to high differences due to the use of a scanner with 16 detector rows and hermaphrodite stylized phantom. The former leads to deviations related to the beam geometry like the cone-beam shape, heel effect or the overbeaming. The latter entails differences in phantom in such a way that positioning of high radiosensitive organs like breast and thyroid could lead to large discrepancies in dose depending on if they are located within the volume directly irradiated or not. Besides, it is important to notice that ICRP computational phantoms, which were used in the studies of this thesis, provide a more realistic and accurate representation of human anatomy. In this way, other authors reported k-factors for generic protocols in different scanners that overestimate effective doses from the 320 multi-slice scanner [30, 31].

Contrarily, for the cardiac protocol performed with the 320 detector-row scanner and described in Paper [II], the ImPACT dosimetry calculator tool and the k-factors reported by other authors [27, 32–37] may underestimate the effective dose a factor of 2 in average phantom and a factor of 3 in female. In addition to the differences in scanner models and phantoms, some methodological aspects such as the correct positioning may cause the dose underestimation. These discrepancies also occur in perfusion CT examinations included in Paper [III] if scanners with narrower geometries are used for dose evaluation in a wide cone-beam scanner. While results from literature [38, 39] overestimate the effective dose in brain protocols, dose in body acquisitions is underestimated. Hence, it is recommended to modify the standard ICRP computational phantoms accordingly for dose estimates of body CT acquisitions where trunk of the patient is scanned with the arms positioned along the head.

The above mentioned deviations on effective dose assessment in standard patients for a 320 detector-row cone-beam scanner can be overcome with the use of the k-factors reported in the different studies of this thesis. Also regarding to the organ doses, a software dosimetric tool is also provided for easily and accurate dose estimates taking into account the technical characteristics of the scanner model. As it is described in Paper [IV], doses reported by other software tools [19, 23] that use outdated scanner models may differ up to 40% from doses reported by SimDoseCT. In the case of tools that in addition to outdated scanners, use stylized phantoms, dose differences can be even more than 100% in some organs due to the inappropriate implementation of the contemporary CT scanners and reference phantoms.

## Chapter 6

# Conclusions

### 6.1 Main conclusions

This dissertation presents a frame of reference for dose estimates in standard patients undergoing CT examinations with a 320 detector-row cone-beam scanner. MC simulation was used to assess organ- and effective doses in the ICRP adult reference computational phantoms from clinical acquisitions and specific protocols performed with this scanner.

According to the objectives of this thesis, the main conclusions can be stated as follows:

A MC simulation program was tailored for dose assessment in CT examinations with a 320 detector-row cone-beam scanner. An accurate reproduction of the scanner operation was achieved by modelling all the technical aspects that have an effect on dose including the x-ray spectrum, the x-ray beam geometry and the acquisition parameters.

The MC simulation program was validated by comparing results from simulations with the actual measurements acquired in the scanner under the same conditions in standard CT dose phantoms. Good agreement was found between results (differences were within 8%).

The MC program in combination with the ICRP anthropomorphic computational phantoms were used to estimate organ- and effective doses in standard adult patients from clinical acquisitions with a 320 multislice CT scanner. Effective doses were in the range of 0.1 and 0.5 mSv/100 mAs for head acquisitions and about 2.2 mSv/100 mAs for body examinations. Organ doses in female were predominantly higher than in male.

The influence of TCM on patient dose was analysed using a renal arteries CTA clinical protocol. With the modulation of the tube current depending on the patient size, the uniformity of the dose distribution increased and doses decreased.

The MC program was used to estimate organ- and effective doses in the ICRP computational phantoms for a cardiac CT protocol (including CT calcium scoring, CT coronary angiography and CT myocardial perfusion) with a 320 multislice CT scanner. Effective doses were 5.6 mSv/100 mAs for female and 2.2 mSv/100 mAs for male. Organ doses in female were two times higher than in male.

The effect on dose of the off-centered positioning of the patient in clinical cardiac CT and the arms positioning during the scan was evaluated. The influence on effective dose of the positioning of the patient was negligible, but the effect of removing the arms

from the scan range may lead to a significant increase on effective dose (between 6 and 8%).

The MC program was employed to assess organ- and effective doses from perfusion CT examinations of the brain, lung tumors and the liver on a 320 detector-row scanner with the ICRP adult computational phantoms. The scan repetition required in these dynamic studies leads to relevant patient radiation exposure resulting in effective doses in the order of magnitude of 4 mSv for brain perfusion and in the range of 23–25 mSv for body perfusion acquisitions. Organ doses in female were mostly higher than in male.

The absorbed dose in radiosensitive organs such as eye lens and skin during perfusion CT studies was evaluated. Results were lower than the dose thresholds published in ICRP guidelines for induction of deterministic effects. The results were correlated with  $CTDI_{vol}$  to establish conversion factors for eye lens and peak skin dose estimation.

Conversion factors (k-factors) to estimate effective dose from DLP were determined for all the studied acquisition protocols. Results established conversion factors about 0.0015 mSv/mGy · cm for head protocols and in the range of 0.01–0.03 mSv/mGy · cm for body CT acquisitions in the 320 multislice scanner.

A software dosimetric tool based on MC simulation was developed to easily assess and report doses for standard patients undergoing CT examinations in a 320 detector-row cone-beam scanner. The tool provides organ- and effective doses in the ICRP reference adult phantoms for all the available protocols in the scanner. Results demonstrated the accurate methodology of the tool and its usefulness in clinical application.

The use of dosimetric tools based on outdated scanners and inaccurate phantoms led to important dose deviations for a 320 detector-row cone-beam scanner that can be avoided with the use of the tools developed in this dissertation.

## 6.2 Future work

The methods described in this thesis such as the k-factors determined for each acquisition protocol and the current version of SimDoseCT become suitable tools to estimate the effective dose and the organ doses in patients for CT examinations with a 320 multislice scanner.

However, the tools provided in the framework of the thesis are focused on standard adult patients. Specially for the body studies, size changes significantly depending on the patient. Thus, the effect of patient size on dose in CT contemporary scanners needs to be analysed in future studies.

One of the most important benefits of MC simulation is versatility as the code can be adapted accurately to reproduce the specific dosimetric question and the actual exposure conditions. Thereby, different phantoms can be implemented in the code to evaluate the influence of different patient sizes, including paediatric patients.

In a short term, some improvements could be performed to extend the SimDoseCT tool. Size-specific dose estimates (SSDE) could be considered if conversion factors to calculate doses from  $CTDI_{vol}$  are also included in the database, such as conversion factors tabulated in AAPM Report 204 [40]. Besides, regarding to the TCM, the tool could be adjusted to take into account a set of tube current values (mAs) depending on the z-tube position (longitudinal modulation). Unfortunately, the implementation of the x-y tube current variation (angular modulation) could introduce an uncertainty since the mAs per angle information is not provided in the DICOM files by the CT scanner.

In a medium term, the great flexibility in implementation of the developed MC simulation program, can allow to extend it to new x-ray diagnostic systems for dose assessment in the latest trends in CT technology. In addition, since dose optimization in CT is based on reducing patient dose without compromising the image quality level required for an appropriate diagnosis, new dosimetric studies that take into account image quality evaluation have to be investigated for the specific protocols used in CT contemporary scanners.



## Chapter 7

# Bibliography

- [1] Kalender WA. *Computed Tomography. Fundamentals, system technology, image quality and applications*. Munich: Publicis MCD Werbeagentur GmbH, 2000
- [2] Hsieh J. *Computed Tomography. Principles, design, artifacts, and recent advances*, 2nd ed. Bellingham: John Wiley & Sons Inc., 2009
- [3] Romans LE. *Computed Tomography for technologists. A comprehensive text*. Baltimore and Philadelphia: Wolters Kluwer Health/Lippincott Williams & Wilkins, 2011
- [4] Calzado A, Geleijns J. Tomografía Computarizada. Evolución, principios técnicos y aplicaciones. *Revista Física Médica* 2010;11:163-180
- [5] Kalender WA. Dose in x-ray computed tomography. *Phys Med Biol* 2014;59:129-50
- [6] Buzug TM *Computed Tomography. From Photon Statistics to Modern Cone-Beam CT*, 1st ed. Heidelberg:Springer-Verlag, 2008
- [7] Rosenberg KM. The open-source Computed Tomography Simulator (CTSim). 2014 (<http://www.ctsim.org/>)
- [8] Geleijns J, Salvado Artells M, de Bruin PW, Matter R, Muramatsu Y, McNitt-Gray MF. Computed tomography dose assessment for a 160 mm wide, 320 detector row, cone beam CT scanner. *Phys Med Biol* 2009;54:3141-59
- [9] Shope TB, Gagne RM, Johnson GC. A method for describing the doses delivered by transmission x-ray computed tomography. *Med Phys* 1981;8:488-495
- [10] International Atomic Energy Agency. Status of computed tomography. Dosimetry for wide cone beam scanners. Vienna: IAEA Human Health, 2011: Reports No 5
- [11] International Commission on Radiological Protection. The 2007 Recommendations of the International Commission on Radiological Protection. ICRP Publication 103. *Ann ICRP* 2007;37:1-332
- [12] Cagnon C, DeMarco J, Angel E, McNitt-Gray M. Estimating Patient Radiation Dose from Computed Tomography. UCLA David Geffen School of Medicine, American Collage of Medical Physics, American Association of Physicists in Medicine 2008
- [13] American Association of Physicists in Medicine. The Measurement, Reporting, and Management of Radiation Dose in CT. Report of AAPM Task Group 23: CT Dosimetry, 2008: Report No 96
- [14] Baró J, Fernández-Varea JM, Mayol R, et al. Simulació Montecarlo del transport d'electrons i fotons d'alta energia. *Revista de Física* 1997;12

- [15] Choonsik L, Jai-Ki L. Computational anthropomorphic phantoms for radiation protection dosimetry: evolution and prospects. *Nuclear engineering and technology* 2006;38
- [16] Zankl M, Petoussi-Henss N, Fill U, Regulla D. The application of voxel phantoms to the internal dosimetry of radionuclides. *Radiat Prot Dosimetry* 2003;105:539-548
- [17] International Commission on Radiological Protection. Adult reference computational phantoms. ICRP Publication 110. *Ann ICRP* 2009;29
- [18] International Commission on Radiological Protection. Managing Patient Dose in Multi-Detector Computed Tomography (MDCT). ICRP Publication 102. *Ann ICRP* 2007;37
- [19] Kalender WA, Schmidt B, Zankl M and Schmidt M A PC program for estimating organ dose and effective dose values in computed tomography. *Eur Radiol* 1999;9:555-562
- [20] Stamm G, Nagel HD. CT-Expo - a Novel Program for Dose Evaluation in CT. *Fortschr Rontgenstr* 2002;174:1570-1576
- [21] Ban N, Takahashi F, Ono K, Hasegawa T, Yoshitake T, Katsunuma Y, Sato K, Endo A, Kai M. Waza-Ari: Computational Dosimetry System for X-Ray CT Examinations II: Development of Web-Based *Radiat Prot Dosim* 2011;146:244-247
- [22] Takahashi F, Sato K, Endo A, Ono K, Yoshitake T, Hasegawa T, Katsunuma Y, Ban N, Kai M. WAZA-ARI: Computational dosimetry system for x-ray CT examinations I: radiation transport calculation for organ and tissue doses evaluation using JM phantom *Radiat Prot Dosim* 2011;146:241-243
- [23] ImPACT. ImPACT's CT dosimetry tool. 2012 (<http://www.impactscan.org/>)
- [24] Ding A, Gao Y, Liu H, Caracappa PF, Long DJ, Bolch WE, Liu B and Xu XG. VirtualDose: a software for reporting organ doses from CT for adult and pediatric patients. *Phys Med Biol* 2015;60:5601-5625
- [25] Salvadó M, López M, Morant JJ, Calzado A. Monte Carlo calculation of radiation dose in CT examinations using phantom and patient tomographic models. *Radiat Prot Dosimetry* 2005;114:364-8
- [26] Geleijns J, Salvadó Artells M, Veldkamp WJH, López Tortosa M, Calzado Cantera A. Quantitative assessment of selective in-plane shielding of tissues in computed tomography through evaluation of absorbed dose and image quality. *Eur Radiol* 2006;16:2334-2340
- [27] Geleijns J, Joemai RMS, Dewey M, De Roos A, Zankl M, Cantera AC, et al. Radiation exposure to patients in a multicenter coronary angiography trial (CORE 64). *Am J Roentgenol* 2011;196:1126-1132
- [28] Morant JJ, Salvadó M, Casanovas R, Hernandez-Giron I, Velasco E, Calzado A. Validation of a Monte Carlo simulation for dose assessment in dental cone beam CT examinations. *Phys Medica* 2012;28:200-209
- [29] Morant JJ, Salvadó M, Hernandez-Giron I, Casanovas R, Ortega R, Calzado A. Dosimetry of a cone beam CT device for oral and maxillofacial radiology using Monte Carlo techniques and ICRP adult reference computational phantoms. *Dentomaxillofac Radiol* 2013;42:92555893

- [30] Deak PD, Smal Y, Kalender WA. Multisection CT protocols: sex- and agespecific conversion factors used to determine effective dose from doselength product. *Radiology* 2010;257:158e66
- [31] Huda W, Magill D, He W. CT effective dose per dose length product using ICRP 103 weighting factors. *Med Phys* 2011;38:1261e5
- [32] Bongartz G, Golding SJ, Jurik AG, et al. European guidelines on quality criteria for computed tomography. EUR 16262 1999.
- [33] Deak P, van Straten M, Shrimpton PC, Zankl M, Kalender WA. Validation of a Monte Carlo tool for patient-specific dose simulations in multi-slice computed tomography. *Eur Radiol* 2007;18:759-772
- [34] Seguchi S, Aoyama T, Koyama S, Fujii K, Yamauchi-Kawaura C. Patient radiation dose in prospectively gated axial CT coronary angiography and retrospectively gated helical technique with a 320-detector row CT scanner. *Med Phys* 2010;37:5579-5585
- [35] Einstein AJ, Elliston CD, Arai AE, Chen MY, Mather R, Pearson GD, et al. Radiation dose from single-heartbeat coronary CT angiography performed with a 320-detector row volume scanner. *Radiology* 2010;254:698-706
- [36] Gosling OE, Roobottom CA. Radiation exposure from cardiac computed tomography. *JACC Cardiovasc Imaging* 2010;3:1201-1202
- [37] Huda W, Tipnis S, Sterzik A, Schoepf UJ. Computing effective dose in cardiac CT. *Phys Med Biol* 2010;55:3675-3684
- [38] Valentin J, International Commission on Radiological Protection. Managing patient dose in multi-detector computed tomography (MDCT): ICRP publication 102. *Ann ICRP* 2007;37:1-79
- [39] Diekmann S, Siebert E, Juran R, et al. Dose exposure of patients undergoing comprehensive stroke imaging by multidetector-row CT: comparison of 320-detector row and 64-detector row CT scanners. *Am J Neuroradiol* 2010; 31:1003-1009
- [40] American Association of Physicists in Medicine. Size-Specific Dose Estimates (SSDE) in Pediatric and Adult Body CT Examinations. AAPM, 2011: report No 204





## Appendix A

# Software registration

### **SimDoseCT: Computed Tomography dose reporting software**

#### **Summary**

The software, called SimDoseCT, is a tool for assessing and reporting doses for standard patients undergoing CT examinations in a 320 detector-row cone-beam scanner. The software is based on MC simulation code, which was developed to calculate organ- and effective doses in the current standard phantoms, namely the ICRP computational adult male and female phantom, for acquisitions with the Aquilion ONE CT scanner (Toshiba). SimDoseCT consists of a graphical user interface coded using the object-oriented programming language C# (Microsoft, USA) connected to a MySQL database, which contains 378504 look-up-tables that were generated with MC simulations. The dose assessment should take into account all relevant technical characteristics of the scanner, like focal spot size, overbeaming, overranging, beam shaping filter, the cone beam geometry and the heel effect. The software should also take into account all possible acquisitions within the scanner, like axial (volumetric), helical and scanogram acquisitions. Hence, the user can select any available protocol in the Aquilion ONE scanner for any scan range of the standard adult male or female and obtain the dose results through the SimDoseCT interface that accurately resembles the user interface of the actual CT scanner. After entering the acquisition protocol in SimDoseCT, the dose results are displayed immediately in the user interface. A patient dose report can be generated and saved. Hence, the software presents a tool for an accurately organ- and effective dose estimation in a 320 detector-row cone-beam scanner with the aim of improving the easy dose evaluation for standard adult patients in CT contemporary scanners.



B B I E  
I  
P  
B  
O



Benelux Office  
for Intellectual Property



## i-DEPOT evidence

Number

105319

Date

11-05-2017

Reference

T-2017/011

Title

SimDoseCT: Computed Tomography dose reporting software

In the name of

FUNDACIÓ URV  
Avda. Paisos Catalans 18  
43007 Tarragona  
Spain

This electronic file constitutes proof that all the included data was submitted to the Benelux Office for - Intellectual Property (BOIP) on the date mentioned and has not been altered subsequently.

Edmond Simon  
Director General BOIP

B B I E

I

P

B

O



Benelux Office  
for Intellectual Property



## Description

The software, called SimDoseCT, is a tool for assessing and reporting doses for standard patients undergoing Computed Tomography examinations in a 320 detector-row cone-beam scanner.

B B I E

I

P

B

O



Benelux Office  
for Intellectual Property



## Attachments

Click on the file to open it. **Attention:** It depends on the settings of your PDF viewer if and how the file will be opened.

- > 63\_CPCT2\_2017 - Acord 2017PAT-10 - Notificació.pdf
- > iDEPOT Information\_SimDoseCT.docx
- > Sol·licitud propietat intel·lectual SimDoseCT.pdf
- > SourceCode\_SimDoseCT.txt
- > User\_manual\_SimDoseCT.pdf



# SimDoseCT

*User Manual*

---



LEIDEN UNIVERSITY MEDICAL CENTER



## Table of Contents

1. Introduction .....	3
2. Programming language and system requirements .....	4
3. Using SimDoseCT .....	5
4. Copyright .....	15

## 1. Introduction

The software, called SimDoseCT, is a tool for assessing and reporting doses for standard patients undergoing Computed Tomography examinations in a 320 detector-row cone-beam scanner. The software is based on Monte Carlo simulation code, which was developed to calculate organ and effective doses in the current standard phantoms, namely the ICRP (International Commission on Radiological Protection) computational adult male and female phantom, for acquisitions with the Aquilion ONE Computed Tomography scanner (Toshiba). SimDoseCT consists of a graphical user interface connected to a MySQL database, which contains 378504 look-up-tables that were generated with Monte Carlo simulations. The dose assessment should take into account all relevant technical characteristics of the scanner, like focal spot size, overbeaming, overranging, beam shaping filter, the cone beam geometry and the heel effect. The software should also take into account all possible acquisitions within the scanner, like axial (volumetric), helical and scanogram acquisitions. Hence, the user can select any available protocol in the Aquilion ONE scanner for any scan range of the standard adult male or female and obtain the dose results through the SimDoseCT interface that accurately resembles the user interface of the actual Computed Tomography scanner. After entering the acquisition protocol in SimDoseCT, the dose results are displayed immediately in the user interface. A patient dose report can be generated and saved.

In summary, the software presents a tool for an accurately organ and effective doses estimation in a 320 detector-row cone-beam scanner with the aim of improving the easily dose evaluation for standard adult patients in Computed Tomography contemporary scanners.

## 2. Programming language and system requirements

SimDoseCT consists of a graphical user interface connected to a MySQL database. The application runs on a PC and shows the same interface as the scan console of the Aquilion ONE CT scanner (software version 4.74). The user can design an acquisition protocol with the same options and user interface as on the scanner console. Once the acquisition protocol is designed the user has the option to visualize the dose values either by selecting a dose tab in the interface or by generating a PDF dose report. Both options will trigger the application to retrieve dose values from the database. The database can either be stored local or accessed as an online database by performing a secure query. The graphical user interface has read-only privileges in the database for security reasons. The user can change any acquisition parameter and the dose will be updated in real-time to show how it affects the organ dose and effective dose. This software is coded using the object-oriented programming language C# (Microsoft, USA).

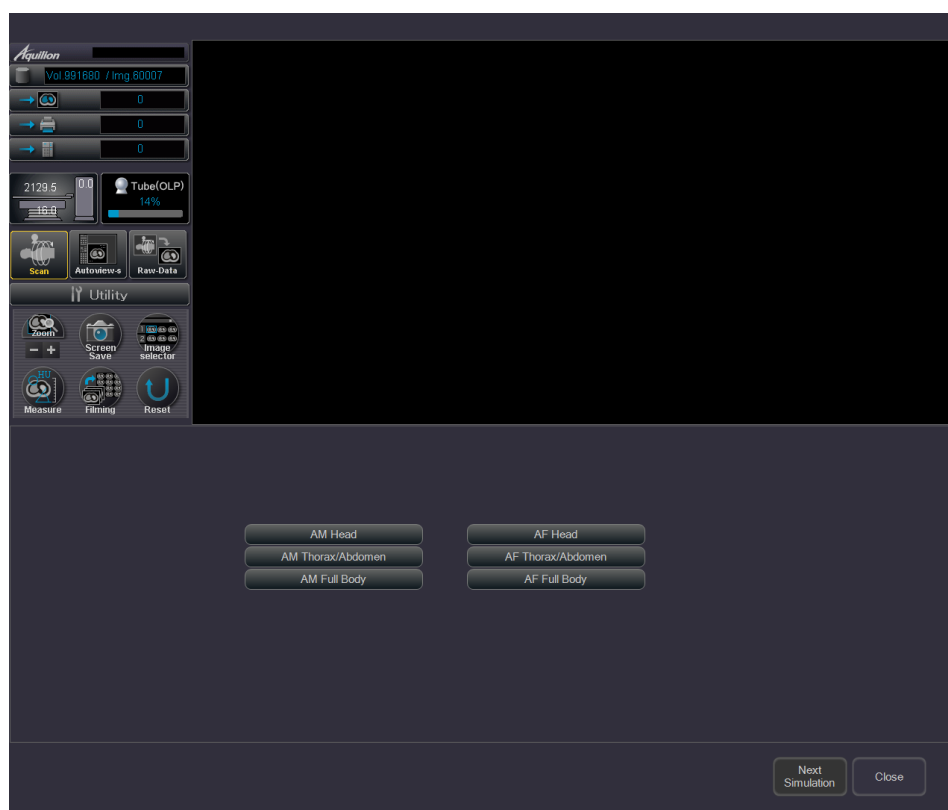
The software requires the installation on user's computer. SimDoseCT can be downloaded from <http://dio.urv.cat/simdosect/> after a user registration. Once installed, the software can be used from the computer, which must be connected to the internet. Every time that the user runs the program, user verification and data updating will be automatically done.

The recommendable resolution of the computer screen is at least 1280 x 1024. If the resolution is lower, scroll bars will be automatically added in the interface with the aim to use the program normally.

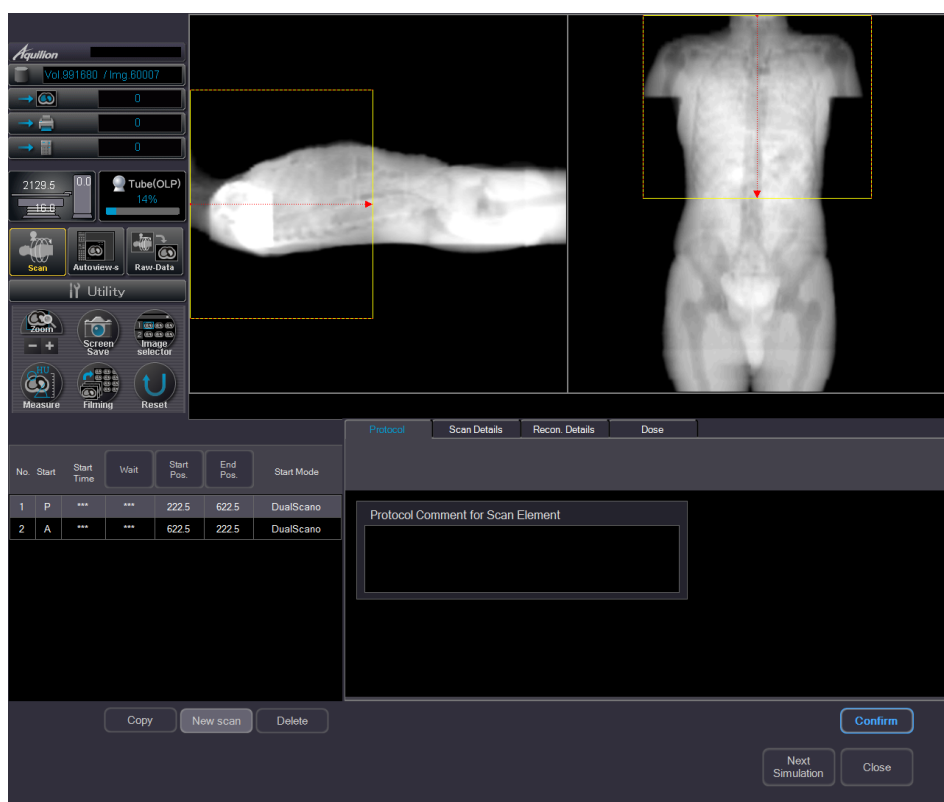
### 3. Using SimDoseCT

SimDoseCT is based on a graphical user interface that accurately resembles the user interface of the actual Aquilion ONE Computed Tomography scanner. For this reason, the use of this software should be easy for the clinical professionals who know how the scanner operates.

**Step 1.** When SimDoseCT is launched, a first menu appears. It includes the path to all clinical protocols (head, thorax/abdomen and full body) in the application for male (AM) and female (AF). You may choose one of the six possible protocols.



**Step 2.** When you click on one of the protocols, two images of a phantom showing the corresponding part of the body are added in the screen, one lateral and one frontal image. In the left lower corner, there is a table with a summary of the different scans of the whole protocol. As in the actual scanner, two orthogonal scanograms are going to be included as default (DualScano). You can write the start and the end position (in cm from the top of the head of the phantom) of the scan range. Alternatively, you can choose the range of the scanning using the yellow boxes in the phantom pictures.



**Step 3.** Other scans can be added in the same whole protocol after the both scanograms clicking the button “New scan”. You can choose the scan mode you prefer (volumetric, S&S, S&V and helical).



**Step 4.** Select again the start and the end position to define the scan range by using the yellow boxes or by directly writing the positions. You can write any comment about the protocol in the enabled box in the tab “Protocol”.



The screenshot shows the Aquilion software interface. The top section displays two axial CT slices with yellow boxes indicating the scan range. The bottom section shows a table with scan parameters and a text box for protocol comments.

No.	Start	Start Time	Wait	Start Pos.	End Pos.	Start Mode
1	P	***	***	222.5	622.5	DualScano
2	A	***	***	622.5	222.5	DualScano
3	P			222.5	432.5	Volumes

Protocol Comment for Scan Element

Buttons: Copy, New scan, Delete, Confirm, Next Simulation, Close

**Step 5.** Clicking on the tab “Scan Details”, you can choose all the acquisition parameters of the examination. You can choose the tube voltage (i.e. 80, 100, 120 and 135 kVp) and the beam shaping filter or FOV (i.e., small, medium and large). The tube current can be selected from 10 to 50 mA in 5 mA steps and from 50 to 580 mA in 10 mA steps. You can also select the rotation time (i.e., 0.35, 0.375, 0.4, 0.45, 0.5, 0.65, 0.75, 1.0, 1.5, 2.0 or 3.0 s). The focal spot size, either large or small, is automatically chosen by the scanner depending on the selected acquisition parameters. The range is automatically determined using the start and the end position that you have chosen. The effective mAs and the total scan time are also automatically calculated. The direction can be *in* or *out*. The control exposure is not yet implemented and it remains at mode *off*.

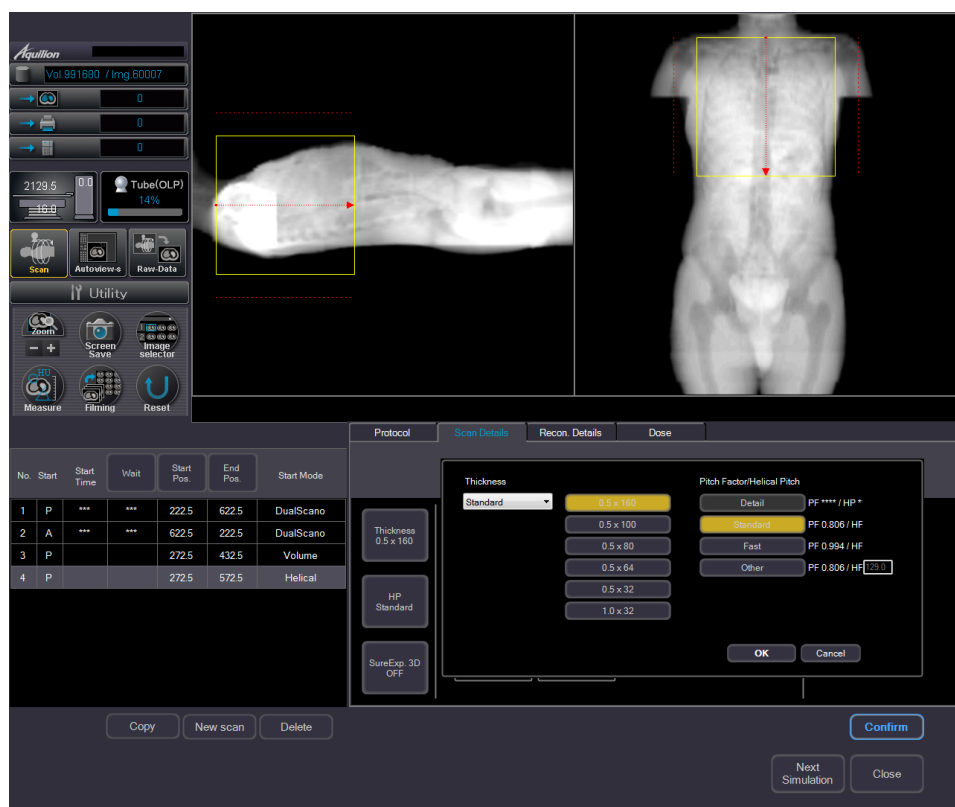




**Step 6.** Clicking on the box “Thickness”, you can select one of the sixteen different beam collimations between 2 and 160 mm (i.e. 160, 140, 128, 120, 100, 80, 60, 50, 40, 32, 20, 16, 12, 8, 4 and 2 mm). There are different options depending on the scan mode that you choose.



**Step 7.** For the helical mode, the helical pitch has to be selected. Clicking the box “HP”, you can choose one pitch value from different options (i.e., detail, standard, fast, other) depending on the thickness.



**Step 8.** When you have defined all the acquisition parameters, click on the tab “Dose” to obtain the dose results from the individual scan that you have selected in the table situated at left of the screen and that appears highlighted. The doses in organs that contribute to the calculation of the effective dose are shown in a table. The doses in other organs or tissues of interest are also indicated. In addition, you obtain the CTDIvol, the DLP and the Effective dose of this individual scan. The effective dose of the whole protocol is also indicated.

The screenshot displays the Aquilion software interface. On the left is a control panel with various icons and settings. The center shows two CT scan images: an axial view on the left and a coronal view on the right. The 'Dose' tab is selected, showing a table of organ doses and effective doses. The table has three columns: Organ Name, Organ Dose (mGy), and Organ Dose x Wt. The data is as follows:

Organ Name	Organ Dose (mGy)	Organ Dose x Wt
Gonads	0.00	0.00
Red Bone Marrow	1.21	0.15
Colon	0.13	0.02
Lung	6.51	0.78
Stomach	0.78	0.09
Urinary bladder	0.01	0.00
Breast	1.01	0.00
Liver	0.86	0.03
Oesophagus	5.93	0.24

Below the table, there are buttons for 'Copy', 'New scan', 'Delete', 'Confirm', 'Next Simulation', and 'Close'. The 'Dose' tab also displays summary statistics: CTDIvol (10.7 mGy), DLP (171.2 mGy.cm), and Eff. Dose Serie (2.23 mSv).

**Step 9.** A patient dose report can be generated and saved clicking on the button “Confirm”. The selected scan parameters for the protocol and the corresponding effective dose,  $CTDI_{vol}$  and DLP are reported in a table. The absorbed dose in all the organs that contribute to the effective dose, including the remainder organs, is listed in a table together with the absorbed dose of other organs or tissues of interest, such as eye lens and testis or ovaries. The report shows also a graph with the organ doses of the eight organs that have the highest contribution to the effective dose. A graphical representation of the scanned region in the phantom is shown to provide a visual control of the selected anatomical region for the scan. The described information is presented for the entire CT examination (page 1) and also for each scanogram and each individual scan in the whole protocol (other pages).



**Step 10.** You can perform a new simulation clicking on the button “Next Simulation” located on the lower right corner. You can also close the program clicking on “Close”.

No.	Start	Start Time	Wait	Start Pos.	End Pos.	Start Mode
1	P	***	***	222.5	622.5	DualScano
2	A	***	***	622.5	222.5	DualScano
3	P			272.5	432.5	Volume
4	P			272.5	382.0	Helical

Organ Name	Organ Dose (mGy)	Organ Dose x Wt
Gonads	0.00	0.00
Red Bone Marrow	1.21	0.15
Colon	0.13	0.02
Lung	6.51	0.78
Stomach	0.78	0.09
Urinary bladder	0.01	0.00
Breast	1.01	0.00
Liver	0.86	0.03
Oesophagus	5.93	0.24

CTDIvol (mGy): 10.7      DLP (mGy cm): 171.2

Eff. Dose Serie (mSv): 2.23

Eff. Dose Total (mSv): \*\*\*

#### 4. Copyright

This software called SimDoseCT is Copyright ©2017. All rights reserved.

By using all or any portion of the software you accept all the terms and conditions of the License Agreement that is detailed in the installation of the program. If you do not agree, do not use this software.

For further queries related to SimDoseCT program contact us through the website <http://dio.urv.cat/simdosect/>.



